
NAWI Graz
Natural Sciences


TU
Graz

AFFIDAVIT

I declare that I have authored this thesis independently, that I have not used other than the declared sources/resources, and that I have explicitly indicated all material which has been quoted either literally or by content from the sources used. The text document uploaded to TUGRAZonline is identical to the present master‘s thesis.

Date

Signature

Acknowledgements

A big thank you to Univ.-Prof. Dipl.-Biol. Dr.rer.nat. Gabriele Berg, who supervised me during my time at the Institute of Envrionmental Biotechnology. She gave me the great opportunity to get in contact with microalgae biotechnology, encouraged me to improve myself and supported me in every step of my Master Thesis. Further I want to thank Dr.techn. BSc MSc Tomislav Cernava and Dipl.-Ing. Dr.techn. BSc Armin Erlacher, who guided me through my time at the institute with a lot of patience, advice and motivation in every situation. Special thanks to Dipl.-Ing. BSc Lisa Krug for every moment we spent together at the institute in the last two years, it was (and actually is) an outstanding pleasure for me to be your colleague and friend.

I want to thank my colleagues at the Institue of Environmental Biotechnology for the great experiences I made during the time of my master's thesis.

Special thanks to BioEnergy International (BDI) for enabling my project and providing the samples.

Another Special thanks to Harald Fischer, Eva Haberler and Nadja Eder who enabled me to study and especially to work at the Institue of Environmental Biotechnology with outstanding flexibility and understanding during the last ten years.

Finally I would like to thank my wonderful family and my dearest friends who support me with so much love, laughter and joy in every area of my life (and in this case: during my time at the university). Being happy without you is impossible.

Abstract

The green microalgae *Chlorella vulgaris* BEIJ is a common primary producer in a wide range of natural ecosystems, and it is widely used for biotechnological approaches, *e.g.* for biofuel production, human nutrition and wastewater treatment. The majority of algae live in close associations with their surrounding microorganisms (microbiome) but this was not yet considered in advanced process designs.

The aim of this study was to identify novel bacterial strains that can improve algal growth in industrial photobioreactors, and to study microbiome associated with naturally occurring microalgae. In order to identify growth-promoting microbes, a strain collection was constructed containing bacteria co-occurring with microalgae in natural environments as well as such obtained from production sites. A novel high-throughput screening assay was established to detect differences in *C. vulgaris* performance during co-cultivation with these bacterial isolates. Further, identified beneficial microbes were characterized with respect to their mode of interaction. In a complementary approach, natural occurring *C. vulgaris* habitats were analyzed by combining cultivation-independent single strand conformation polymorphism gel electrophoresis (SSCP) and Illumina-based 16S and 18S rRNA gene fragment sequencing.

Out of 726 isolated bacteria 17 strains were identified as *C. vulgaris* growth promoters. Ten *Pseudomonas* strains were characterized as common genus among the growth promoting isolates. The most effective isolate was identified as *Pseudomonas trivialis* 2Ca3. Besides microalgae growth promotion, *P. trivialis* 2Ca3 additionally disclosed various properties that are well described in context of plant growth promotion, *e.g.* siderophore production, protease activity, phosphate solubilization and quorum sensing. Microbial fingerprints performed by SSCP analyses of 16S and 18S rRNA genes provided a first but only limited insight into the eukaryotic and prokaryotic community structure of natural habitats where *C. vulgaris* was expected. Barcoded 18S rRNA gene fragment sequencing revealed the absence of *C. vulgaris* in all examined samples, but a high abundance of other microalgae, especially from the family of *Chlamydomonadaceae*. Furthermore, the taxonomic analysis showed that the eukaryotic community was habitat specific, but not dependent on the sampling site. Analyzing the 16S rRNA gene library uncovered *Proteobacteria* and *Bacteroidetes* as the most prominent phyla within snowfield specimens, whereas freshwater samples mainly consisted of *Proteobacteria* and *Actinobacteria*. Comparing samples at lower taxonomic levels indicated a location independent, but habitat specific bacterial community structure. Despite *C. vulgaris* was not

present in the high altitude environmental samples, strong *C. vulgaris* growth promoting strains were identified among the isolates, especially members belonging to the genus *Pseudomonas*.

Further characterization of algae growth promoting bacteria (AGPB) provides the potential to improve *C. vulgaris* mass production in industrial scale. Taking a deeper look into *C. vulgaris* and its co-occurring microbiome in their natural habitat provided even more knowledge for the application into prospective biotechnological approaches.

Kurzfassung

Die Grünalge *Chlorella vulgaris* BEIJ. ist ein Primärproduzent, der weltweit in verschiedensten Ökosystemen vorkommt. Dank schnellem Wachstum und Flexibilität hinsichtlich Wachstumsbedingungen ist *C. vulgaris* einfach zu kultivieren. Zudem weist die Grünalge verschiedenste nutzbare Eigenschaften auf, wie die Produktion von kommerziell relevanten Substanzen oder die Fähigkeit Kohlenstoff durch Photosynthese zu fixieren. Aufgrund dieses vielversprechenden biotechnologischen Nutzens wurde *C. vulgaris* in Sektoren wie Biotreibstoffproduktion, Ernährung und Abwasseraufbereitung, mehr Aufmerksamkeit zu Teil. Ein Ziel dieser Arbeit war die Identifizierung von neuen Bakterienstämmen, die eine Steigerung der Biomasseproduktion von Algen in industriellen Photobioreaktoren ermöglichen, da ein Großteil der bekannten Algenspezies in enger Verbindung mit co-existierenden Mikroorganismen steht. Dadurch ist eine sterile Kultivierung kaum durchführbar. Folglich muss dieses Mikrobiom auch in Biomasse-Produktionssystemen von größerem Maßstab beachtet werden. Um jene Mikroorganismen zu identifizieren, wurden Algen-assoziierte Bakterien aus der Umwelt wie auch aus industriellen Photobioreaktoren isoliert und eine Bakterien-Bibliothek erstellt. Ein neues Screening System wurde entwickelt, um die unterschiedlichen Auswirkungen einzelner Isolate auf das Wachstum von *C. vulgaris* zu bestimmen. Des weiteren wurden jene Isolate, welche als wachstumsfördernd identifiziert werden konnten, bezüglich ihrer Interaktion mit der Alge charakterisiert. Ein weiteres Ziel war die Analyse von *C. vulgaris* in ihrem natürlichen Lebensraum mittels einer mehrphasigen Versuchsreihe. Dabei wurden kultivierungsunabhängige Versuche mit spezifischen taxonomischen Markern (16S rRNA, 18S rRNA) und molekularbiologischen Nachweismethoden (genetische Fingerabdrücke via SSCP, Illumina Amplikon Sequenzierung) miteinander kombiniert.

Von 726 isolierten Bakterien wurden 17 als *C. vulgaris*-wachstumsfördernd identifiziert. Von diesen gehörten zehn zur Gattung *Pseudomonas*. Besonderes Augenmerk lag auf *Pseudomonas trivialis* 2Ca3, der das Wachstum der Alge signifikant steigerte und zudem verschiedene Fähigkeiten im Zusammenhang mit Pflanzenwachstumssteigerung zeigte. Zu diesen gehörten zum Beispiel die Produktion von Eisenchelatoren (Siderophore), Protease-Aktivität, Phosphat Solubilisierung und Quorum Sensing. Das genetische Fingerprinting via SSCP gab nur begrenzte Einsicht in die Struktur der eukaryotischen und prokaryotischen Umgebung der vermeintlichen *C. vulgaris* Habitate. Die eukaryotische Analyse, basierend auf der 18S rRNA Genfragmentsequenzierung, offenbarte, dass sich kein *C. vulgaris* unter den untersuchten Proben befand, zeigte aber jedoch einen hohen Anteil anderer Mikroalgen,

besonders der Familie *Chlamydomonadaceae*. Weiters zeigte die taxonomische Analyse, dass die Zusammensetzung der eukaryotischen Umgebung habitatspezifisch, aber unabhängig vom Ort der Probennahme ist. Die Analyse der 16S rRNA Genfragmentsequenzierung enthüllte *Proteobacteria* und *Bacteroidetes* als häufigste bakteriellen Stämme innerhalb der Schneefeldproben. Die Süßwasserproben hingegen bestanden vorwiegend aus *Proteobacteria* und *Actinobacteria*. Der Vergleich der Proben auf niedrigeren taxonomischen Ebenen wies auf eine ortsunabhängige, aber habitatspezifische bakterielle Zusammensetzung hin. Obwohl *C. vulgaris* nicht in den hochalpinen Umweltproben gefunden werden konnte, wurden aus jenen *C. vulgaris*-wachstumsfördernde Bakterien isoliert, welche vor allem zur Gattung der Pseudomonaden gehörten. Deren weitere und detailliertere Charakterisierung hinsichtlich Algenwachstumsförderung könnte Potential zur Verbesserung von *C. vulgaris* Massenkultivierungsanlagen bieten. Durch die Isolierung von *C. vulgaris* und dem natürlich assoziierten Mikrobiom könnten weitere nützliche Kenntnisse für die Anwendung in zukünftigen biotechnologischen Verfahren gewonnen werden.

Content

I. Introduction

1.1 Algae – a general introduction

Phycology, deriving from the Greek word *phykos* "seaweed", is the study about algae. Algae in turn is the plural from the Latin word *alga,* also meaning "seaweed". As algae are organisms performing photosynthesis but lacking leaves, stems and roots, they are thallophytes (Lee, 2018). Algae species occur ubiquitous and are present in a wide variety of habitats, including fresh-, brackish- and seawaters (aquatic), soil (terrestrial), on and within plants (epi- and endophytic), on rocks (lithophytic), deserts, hot springs (thermal), permanent snowfields (cryophytic) or in form of phytoplankton (Atkinson, 1972; Sharma, 1986). Furthermore according to Ahmadjian (1967) certain alga genera live in symbiotic association with fungi, further called lichens. Lee (2018) classified algae in four different taxonomic groups: prokaryotic blue-green algae, commonly called cyanobacteria; eukaryotic algae with chloroplasts surrounded by the two membranes of the chloroplast envelope (*Archaeplastida*), including red algae (*Rhodophyta*) and green algae (*Chlorophyta*); eukaryotic algae with chloroplasts surrounded by one membrane of the chloroplasts endoplasmic reticulum, including euglenoids (*Euglenophyta*) and dinoflagellates (*Dinophyta*); eukaryotic algae with chloroplasts surrounded by the two membranes of the chloroplasts endoplasmic reticulum, including *Cryptophyta* and *Heterokontophyta* like *Chrysophyceae* (golden-brown algae), *Bacillariophyceae* (diatoms) or *Xanthophyceae* (yellow-green algae). Algae species may occur unicellular (microalgae) or multicellular (macroalgae, seaweed) (Benemann *et al.*, 1978). The size of a microalgae can range from a few micrometers up to a few hundreds of micrometers, dependent on species. Nevertheless they are capable of producing half of the atmospheric oxygen through photosynthesis by using carbon dioxide for autotrophic growth. To date the biodiversity of microalgae comprises around 20,000-800,000 species (Oncel, 2013; Hu *et al*., 2008).

1.2 Potential of microalgae in industrial applications

Over the last decades, microalgae gained more attention for commercial use and industrial application due to their wide range of useful characteristics. Several fields within the use of algal biomass have unfolded. Microalgae are producers of many bioproducts such as carbon compounds, polysaccharides, lipids, pigments, proteins, vitamins and antioxidants (Brennan and Owende, 2010). The use of microalgal biomass as renewable and sustainable feedstock in bioenergy production was established as they are one of the most promising raw material to

compensate and balance the increasing demand for fuel energy (Harun *et al.*, 2010). Microalgae-based biofuels are non-polluting, non-toxic and feature a high potential of fixing global carbon dioxide (Gendy and El-Temtamy, 2013). Additionally, microalgae are natural producers of commercial relevant substances. As microalgae produce vitamins and essential amino-acids beside diverse carbohydrates they are used as nutrients and protein-rich food ingredients (Borowitzka, 1998; Guil-Guerrero *et al*., 2004). Several microalgal species find application to the biopharmaceutical industry by producing health-promoting substances; One example are polyunsaturated fatty acids with a therapeutic value for chronic diseases (Adame-Vega *et al.,* 2011). Some pigments deriving from microalgae exhibit a protective effect against free radicals and oxidative stress-associated diseases. These antioxidative compounds prevent oxidative cell damage and peroxidation processes and are nowadays available as food additives (Liang *et al.,* 2004).

Many different species of microalgae provide potential for large scale culturing. To achieve a sustainable, feasible and economically viable microalgae-based industry, modern cultivation systems targeting microalgae biomass production are constructed. These have to be optimized concerning growth conditions and culturing methods in order to obtain a constant and robust microalgae growth. Apart from negative effects like growth reduction, algae-bacteria interactions may provide high potential in beneficially affecting microalgae mass production. Therefore analyzing the microalgae co-occurring microbiome in natural habitats, but also from artificial cultivation processes, may lead to better understanding of these algae-bacteria communities and facilitate the development of more efficient algae biotechnological processes (Fulbright *et al.,* 2018).

1.3 Microalgae-bacteria interactions and their potential

The majority of all described algae species live in close associations with distinct microorganisms during their whole lifetime (Dittami *et al.,* 2014). Attempts to remove these microorganisms in the frame of industrial algae mass cultivation approaches failed in many cases. More interestingly, if axenic biomass production is achieved, the microalgae growth is often constrained. This leads to the assumption that the relation between microalgae and bacteria is from high importance for the algae viability (Hom *et al.*, 2015). Interactions between algae and bacteria occur in various forms concerning nutrient exchange, horizontal gene transfer or signal transduction. They have potential to stimulate algae growth, alter morphogenesis and germination (Krediet *et al.,* 2013) and support the algae to cope with harsh environmental conditions (Xie *et al.,* 2013). On the other side many microorganisms

might affect the algae growth negatively (Le Chevanton *et al.,* 2013; Kim *et al.,* 2014). These microbes present big constraints during the scale-up process from laboratory experiments to industrial microalgae mass production (Carney and Lane, 2014). Thus examining the microbiome naturally co-occuring with microalgae and the assessment of prevalent interactions may improve controlling and monitoring of large-scale algae mass production systems (Mendes and Vermelho, 2013).

1.3.1 Beneficial interplay of co-occurring microorganisms

According to Seymour *et al.* (2017) mutualistic relations between algae and bacteria are prevalent. In these common relations both, algae species and bacterial species, benefit each other (Copper and Smith, 2015). Co-cultivation of algae with different bacteria (Le Chevanton *et al.,* 2013; Sison-Mangus *et al.,* 2014; Biondi *et al.,* 2017) revealed multiple effects on the growth of microalgae, particular concerning metabolite exchange. With regard to algae biotechnology accelerating the algae growth rate and increasing the algae cell count are two factors that can be addressed for optimizations.

1.3.1.1 Nutrient provision by bacteria

For growth algae need carbon dioxide, inorganic nitrogen and phosphorus sources together with micronutrients and cofactors (Singh and Das, 2014). A specific co-occurring bacterial community can provide these nutrients in an appropriate amount (Clarens *et al.,* 2010). For this reason, many microalgae live in symbiotic relations with surrounding bacteria. For instance algae are capable of releasing dissolved organic matter, fixed carbon and signaling molecules to nurture bacterial communities located in the phycosphere (Amin *et al.,* 2012). In exchange bacteria have the ability to degrade a broad range of organic compounds and provide the essential CO_2 for the algae (Mouget *et al.,* 1995; Subashchandrabose *et al.,* 2011). Algae prefer ammonium (NH_4) as nitrogen source, which can be provided by nitrogen-fixing bacteria through reduction of atmospheric dinitrogen (N_2) (Singh and Das, 2014). Moreover, algae only consume ionic phosphorus (P_i) that has to be derived by hydrolysis of organic phosphorus (P_o) (Zhu *et al.,* 2013). P_o hydrolysis is performed by phosphatases of P_o-decomposing bacteria (Kononova and Nesmeyanova, 2002). Despite these macronutrients algae growth is also dependent on the availabilty of micronutrients like vitamins, iron and signal molecules like phytohormones. There are specific bacteria that provide algal hosts with siderophores for iron-assimilation (Amin *et al*., 2009), synthesize the phytohormone indole-3-acetic-acid for cell division promotion (Amin *et al.,* 2015) or ensure the sufficient vitamin B supply for algae as Croft and colleagues (2005) showed that 171 out of 326 examined algae

species lack vitamin B_{12} synthesis pathway. In figure 1.1 general interactions between microalgae and symbiotic bacteria are displayed.

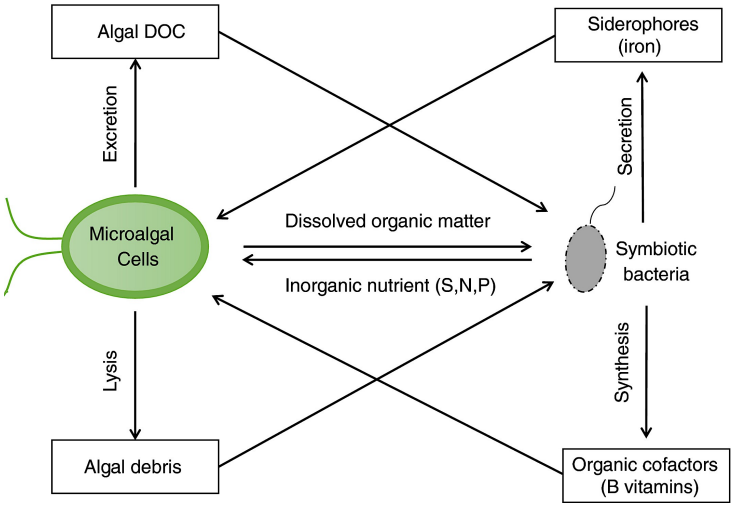

Figure 1.1: A simplified diagram of interactions between microalgae and symbiotic bacteria. DOC = dissolved organic carbon (adapted from Yao *et al.,* 2018).

1.3.1.2 Better adaption to environmental conditions

Another benefit caused by algae-bacteria co-occurrences is a better adaption to changing or harsh environmental conditions. For instance specific cobalamin-producing bacteria can avoid algae cell death caused by increased temperatures through circumvention of the cobalamin-independent methionine synthase (Xie *et al.,* 2013). Another case of improved adaption to environmental conditions caused by associated bacteria is the marine alga *Picochlorum* sp. SENEW3. This green alga displays an increased salt tolerance that originated from horizontal gene transfer (Wang *et al.*, 2014). It contains 24 additional functional genes in response to salt stress, which derived from bacteria (Foflonker *et al*., 2015).

1.3.2 Negative effects of bacteria on algae

There are many cases of bacterial parasitism on algae, where the bacterial species lives on the expense of the algae species. Algicidial effects like algae cell lysis through the activity of glucosidases, chitinases or cellulases that were secreted by bacteria (Affi *et al.*, 1996); algae growth decrease caused by nutrient competition with bacteria were also observed (Ramanan *et al.,* 2016). Zozaya-Valdés and colleagues (2017) found algae-associated bacterial families that were implicated in bleaching of the marine macroalgae *Delisea*. Ashen and Goff (2000) as well as Wang and colleagues (2008) examined the effects of gram-negative bacteria on seaweed; they determined various bacterial genera to be responsible for rot symptoms (Ashen

and Goff, 2000) and galls (Wang *et al*., 2008). Another study performed by Ivanova and colleagues (2014) identified *Microbacterium* sp. LB1 as responsible for cell lysis of laboratory cultures of the green algae *Choricistis minor*, which resulted in a dry weight reduction of 34%. Considering these versatile negative effects of bacteria on algae, the associated bacterial community is a main factor in artificial microalgae growth processes. During cultivation processes the co-cultivation of unwanted eukaryotic or prokaryotic organisms is hardly possible to avoid, so it has to be monitored severely. According to Pienkos and Darzins (2009) these co-cultivated organisms in large-scale algae production also include viruses, parasites and bacterial pathogens. These might infect algae cells and are subsequently a main risk in algae biomass production. To date there is little knowledge about these associated microbiomes in industrial scale. Hence controlling and predictions of a microalgae cultivation process concerning bacterial contamination is difficult.

1.4 *Chlorella vulgaris* cultivation

The microalgae *Chlorella vulgaris* BEIJ belonging to the genus *Chlorella,* was found 1889 by the Dutch microbiologist Martinus Willem Beijernick (Beijernick, 1890). It is a green, unicellular freshwater algae that is present ubiquitously since the pre-Cambrian period (von Ditfurth, 1972). *C. vulgaris* microscopic cells have a diameter between two and ten μm and exhibit a cellular structure similar to a plant.

1.4.1 Reproduction

C. vulgaris is a non-motile reproductive microalgae which uses autosporulation to multiply. Autosporulation is the most common reproduction system within algae. Four daughter cells are formed inside the mother's cell wall. After maturation of the daughter cells they are liberated by rupturing the cell wall. The remnant of the mothercell then serves as feed for the newly formed cells (Figure 1.2), (Yamamoto *et al.,* 2004).

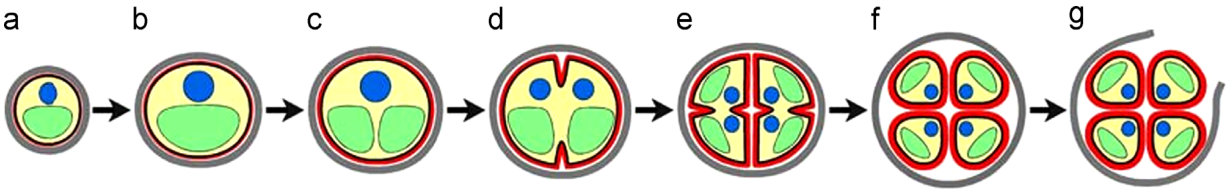

Figure 1.2: Schematic reproduction of *C. vulgaris*. (a) early cell-growth phase; (b) late cell-growth phase; (c) chloroplast dividing phase; (d) early protoplast dividing phase; (e) late protoplast dividing phase; (f) daughter cells maturation phase and (g) hatching phase (adapted from Yamamoto *et al.*, 2005).

1.4.2 Morphology

The rigidity of the cell wall is responsible for the cells integrity and protects it against invaders and environmental influences. Its structure and composition varies depending on the algae growth phase. During the early cell-growth phase the newly formed cell wall is fragile and consists of a two nm thin electron-dense unilaminarlayer. It increases its thickness to 17-21 nm after maturation (Yamamoto *et al.,* 2004) when a microfibrillar layer is formed composed of glucosamine, which is responsible for the cells rigidity (Yvonne and Tomas, 2000). Composition and structure of the mature cell wall are depending on growth and environmental conditions. The *C. vulgaris* cytoplasm consists of water, soluble proteins and minerals. It embeds cell organelles like the nucleus, mitochondria, vacuoles, the chloroplast and the Golgi body (Figure 1.3). The mitochondria are surrounded by a layer membrane and include a part of the genetic material as well as the respiratory apparatus. The whole organelle is enclosed by the outer membrane composed of an equal ratio of proteins and phospholipids, while the inner membrane consists of thrice more proteins than phospholipids. It surrounds the matrix, the internal space where the majority of the mitochondrial proteins is situated (Solomon *et al*., 1999). Every *C. vulgaris* cell contains one single chloroplast, that is enclosed by a double-phospholipid-membrane. Under unfavorable growth conditions the chloroplast forms starchgranules, composed of amylose and amylopectin. The center of the carbon dioxide fixation is the pyrenoid, which contains high levels of ribulose-1,5-bisphosphate-carboxylase-oxygenase (RuBisCO). The green color of *C. vulgaris* is originated from the dominant pigment chlorophyll, which is synthesized in a cluster of fused thylakoids in the chloroplast (Van den Hoek *et al.,* 1995).

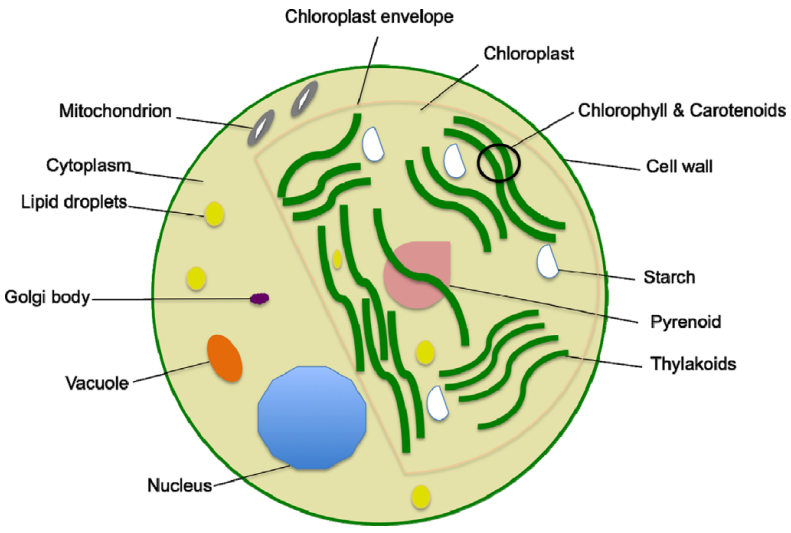

Figure 1.3 : Schematic *C. vulgaris* cell structure (adapted from Safi *et al*., 2014).

1.4.3 Primary composition

1.4.3.1 Proteins

In the composition of microalgae proteins have an important role as they are involved in main functions such as growth, repair and maintenance of the cells, chemical communication, regulation of cellular activity and defense against invaders (Solomon *et al*., 1999). The protein content in *C. vulgaris* presents about 50% of the total dry weight and is dependending on growth conditions. *C. vulgaris* exhibits an amino acid profile similar to the suggested standard profile for human nutrition proposed by World Health Organisation (Faheed *et al*., 2008) (Table 1.1).

Table 1.1: Amino acid profile from *C. vulgaris* expressed in g × 100 g^{-1} of protein (Faheed *et al.,* 2008; adapted from Safi *et al.,* 2014). NA = not available.

Amino Acid	*Chlorella vulgaris*	Recommendation from WHO
Aspartic Acid	9.30	NA
Threonine	5.30	4.00
Serine	5.80	NA
Glutamic Acid	13.70	NA
Glycine	6.30	NA
Alanine	9.40	NA
Cysteine	NA	3.50
Valine	7.00	5.00
Methionine	1.30	NA
Isoleucine	3.20	4.00
Leucine	9.50	7.00
Tyrosine	2.80	6.00
Phenylalanine	5.50	NA
Histidine	2.00	NA
Lysine	6.40	5.50
Arginine	6.90	NA
Tryptophan	NA	1.00
Proline	5.00	NA

1.4.3.2 Lipids

C. vulgaris can reach 5-40% lipid content per dry weight of biomass under optimal growth conditions (Becker, 1994). The mixture of lipids is mainly composed of glycolipids, waxes, hydrocarbons, phospholipids and free fatty acids (Lee, 2008; Hu *et al.,* 2008). All these components are synthesized by the chloroplast and located on the cell wall and on the membranes of the chloroplast and the mitochondria. Further the lipid content can reach up to

58% under unfavorable growth conditions (Mata *et al*., 2010; Becker, 1994), whereas mainly triacylglycerols are produced in that case. These triacylglycerols accumulate as storage lipids in the cytoplasm and in the inter-thylakoid space of the chloroplast (Hu *et al.,* 2008). Changes in the fatty acid profile depending on given growth conditions are consequently suitable for different industrial applications. For biodiesel production a high amount of saturated and monounsaturated fatty acids (palmitic acid C16:0, stearic acid C18:0, palmitoleic acid C16:1, oleic acid C18:1) is required and generated under good growth conditions (Zheng *et al.,* 2011). Contrary a fatty acid profile for nutritional use with a high content of polyunsaturated fatty acids can be achieved under unfavorable conditions (Chen *et al.*, 2011).

1.4.3.3 Carbohydrates

As already mentioned *C. vulgaris* is capable of synthesizing high amounts of starch, which is located in the chloroplast and serves as energy storage. Additionally, microalgae produce a structural polysaccharide cellulose that is located at the cell wall and serves as protective fibrous barrier. Beside these two main carbohydrates *C. vulgaris* synthesizes β-1,3-glucan that provides health and nutritional benefits (Lordan *et al*., 2011).

1.4.3.4 Pigments

As *C. vulgaris* is a green algae its most abundant pigment is chlorophyll, located in the thylakoids of the chloroplast. Additionally, the algae contains other pigments such as different carotenoids like β-carotene, astaxanthin, cantaxanthin, lutein or types of chlorophylls like pheophytin-a and –b, as accessory substances. For instance, primary carotenoids which are associated with chlorophyll are responsible for trapping light energy and transferring it into the photosystem. They work as photoprotectors as they defend chlorophyll molecules against degradation or bleaching during strong exposure to oxygen (Solomon *et al.,* 1999). Due to their versatile therapeutic properties pigments produced by *C. vulgaris* are highly rated for commercial use. According to Gouveia and colleagues (2005) these pigments have an antioxidant activity. Furthermore they prevent retina degeneration (Granado *et al.,* 2003; Fernandez-Sevilla *et al.,* 2012), have potential to regulate blood cholesterol, prevent chronic diseases and are capable of strengthening the immune system (Cha *et al*., 2008; Tanaka *et al.,* 1984).

1.5 Industrial production and commercial applications of *Chlorella vulgaris*

Due to its versatile properties *C. vulgaris* has high potential for various biotechnological applications, *e.g.* production of biodiesel, food supplementation, wastewater treatment or sustainable energy production (Safi *et al.,* 2014). The first mass cultivation approach for *Chlorella* took place in Boston, United States of America (Little, 1953), followed by different production approaches in Israel (Evenari *et al*., 1953), Japan (Mitsuya *et al.,* 1953) and Germany (Gummert *et al.,* 1953). In 1961 the Chlorella Institute in Tokyo established the first mass cultivation system for commercial use of *Chlorella* (Iwamoto, 1958; Takechi, 1965). Since then the annual commercial mass cultivation of *C. vulgaris* increased from 200 t per year (1975) to 2000 t per year in 2009 (Brennan and Owende, 2010), establishing different large-scale processes for microalgae biomass production.

C. vulgaris is highly suitable for mass production because of its rapid growth rate and its resistance against harsh environmental conditions and invaders. *C. vulgaris* is able to grow under different sets of conditions; conditions during mass cultivation can be modified and thus result in different outcomes. Under unfavourable growth conditions, such as nitrogen and phosphorus limitation, high levels of CO_2, intense exposure to light or increased temperature (Converti *et al*., 2009; Lv *et al*., 2010; Pribyl *et al*., 2012; Widjaja *et al.,* 2009) the biomass production decreases and the cells produce more lipids and starch (Pribyl *et al.,* 2013). During favorable growth conditions the biomass and the protein content increase. In order to target a specific product or a specific activity the microalgae growth techniques can be adapted accordingly. A general schematic *C. vulgaris* production process can be seen in figure 1.4.

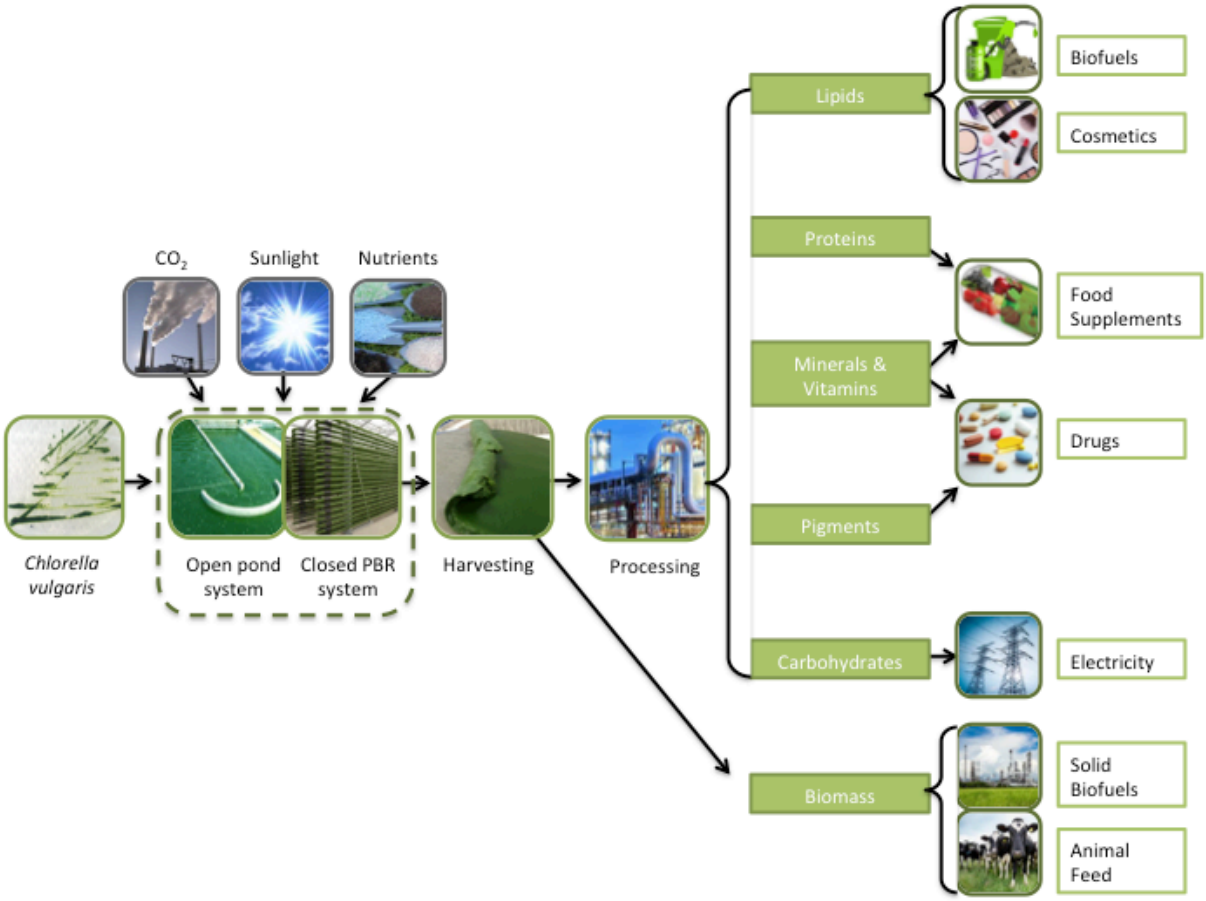

Figure 1.4: Scheme of an autotrophic *C. vulgaris* large-scale production process. PBR = photobioreactor.

1.5.1 Biofuels and bioethanol

Considering the harmful consequences of fossil based fuels for the environment sustainable and renewable energy sources have to be established. Compared to soybean, corn, rapeseed or lignocellulosic as feedstocks for biofuel production, microalgae are advantageous as alternative energy source as they do not compete with food production and do not require land to grow (Singh *et al.,* 2011). *C. vulgaris* has the ability to store large amounts of lipids, especially when grown in a mixotrophic system under favorable growth conditions. Then its fatty acid profile seems to be suitable for biodiesel production (Wang *et al.,* 2013). Beside accumulation of lipids *C. vulgaris* is also capable of producing starch in high levels, which is considered as a good source for bioethanol production. As an example Hirano *et al.* (1997) achieved an ethanol conversion rate of 65% after starch extraction from *C. vulgaris*, saccharification and fermentation with yeast.

1.5.2 Human nutrition

Because *C. vulgaris*-derived products provide various health benefits like antioxidant activity, a richness in proteins or lipids and vitamins, the microalga is of high interest for food industries and the healthcare sector. Substances produced by *C. vulgaris* are used as a food supplement or colorant in different forms like capsules, tablets, extracts, powder or as ingredient (Liang *et al.*, 2004). Since there are no clear official legislations concerning quality and requirements of microalgae, *C. vulgaris* is more often used as nutraceutical (Grobbelaar, 2003; Golati *et al*., 2006).

1.5.3 Wastewater treatment

Beside producing various industrially relevant compounds, *C. vulgaris* is also able to fix carbon dioxide, absorb nitrogen and phosphorus and reduce the chemical oxygen demand and can therefore be utilized for several industrial purposes. Since microalgae need vital nutrients (nitrogen and phosphorus), carbon dioxide and heavy metals for their growth, they imply a pathway to remove them from water. This is used in wastewater treatment processes as all these substances are present in wastewater from textile, sewage, municipal or agricultural sources (Aslan and Kapdan, 2006; Feng *et al.,* 2011; Lau *et al.,* 1996; Lim *et al.,* 2010; Silva-Benavides and Torzillo, 2012; Valderrama *et al.,* 2002; Yun *et al.,* 1997). Additionally growing microalgae is advantageous in wastewater treatment as part of a biomass production process since chemical remediation can be avoided and the use of microalgae may reduce the need of fresh water (Brennan and Owende, 2010).

1.6 Improving industrial production of algae biomass with nature-based strategies

Interactions between algae and bacteria are many-sided and nowadays seen as promising way to improve algae biotechnology in a natural way (Figure 1.5). Additionally, more knowledge of related co-cultivated bacteria may help to establish a stable production process and enable improved controlling and monitoring within (Lian *et al.,* 2018).

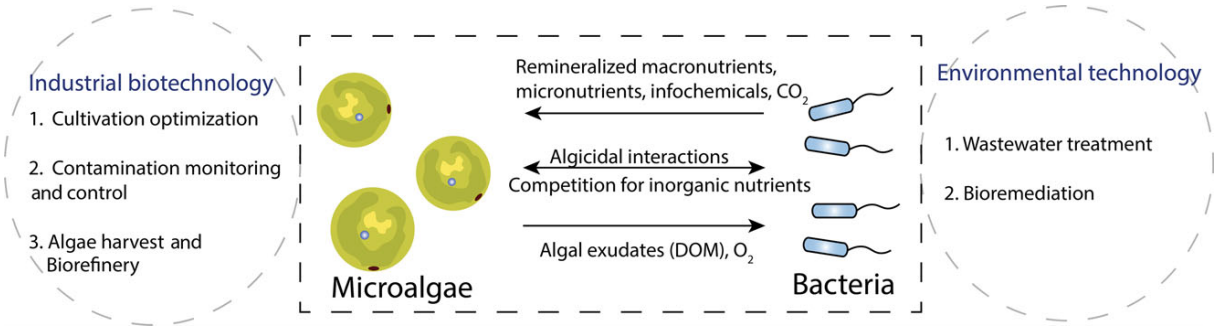

Figure 1.5: Potential applications of algae-bacteria interactions in industrial and environmental biotechnology. DOM = dissolved organic matter. (adapted from Lian *et al.,* 2018).

Though the number of cultivation-independent studies has increased over the last years due to next-generation-sequencing methods, there are few studies concerning the bacterial community within microalgae production systems. This limited knowledge prevents general statements concerning microalgae-associated bacterial communities and predictions in context of large-scale algae production processes (Lian *et al.,* 2018). Otherwise single interactions between bacteria and algae were analyzed and have the potential to be implemented into algae technology (Le Chevanton *et al.,* 2013; Sison-Mangus *et al.,* 2014; Biondi *et al.,* 2017).

For instance, CO_2 levels are one of the limiting factors during open microalgae biomass processes, as gas transfer is dependent on environing air (Putt *et al.,* 2011). In order to guarantee a constant high CO_2-supply additional CO_2-enriched gas is often used, which comes along with additional cost (Clarens *et al.,* 2010). The co-cultivation of specific bacteria that degrade organic compounds and subsequently provide further CO_2 for the algae may circumvent these costs (Mouget *et al.,* 1995; Subashchandrabose *et al.,* 2011). Many bacteria are known to suppress algae growth. On the one side these bacteria may be applied to control unwanted microalgae or cyanobacterial blooms (Kim *et al.,* 2008). On the other side co-occurring detrimental bacteria in large-scale biomass production systems are responsible for losses regarding production yield and efficiency (Fuentes *et al.,* 2016).

More insight into interactions and relations between microalgae and their surrounding bacterial community may provide new approaches in algae biotechnology concerning yield acceleration and cost reduction (Fuentes *et al.,* 2016).

1.7 Implementation of bacterial consortia for industrial purposes

Mixed bacterial communities are omnipresent in nature. Nowadays they are used in biotechnological processes like bioremediation or wastewater treatment. Using bacterial consortia is far more complex than the use of monocultures but provides many advantages. Microbial consortia are capable of performing more complicated tasks and show higher robustness against environmental changes. Hence engineering artificial bacterial consortia is from high interest in biotechnological processes (Brenner *et al.,* 2008). With respect to algae biotechnology plenty algae growth-affecting strains were identified (Kim *et al*., 2014; Hernandez *et al.,* 2009). As microalgae are naturally surrounded by bacteria in their phycosphere, the engineering of a defined advantageous microalgal-bacterial consortium and its application into algae cultivation processes might be promising for prospective large-scale approaches (Cho *et al.*, 2014).

1.8 *Chlorella vulgaris* interactions with bacteria

C. vulgaris is one of the best studied and most applied microalgae so far. There are many studies concerning *Chlorella vulgaris*-bacteria interactions and subsequent implementation into large-scale bioprocesses (Lian *et al.*, 2018). For example *Baciullus pumilus* ES4 promotes *C. vulgaris* growth through nitrogen fixation under axenic conditions (Hernandez *et al.*, 2009), co-cultivation with *Rhizobium* sp. leads to increased cell count and growth rate (Kim *et al.*, 2014) and Bashan and Gonzalez (2000) determined higher *C. vulgaris* cell counts when co-immobilized with the plant growth-promoting bacterium *Azospirillum brasiliense* in alginate beads. Implementation of a bacterial consortium consisting of *Flavobacterium* sp., *Rhizobium* sp., *Hyphomonas* sp. and *Sphingomonas* sp. results in increased cell density by over 100% (Cho *et al.*, 2014). These studies are appropriate examples how co-occurring microbes are able to affect microalgae growth. Furthermore, finding *C. vulgaris* beneficial strains and their targeted implementation as single strains or in form of defined consortia is of high interest for prospective bioindustrial applications.

1.9 Objectives of the study

C. vulgaris is one of the most promising microalgae concerning prospective alternative biotechnological approaches. The impact of co-occurring microbes is from great extent since they are able to affect the microalgae life in various ways. Gaining more knowledge about these associated bacteria may lead to improvements regarding mass cultivation yield and quality.

Principle aims of the study were (I) the examination of *C. vulgaris* and its co-occurring microbiome in natural and artificial environments, (II) screening for growth-promoting or –suppressing bacterial strains and (III) unravelling their way of interaction with the microalgae. Thereby (IV) a novel high-throughput screening system to identify algae growth-affecting microbes was developed.

II. Material & Methods

2.1 Experimental design

The algal strains used in this study were isolated from photobioreactors (PBR) in a previous project (Krug, 2016) where they were identified as co-cultivated microalgae during industrial-scale cultivation of the green microalgae *Haematococcus pluvialis*. The strains used in this work are deposited in the strain collection of the Institute of Environmental Biotechnology (Graz University of Technology).

In the two-step approach, the co-occurring microbiome of *C. vulgaris* in an artificial environment (PBR) was investigated. Additionally, eukaryotes and bacteria associated with microalgae in their natural environment were examined. To analyze the *C. vulgaris* co-occurring prokaryotes and eukaryotes, samples from an artificial environment and different environmental habitats were analyzed and compared. For this purpose, cultivation dependent and independent approaches were designed and performed (Figures 2.1; 2.2).

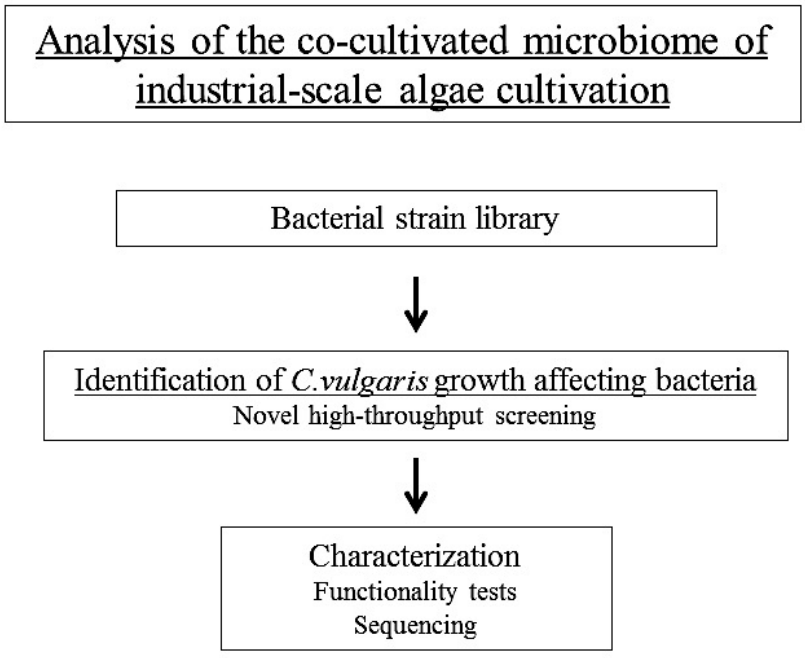

Figure 2.1: Workflow scheme for samples taken from production sites (photobioreactors).

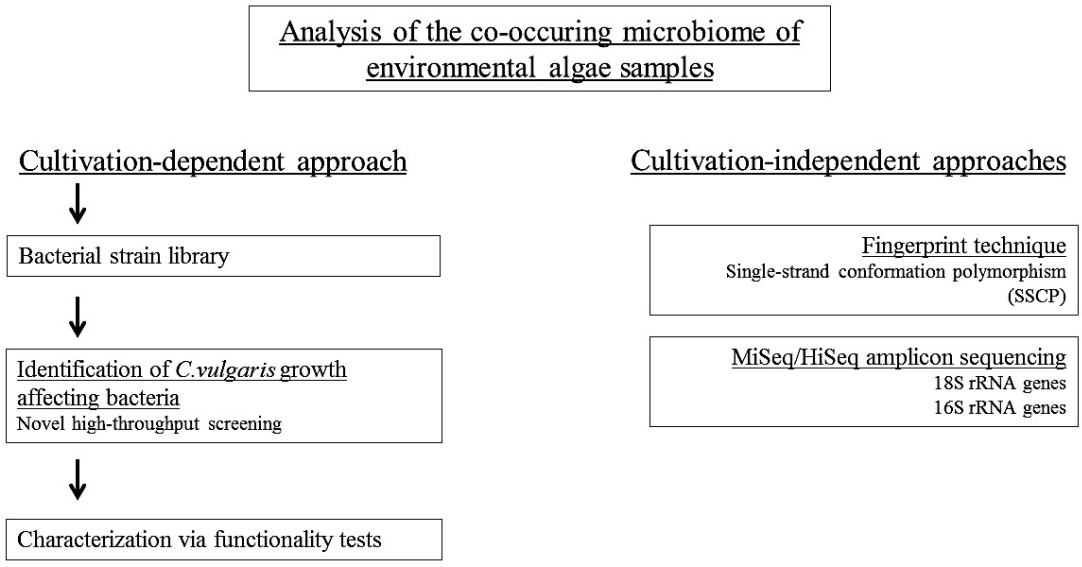

Figure 2.2: Workflow scheme for environmental samples taken from different spots in Styria (Austria).

2.2 Microalgae strains for growth evaluations

The main model microalgae used in this study *C. vulgaris* was isolated and identified in a previous study (Krug, 2016). Microalgae were cultivated in Erlenmayer Flasks and/or on agar plates using sterile Bold's Basal Medium (BBM) (Bischoff and Bold, 1963) at 23 °C. The lighting was supplied by cool-white fluorescent lamps TL-D 36W/840 REFLEX Eco (Philips, Netherlands) with an intensity of 3350 lm under natural light conditions (16-h-8-h light-dark cycle).

2.3 Bacterial strains for co-cultivation experiments

2.3.1 Plant biocontrol strains

A total of 24 plant biocontrol strains stored at the Institute of Environmental Biotechnology (Graz University of Technology) were used for growth promotion screenings with the model microalgae (Table 2.1).

Table 2.1: Plant biocontrol strains from the Institute of Environmental Biotechnology that were tested for microalgae growth promotion.

1	*Serratia plymuthica* 3Re4-18
2	*Streptomyces tauricus* RE2-6-8
3	*Pseudomonas aurantiaca* SDK 2-2-6
4	*Pantoea ananatis* BLBT 1-08
5	*Stenotrophomonas rhizophila* ep17
6	*Serratia plymuthica* HRO C48
7	*Stenotrophomonas rhizophila* P69
8	*Bacillus pumilis* BB-1-3-5
9	*Pseudomonas fluorescens* L13-6-12
10	*Bacillus subtilis* B2g
11	*Pseudomonas poae* Re × -1-1-14
12	*Paenibacillus polymyxa* Pb71
13	*Burkholderia sp.* C1 ecto 15
14	*Pseudomonas trivialis* 3Re-2-7
15	*Pseudomonas putida* 1T1
16	*Streptomyces* Ca 1-25a
17	*Pseudomonas filiscidens* B2R2-1-2-3
18	*Stenotrophomonas rhizophila* ep14
19	*Micorbacterium sp*. Rübe 1-3-26
20	*Microbacteriaceae* C1 ecto 9
21	*Kytococcus sedentarius* L3 ecto 15
22	*Sinorhizobium sp.* W4-7
23	*Serratia plymuthica* 3RP8
24	*Burkholderia bryophila sp.* Nov. A5

2.3.2 Isolation of bacterial isolates from photobioreactors

Samples from photobioreactors with different capacities and growth conditions were used for the isolation of additional bacterial strains (Table 2.2).

Table 2.2: Sample overview from photobioreactors with different growth conditions.

sample ID	origin	growth conditions	picked bacterial isolates
A	Demo B 10100 green	no data	63
B	5 L PBR	carbon-source CO_2	52
C	5 L PBR	carbon-source Acetic acid	56
D	reactor 4 17016	carbon-source CO_2 + intense light	71
E	reactor 3 17015	carbon source Acetic acid pH 3.9 + intense light	17
F	reactor 3 17015	carbon source Acetic acid pH 7.5 + intense light	34

2.3.3 Sampling of *C. vulgaris* isolates and co-occurring bacteria from the environment

Environmental samples were collected from five different sites located in Styria (Austria) using 50 mL tubes (Sarstedt, Germany) and FLOQSwabs (Copan Diagnostics, USA), respectively (Figures 2.3, 2.4; Table 2.3). A red-green-colored puddle on a white garden chair in the suburban region of Graz was sampled (G – Graz, N 47°3'39.536" E 15°27'29.308"). In total three replicates were taken. In addition, six biological replicates were taken from white tiles in a rural region near Liezen (P – Ennstal, N 47°35'27.870" E 14°21'24.075"). In total 37 samples from three different locations were taken from snowfields, lakes and stagnant waters in high altitude (1000 m – 2400 m): 1 – Triebener Tauern (N 47°26’24.695’’ E 14°34’34.556’’); 2 – Drei Lacken (N 47°26’17.275’’ E 14°27’12.86’’); 3 – Seetaler Alpen (N 47°3’56.128’’ E 14°34’0.318’’).

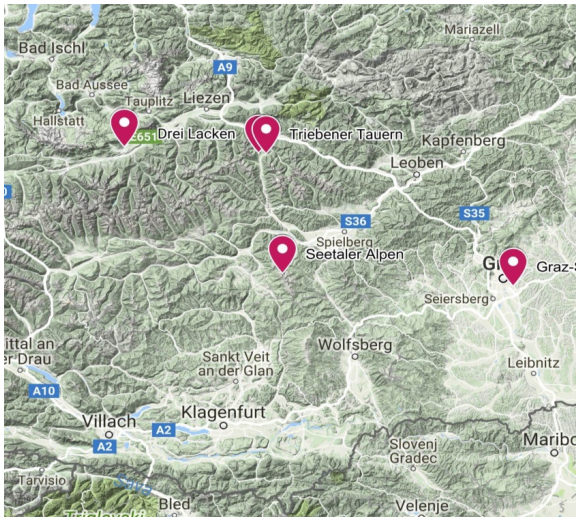

Figure 2.3: Sampling locations in Styria (Austria) where putative *C. vulgaris* strains were taken.

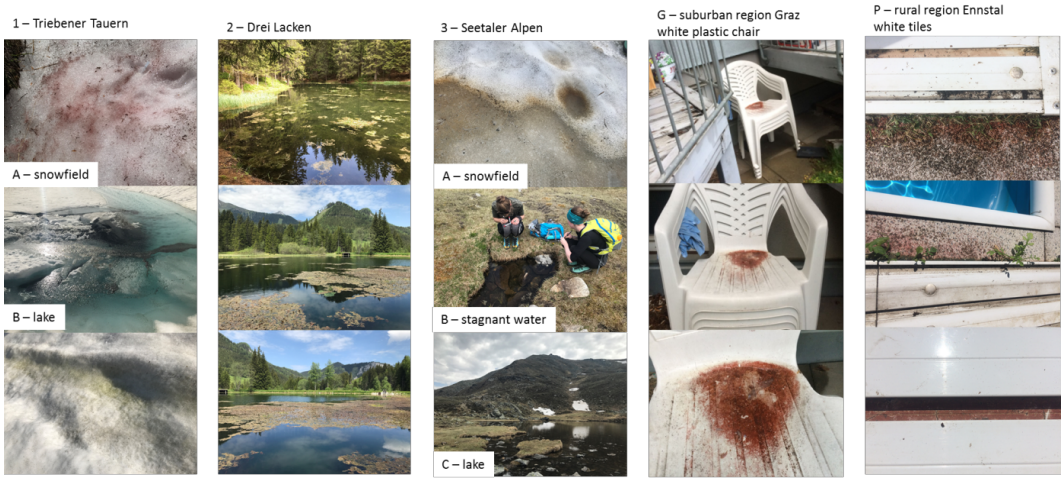

Figure 2.4: Insight into the sample collection. Putative *C. vulgaris* strains were isolated from various habitats including colored snowfields and stagnant water.

Table 2.3: Overview of the environmental samples from different habitats.

sample ID	location	number of sampling spots	number of biological replicates	habitat
G	Graz	1	3	water / chair
P	Ennstal	1	6	water / tile
1	Triebener Tauern	2	14	snowfield
2	Drei Lacken	3	6	water
3	Seetaler Alpen	5	17	water / snowfield

2.4 General Methods

2.4.1 Total community DNA extraction

For each examined sample 2 mL of algae suspension were centrifuged at 13,000 rpm for 20 minutes at 4° C. The supernatant was discarded and the resulting pellets were used for total community DNA extraction. Obtained pellets were used for extraction of the total community DNA using the FastDNA SPIN Kit for soil (MP Biomedicals, Germany). Pellets were treated according to manufacturer's protocol. 978 µL sodium phosphate buffer and 122 µL MT buffer were added to respective pellets. Homogenization of the pellets was done using a FastPrep FP120 instrument (MP Biomedicals, Germany) for 30 seconds at a speed of 5.5 m × s^{-1}. After 15 minutes of centrifugation at 14,000 × g 250 µL protein precipitation solution (PPS) were added to the supernatant. After another 5 minutes of centrifugation at 14,000 × g 1 mL binding matrix solution was added to the supernatant. Then the tubes were inverted for 2 minutes by hand and placed in a rack for 10 minutes to allow settling of the silica matrix. Approximately 700 µL supernatant were discarded. Resuspended binding matrix was transferred to a spin filter with subsequent centrifugation at 14,000 × g for 1 minute. Then the pellet was resuspended in 500 µL SEWS-M and centrifuged for another minute at 14,000 × g. The catching tube was discarded and replaced by a new clean catching tube. After air drying the spin filter for 5 minutes the binding matrix was resuspended in 56 µL ultrapure water. To provide better binding, the matrix was incubated for 5 minutes at 55 °C. After another centrifugation step (14,000 × g, 1 minute) DNA was ready for further processing and stored at -20 °C until further use.

2.4.2 DNA extraction from pure cultures

To obtain DNA from pure cultures, respective colonies were picked using a sterile pipette tip and re-suspended in 300 µL 0.85% NaCl. For mechanical lysis suspensions were transferred in sterile Eppendorf tubes filled with glass beads. Samples were heated up to 96 °C for 3 minutes and subsequently cooled down on ice for one minute. Then cells were processed in a FastPrep FP120 instrument for 30 seconds at 6.5 m × s^{-1} twice. After a final centrifugation step (4,000 rpm, 3 minutes, 18 °C) DNA was ready for further processing and stored at -20 °C for further use.

2.4.3 Purification of the extracted DNA for further analysis

PCR products were purified using Wizard SV PCR DNA clean-up system (Promega, USA) according to manufacturer's protocol. An equal volume of membrane binding solution was

added to the PCR amplification and then transferred to the minicolumn assembly. After incubation for 1 minute the samples were centrifuged (16,000 × rcf, 1 minute) and the flowthrough was discarded. 700 µL membrane wash solution were added to the minicolumn and centrifuged for another minute at 16,000 × rcf. The flowthrough was discarded and another 500 µL membrane wash solution were added to the minicolumn and centrifuged at 16,000 × rcf for 5 minutes. After evaporation of the residual membrane wash solution (centrifugation with open lid, 12,000 × rcf, 2 minutes and subsequent incubation for 30 minutes at room temperature) 36 µL nuclease free water were added to the minicolumn. After another incubation for 15 minutes at room temperature the samples were centrifuged at 16,000 × rcf for 1 minute to obtain purified DNA for further analysis.

2.5 Determination of algae cell number

2.5.1 Drop plate technique

To determine the total algae cell number samples were diluted up to 10^{-3} with 0.85% NaCl. 10 µL of each were plated in stripes on BBM agar plates and resulting cfu × mL were determined after 7 days of incubation at 23 °C under natural light conditions (16-h-8-h light-dark cycle).

2.5.2 *Chlorella vulgaris* fluorescence intensity measurement

To determine the *C. vulgaris* cell number the algal chlorophyll a was measured using fluorometry and subsequently correlated with the respective cfu × mL^{-1}. To determine the fluorescence emission maximum of *C. vulgaris* a fluorescence intensity scan of a pure *C. vulgaris* culture was performed using an infinite M200 spectrofluorimeter (TECAN, Switzerland). *C. vulgaris* was excited at 450 nm wavelength and fluorescence emission was detected at wavelengths ranging from 580 to 760 nm.

By using the fluorescence emission maximum *C. vulgaris* cell number was correlated with the respective fluorescence intensity. Therefor a *C. vulgaris* preculture was grown in a 100 mL Erlenmayer Flask including 20 mL liquid BBM for 5 days. Subsequently the preculture was diluted with 0.85% NaCl (Table 2.4). Fluorescence intensity was measured (excitation: 450 nm; emission: 685 nm) and serial dilution of respective suspensions were plated on BBM agar. After 7 days of incubation cfu × mL^{-1} were determined.

Table 2.4: Prepared dilutions of *C. vulgaris* for correlation with the respective fluorescence intensity.

***C. vulgaris* pure culture [µL]**	**NaCl (0.85%) [µL]**	**ratio**
100	0	1:0
90	10	9:1
80	20	4:1
70	30	7:3
60	40	3:2
50	50	1:1
40	60	2:3
30	70	3:7
20	80	1:4
10	90	1:9
0	100	0:1

2.6 Growth promotion experiments

2.6.1 Novel rapid high-throughput screening for *C. vulgaris* growth-affecting microbes

In order to evaluate the potential for microalgae growth promotion or suppression a novel high-throughput screening was established. It bases on the co-cultivation of *C. vulgaris* and single bacterial strains. *C. vulgaris* growth was detected via fluorometry over time and compared with an axenic culture to identify algae growth-affecting bacteria.

2.6.1.1 Preparation of the *C. vulgaris* inoculum

C. vulgaris cultures were prepared in 300 mL Erlenmayer Flasks filled with liquid BBM and inoculated with a single *C. vulgaris* colony using an inoculation loop. Microalgae precultures were grown over night.

2.6.1.2 Design and initial approach of a novel high-throughput screening method using 24 plant biocontrol strains

The Institute for Environmental Biotechnology, Technical University of Graz, provided 24 plant biocontrol strains (Table 2.1). All strains were initially screened for potential *C. vulgaris* growth affection under sterile conditions. Screening was performed in 96 well-plates (Sarstedt, Germany) filled with 200 µL of *C. vulgaris* preculture. Microalgae were inoculated with single bacterial colonies using sterile toothpicks. Each strain was examined in eightfold replicates. An axenic *C. vulgaris* culture served as growth control. Sterile BBM served as negative control. After four days of incubation fluorescence intensity was measured (excitation: 450 nm; emission: 685 nm). Statistical analysis was performed using SPSS Statistics 23 (IBM, Austria).

2.6.1.3 Approach with the four most promising biocontrol strains

Based on the initial screening the most promising algae growth-affecting strains were selected for further studies. Screening was performed as described above. In order to confirm growth-affecting efficiency *C. vulgaris* was inoculated with *S. plymuthica* 3Re4-18, *S. rhizophila* ep17, *P. fluorescens* L13-6-12 and *Sinorhizobium* sp. W4-7 respectively, each in fourfold replicates. The cultures were incubated and fluorescence intensity was measured periodically over nine days (excitation: 450 nm; emission: 685 nm).

2.6.1.4 Identification of a positive and a negative control strain for further sample analysis

S. plymuthica 3Re4-18 negatively influenced algae growth and was therefore used as negative control in further experiments. Previous studies showed that co-cultivation with *S. rhizophila* ep17 and *Sinorhizobium* sp. W4-7 results in increased microalgae biomass formation. These strains therefore served as positive controls in further studies. For that purpose, the respective growth curves of these three strains were determined and OD_{600} was correlated with the respective cfu × mL^{-1}. 100 mL Erlenmayer Flasks were filled with 30 mL NB media and inoculated with an OD_{600} of 0.05 each. OD_{600} was measured at hourly intervals over 4 h using a BioPhotometer (Eppendorf, Germany). Serial dilutions of the cultures were then individually plated on NA and incubated over night at 30 °C to determine the respective cfu × mL^{-1}.

2.6.1.5 Optimization of the density of the bacterial inoculum

In order to evaluate the effect of differing bacterial cell numbers on *C. vulgaris* growth a defined number of algae cells were inoculated with bacterial cell suspensions of specific cell density.

The cavities of a 96 well-plate were filled with liquid BBM and inoculated with 10^4 *C. vulgaris* cells. Subsequently the microalgae were co-inoculated in triplicates with 10^3 and 10^6 cells of *S. plymuthica* 3Re4-18, *S. rhizophila* ep17 and *Sinorhizobium* sp. W4-7, respectively. An axenic *C. vulgaris* culture served as algae growth control while single bacterial cultures served as bacterial growth controls. Sterile BBM served as negative control. Fluorescence intensity was measured *in vitro* (excitation: 450 nm; emission: 685 nm) periodically over eight days and serial dilutions of respective suspensions were plated on NA and BBM agar to determine algae and bacteria cfu × mL^{-1}.

2.6.2 Identification of microalgae growth-affecting microbes from the environment

2.6.2.1 Bacterial strain library and isolation of single colonies

In order to generate strain libraries dilution series of each sample were plated on BBM, Reasoner's 2 agar (R2A) and Nutrient agar (NA) and grown overnight at 30 °C.

Single colonies were randomly selected and picked using sterile toothpicks. In total 726 bacterial strains were isolated and maintained on respective media.

2.6.2.2 A novel high-throughput screening to identify algae-growth affecting microbes

High-throughput screening was proceeded in 96-well plates filled with 290 µL liquid BBM and inoculated with 10 µL *C. vulgaris* preculture. Subsequently wells were co-inoculated with bacterial isolates in duplicates using a sterile toothpick. An axenic *C. vulgaris* culture served as growth control. Sterile BBM served as negative control. *S. plymuthica* 3Re4-18 served as negative co-cultivation control. *Sinorhizobium* sp. W4-7 served as positive co-cultivation control. High-throughput screening was conducted with all bacterial isolates from environmental sampling sites. Approaches were screened after six days of incubation *in vitro* by fluorometry technique (excitation: 450 nm; emission: 685 nm) for the presence of microalgae growth-affecting activity.

Based on the initial screening experiments were repeated with the most promising strains in 18-fold replicates. Statistical analysis was performed using SPSS Statistics 23.

2.7 Characterization of identified algae-growth affecting microbes

A total of 17 algae-associated bacterial strains were characterized phenotypically by their differing properties (Table 2.5).

Table 2.5: Further characterized algae-associated bacterial strains and their origin.

sample ID	origin
1Ab3	Triebener Tauern snowfield A
1Bg2	Triebener Tauern snowfield B
2Bb9	Drei Lacken pond B
2Ca3	Drei Lacken pond C
3Aa4	Seetaler Alpen snowfield A
3Ab1	Seetaler Alpen snowfield A
3Ac7	Seetaler Alpen snowfield A
3Ac8	Seetaler Alpen snowfield A
3Ba6	Seetaler Alpen water A
3Dc5	Seetaler Alpen snowfield B
3Ea4	Seetaler Alpen snowfield C
3Eb1	Seetaler Alpen snowfield C
A24	PBR A
C16	PBR C
G76	Graz
G97	Graz
G99	Graz

2.7.1 Screening for phosphate solubilization of algae growth-promoting strains

In order to evaluate the ability to solubilize phosphate respective bacterial colonies were transferred to National Botanical Research Institute`s phosphate growth agar (NBRIP) (Nautiyal, 1999). *Pseudomonas* sp. served as positive control. Isolates were grown for 14 days at RT and afterwards presence (phosphate solubilizing positive) or absence (phosphate

solubilizing negative) of visible halo zones at the isolates growth sites on the plates was noted.

2.7.2 Protease activity of isolated strains

To perform screening for protease activity 50 g skim milk dry powder (Bio Magermilch Pulver, Heirler Cenovis GmbH, Germany) was reconstituted with 500 mL of distilled H_2O and autoclaved at 121 °C for 7 min. Likewise 500 mL of 2.00% agar solution were sterilized. Before plating, solutions were mixed thoroughly. Bacterial isolates were streaked out and grown for 2 days at RT. Afterwards presence (protease active) or absence (no protease activity) of visible halo zones at the isolates growth sites on the plates was noted.

2.7.3 N-Acylhomoserine lactone production of algae-associated bacterial strains

Screening for AHL production was performed based on the studies of Morohoshi and colleagues (2008) and McClean and colleagues (1997). Bacteria were plated on NA plates as displayed in figure 2.5. *Chromobacterium violaceum* CV026 served as indicator strain as it is able to produce the violet pigment violacein in the presence of exogenous N-hexanoyl-L-homoserine lactone (C6-HSL). *S. plymuthica* 3Re4-18 served as positive control as it produces C6-HSL. Isolates were grown over night at RT. If present violet coloration of the indicator strain (positive AHL-production) was noted afterwards.

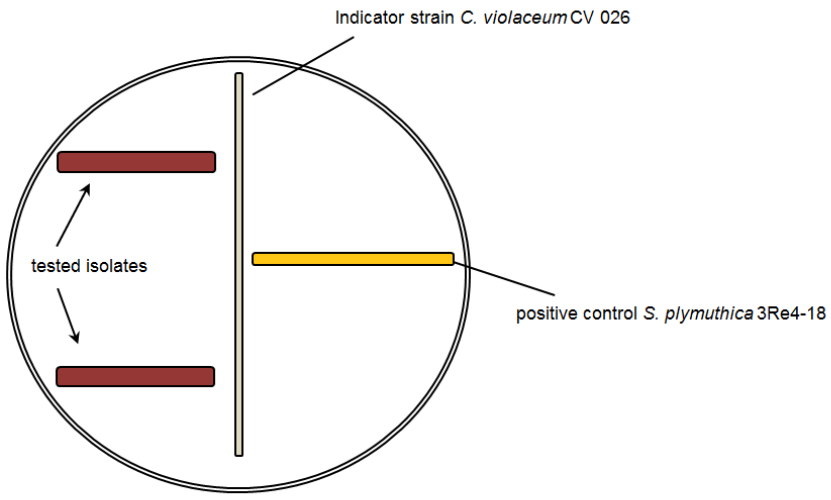

Figure 2.5: Pattern of application for AHL-producing bacterial isolates.

2.7.4 Siderophore production by bacterial isolates

Siderophore production was tested as follows: 400 mL of 1.50% agar LB (Lennox) medium (Carl Roth, Germany) medium was sterilized and mixed thoroughly with 100 mL staining solution (98 mL dH_2O; 1 mL 0.01 M $FeCl_3$; 1 mL 0.1 M HCl; 0.605 g Chrome Azurol-S (CAS); 0.073 g cetyltrimethylammonium bromide (CTAB)). After plate-pouring bacterial isolates were streaked out and incubated for 14 days at RT. Then the presence (siderophore production positive) or absence (siderophore production negative) of yellow halo zones at the isolates growth sites on the plates was noted.

2.8 Cultivation independent methods

2.8.1 Identification of microalgae growth-affecting bacteria

All 17 microalgae-associated bacterial strains (Table 2.5) were characterized genotypically by aligning PCR-amplified 16S rRNA gene sequences against the NCBI nucleotide collection database. DNA of putative pure cultures were extracted using the respective protocol. The PCR was performed by using a total volume of 30 µL containing 16.20 µL ultrapure water, 6.00 µL 5 × Tag&Go Mastermix, 1.50 µL of each primer [5 µM], 1.80 µL $MgCl_2$ [25 mM] and 3 µL template. 16S rRNA genes were amplified using the universal primer pair 27F (5‘-AGA GTT TGA TCM TGG CTC AG-3‘)/1492R (5‘- CGG TTA CCT TGT TAC GAC TT-3‘), (95 °C, 4 min; 30 cycles of 95 °C; 30 sec; 57 °C, 30 sec; 72 °C, 90 sec; final extension at 72 °C, 5 min). PCR products were purified using Wizard SV PCR product clean-up system and DNA concentration was measured using a Nanodrop UV-Vis spectrophotometer (Thermo Fisher Scientific, USA). For Sanger-Sequencing samples were pooled equimolar and processed by LGC Genomics GmbH (Berlin, Germany). 16S rRNA sequences were subsequently aligned against the NCBI nucleotide collection database using the BLAST algorithm (Altschul *et al.,* 1997).

2.8.2 Microalgal colony picking and insight into occurring algae community

In order to get an insight into the occurring microalgae community of natural habitats, single potentially microalgae colonies of environmental samples from Drei Lacken and Seetaler Alpen were picked from initially plated serial dilutions using sterile toothpicks. Colonies were streaked out and maintained on BBM agar plates in the green house. DNA from pure cultures was isolated using the respective protocol. 18S rRNA genes were amplified using the universal primer pair NS1 (5′-GTAGT CATAT GCTTG TCTC-3′)/NS8 (5′-TCCGC AGGTT CACCT ACGGA-3′) (White *et al.,* 1990), (95 °C, 4 min; 40 cycles of 94 °C, 1 min; 50 °C, 2 min; 70 °C, 3 min; final extension at 72 °C, 10 min). Subsequently PCR products were purified using the Wizard SV PCR product clean-up system and DNA concentration was measured using a Nanodrop UV-Vis spectrophotometer. For Sanger-Sequencing samples were pooled equimolar and processed by LGC Genomics GmbH. 18S rRNA sequences were subsequently aligned against the NCBI nucleotide collection database using the BLAST algorithm (Altschul *et al.,* 1997).

2.8.3 Analysis of the community structure by single-strand conformation polymorphism

In order to analyze the eukaryotic community and its co-occurring microbiome single-strand conformation polymorphism (SSCP) was performed for environmental samples of Triebener Tauern, Drei Lacken and Seetaler Alpen. Detailed information about the samples and primers are given in Tables 2.6 and 2.7.

Table 2.6: Sample overview for SSCP analysis.

sample ID	biological replicates	origin	habitat	18S rRNA SSCP	16S rRNA SSCP
1A	abcdefg	Triebener Tauern	snowfield	yes	yes
1B	abcdeg		snowfield	yes	yes
2A	ab	Drei Lacken	water	no	yes
2B	ab		water	yes	yes
2C	ab		water	no	yes
3A	abc	Seetaler Alpen	snowfield	yes	yes
3B	abcd		water	yes	yes
3C	abcd		water	yes	yes
3D	abcde		snowfield	yes	yes
3E	abc		snowfield	yes	yes

Table 2.7: Primers used for amplification of 16S rRNA genes and 18S rRNA genes for SSCP analysis.

Primer	Sequence (5‘ – 3‘)	target	references
515f 806rP	GTGYCAGCMGCCGCGGTAA GGACTACHVGGGTWTCTAAT	16S rRNA	Caporaso *et al.,* 2012
1391f EukBrP	AATGATACGGCGACCACCGAGATCTACAC CAAGCAGAAGACGGCATACGAGAT	18S rRNA (V9)	Amaral *et al.,* 2009 Caporaso *et al.,* 2012 Vestheim *et al.,* 2008

2.8.3.1 Amplification of marker gene fragments for SSCP analysis

Community pattern analysis was proceeded by using two complementary approaches. For SSCP analysis 18S rRNA genes and 16S rRNA genes were amplified using specific primers.

DNA was extracted using the FastDNA SPIN Kit for soil. For amplification of the bacterial rRNA gene sequence, universal primers 515f and 806rP were used (Caporaso *et al*., 2012).

The PCR was performed by using a total volume of 60 µL containing 36.3 µL ultrapure water, 12 µL 5 × Taq&Go ready-to-use Mastermix (MP Biomedicals, USA), 2.4 µL of each primer (10 µM), 0.45 µL pPNA [100 µM], 0.45 µLmPNA [100 µM] (Lundberg et al., 2013) and 6 µL template (96 °C, 5 min; 30 ccycles of 96 °C, 1 min; 78 °C, 5 sec; 54 °C, 1 min; 74 °C, 1 min; final extension at 74 °C, 10 min).

For amplifying the 18S rRNA gene sequence of the eukaryotic community, the primers 1391f and EukBrP covering the variable region 9 (V9), were used (Amaral *et al*., 2009; Caporaso *et al.*, 2012; Vestheim *et al.,* 2008). The PCR was performed using a total volume of 60 µL containing 40.8 µL ultrapure water, 12 µL 5 × Taq&Go Mastermix, 0.6 µL of each primer [10 µM] and 6 µL template (98 °C, 5 min; 10 cycles of 98 °C, 10 sec; 53 °C, 10 sec; 72 °C, 30 sex; 20 cycles of 98 °C, 10 sec; 48 °C, 30 sec; 72 °C, 30 sec; final extension at 72 °C, 10 min).

2.8.3.2 SSCP analysis of eukaryotic and bacterial communities

PCR products were purified by the Wizard SV PCR clean-up system before a λ-exonuclease digestion and DNA single-strand folding according to Schwieger and Tebbe (1998) were performed. 12 µL of each DNA product, amplified with 515f/806rP and 1391f/EukBrP and in case of 18S rRNA SSCP analysis additionally 6 µL of *C. vulgaris* and *H. pluvialis* pure DNA extract were applied on the gel. The polyacrylamide gel electrophoresis was proceeded on a TGGE apparatus (Biometra, Germany). 16S rRNA genes were analyzed on an 8% (wt vol^{-1}) acrylamide gel that run at 26 °C and 400 V for 26 h. 18S rRNA genes were analyzed on a 9.5% (wt vol^{-1}) acrylamide gel at 26 °C and 400 V run for 15 h. The procedure of SSCP analysis was performed according to Schwieger and Tebbe (1998). Afterwards the gels were silver-stained according to Bassam et al. (1991).

2.8.3.3 Identification of SSCP bands and GelComparII analysis

Computer-assisted evaluation of bacterial and eukaryotic communities obtained by SSCP was performed using the GelComparII software (Applied Math, Belgium). The silver-stained SSCP gels were scanned using a transmitted light scanner (Epson perfection 4990 Photo, Japan) to obtain digitalized gel images. After normalizing the gels and subtraction of the background, cluster analysis was performed using „Dice“ as similarity coefficient.

A total of 21 selected bands from the 18S rRNA fingerprint profiles were excised using a sterile scalpel and subsequently eluted by suspending the gel slice in 150 µL elution buffer

containing 0.5 M ammonium acetate, 10 mM magnesium acetate tetrahydrate, 1 mM EDTA (pH 8.0) and 0.1% (wt vol^{-1}) SDS for 5 days at 4 °C. DNA extraction was performed using ethanol precipitation, centrifugation and resuspension in 10 mM Tris-HCl (pH 8.0). The gel-extracted DNA was reamplified and PCR products were purified using the Wizard SV PCR product clean-up system. DNA concentration was measured by using a Nanodrop UV-Vis spectrophotometer. For Sanger-Sequencing samples were pooled equimolar and processed by LGC Genomics GmbH. 18S rRNA sequences were subsequently aligned against the NCBI nucleotide collection database using the BLAST algorithm (Altschul *et al.,* 1997).

2.8.4 Illumina MiSeq/HiSeq sequencing of 16S rRNA gene and 18S rRNA gene region amplicons

The 16S rRNA gene sequences and 18S rRNA gene sequences were each amplified doing three technical replicates. The products of three independent PCR reactions with two different primer pairs were pooled and purified using the Wizard SV PCR clean-up system. Detailed overview of samples used for amplification analysis is provided in Table 2.8. Primers used in this study are provided in Table 2.9. Detailed information about the primer constructs can be found in the appendix 7.6; Table 7.20.

Table 2.8: Sample overview of amplicon analysis.

Sample ID	biological replicates	origin	habitat
1A	abcdefg	Triebener Tauern	snowfield
1B	abcdeg		snowfield
2A	ab	Drei Lacken	water
2B	ab		water
2C	ab		water
3A	abc	Seetaler Alpen	snowfield
3B	abcd		water
3C	abcd		water
3D	abcde		snowfield
3E	abc		snowfield
G	123	Graz	dried puddle
P	123456	Ennstal	dried puddle

Table 2.9: Primers used for amplification of 16S rRNA genes and 18S rRNA genes for Illumina sequencing.

Primer	Sequence (5‘ – 3‘)	target	references
515f 806r	GTGYCAGCMGCCGCGGTAA GGACTACHVGGGTWTCTAAT	16S rRNA	Caporaso *et al.,* 2012
golay_1391f golay_EukBr	ATGGTAATTGTGTACACACCGCC AGTCAGCCAGGGTGATCCTTCTGCAGGTTCA CCTAC	18S rRNA (V9)	Amaral *et al.,* 2009 Caporaso *et al.,* 2012 Vestheim *et al.,* 2008

2.8.4.1 Amplification of 16S rRNA gene fragments for Illumina Sequencing

The 16S rRNA fragments in the different environmental samples were amplified for Illumina sequencing using eubacterial barcoded primers 515f and 806r (Caporaso *et al.,* 2012). The

eight, nine and ten, respectively, base long barcode sequences are part of the primer. PNA was added to the PCR mix to prevent the amplification of unwanted sequences such as mitochondrial (mPNA) or plastidal (pPNA) RNA from eukaryotes (Lundberg *et al.,* 2013). The PCR was performed by using a total volume of 30 µL containing 20.15 µL ultrapure water, 6.00 µL 5 × Tag&Go Mastermix, 1.20 µL of each primer [5 µM], 0.225 µL pPNA [100 µM], 0.225 µL mPNA [100 µM] and 1 µL template. The cycling program was adjusted to an initial denaturation at 96 °C for 5 min, followed by 30 cycles of 96 °C for 1 min, 78 °C for 5 sec, 54 °C for 1 min and 74 °C for 1 min. Final extension was done at 74 °C for 10 min.

2.8.4.2 Amplification of 18S rRNA gene fragments for Illumina Sequencing

18S rRNA gene fragments of eukaryotic compartments were amplified using universal eukaryotic primers golay_1391f_pad and golay_EukBr_primer_pad (Vestheim *et al.,* 2008; Caporaso *et al.,* 2012; Amaral *et al.,* 2009). The PCR was performed by using a total volume of 20 µL containing 14.60 µL ultrapure water, 4.00 µL × 5 Taq& Go Mastermix, 0.20 µL of each primer [10 µM] and 1 µL template (98 °C, 5 min; 10 cycles of 98 °C, 10 sec; 53 °C, 10 sec; 72 °C, 30 sec; 20 cycles of 98 °C, 10 sec; 48 °C, 30 sec; 72 °C, 30 sec; and final extension at 72 °C for 10 min). To apply the barcodes for sequencing an additional PCR was performed. Each PCR-product served as template for a PCR reaction containing 20.60 µL ultrapure water, 6 µL × 5 Taq&Go Mastermix, 1.20 µL of each barcode-primer [10 µM] and 1 µL template (95 °C, 5 min; 10 cycles of 95 °C, 30 sec; 56 °C, 30 sec; 72 °C, 30 sec; and final extension at 72 °C for 10 min).

2.8.4.3 Bioinformatics and statistical analysis

Joining forward and reverse read pairs was done using software package QIIME 1.9.1. (Caporaso *et al.,* 2010). After removing barcodes, primer and adapter sequences reads as well as metadata were imported to QIIME 2 (2017.12 release). The DADA2 algorithm (Callahan *et al.,* 2016) was used to demultiplex, denoise and truncate reads in order to generate ribosomal sequence variants (RSVs), which were then summarized in a feature table. Chimeras were identified by using the VSEARCH uchime_denovo method (Rognes *et al.,* 2016) and subsequently removed. Phylogenetic metrics were constructed by aligning representative sequences using the mafft program. After the multiple sequence alignment was masked and filtered a phylogenetic tree was generated with FastTree.

The prokaryotic taxonomic analysis was based on a customized naïve-bayes classifier trained on 16S rRNA gene OTUs clustered at 99% similarities with the SILVA128 database release

and trimmed to a length of 400 bp. Features assigned to mitochondria and chloroplasts were removed from the table. The dataset was normalized to 64,000 reads per sample to account a variation in the samples. Normalized feature tables served as input for following alpha and beta diversity analyses using QIIME 2 core diversity metrics. Principal Coordinate Analysis (PCoA) plots were constructed by calculating the unweighted UniFrac distance matrix (Lozupone *et al.,* 2007).

The eukaryotic taxonomic analysis was based on a customized naïve-bayes classifier trained on 18S rRNA gene OTUs clustered at 99% similarities with the SILVA128 database release and trimmed to a length of 200 bp. The dataset was normalized to 11,000 reads per sample to account a variation in the samples. Feature table was reduced by retaining only features with an absolute abundance of more than 100 overall samples.

III. Results

3.1 Optimized quantification of the microalgae cells

3.1.1 Determination of the fluorescence emission maximum for *Chlorella vulgaris*

In order to determine the microalgae cell number the fluorescence intensity of an algae culture was correlated with the respective cfu × mL^{-1} determined with classic plate tests. Therefore, the *C. vulgaris* fluorescence emission maximum was determined. The fluorescence intensity scan showed an emission maximum at 685 nm (Figure 3.1).

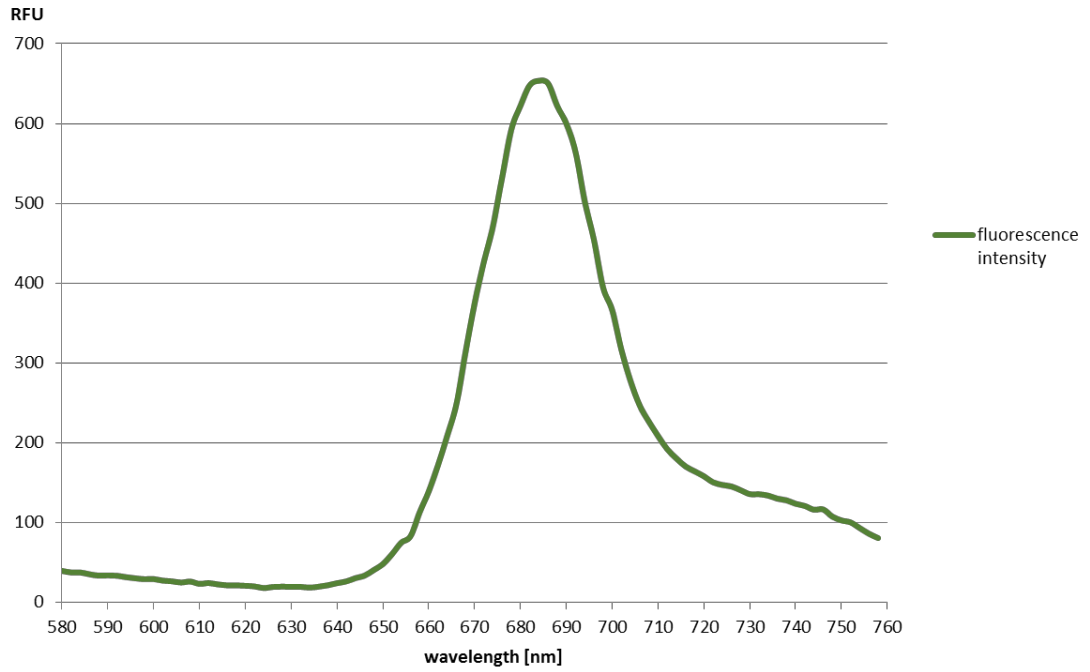

Figure 3.1: *C. vulgaris* fluorescence intensity scan. Microalgae were excited with 450 nm. The microalgae showed an emission maximum at 685 nm. RFU = relative fluorescence units.

3.1.2 Fluorescence intensity-based analysis of microalgae cultures allows a fast quantification of cell numbers

Correlating the fluorescence intensity of the *C. vulgaris* dilution series with the respective cfu × mL^{-1} enabled the determination of microalgae cell number (Figure 3.2). The resulting equation was used for further cell count determination (Figure 3.3).

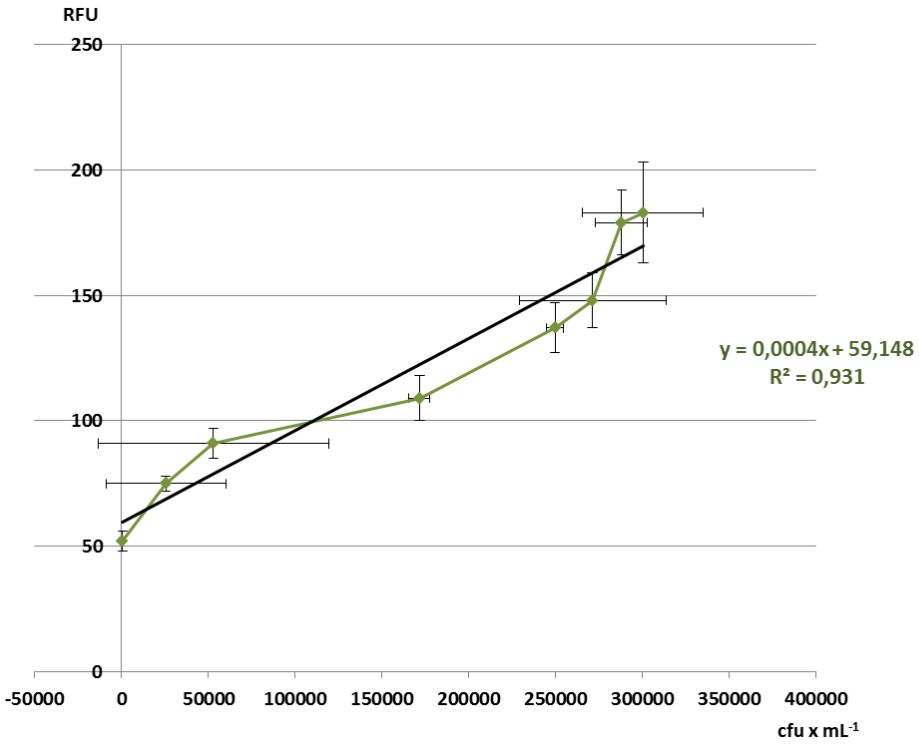

Figure 3.2: Correlation of the *C. vulgaris* fluorescence intensity with the respective cfu × mL^{-1}. RFU = relative fluorescence units.

$$\mathbf{y = 0.0004 \times x + 59.148}$$

$$\mathbf{cfu \times mL^{-1} = \frac{RFU - 59.148}{0.0004}}$$

Figure 3.3: Equation to determine microalgae cell number. y = relative fluorescence intensity; RFU = relative fluorescence units; x = cfu × mL^{-1}.

3.2 Different plant biocontrol strains were identified as microalgae growth-affecting microbes

The individual co-cultivation of *C. vulgaris* with confirmed plant biocontrol agents (BCAs) resulted in varying fluorescence intensity compared to the axenic *C. vulgaris* culture (Figure 3.4).

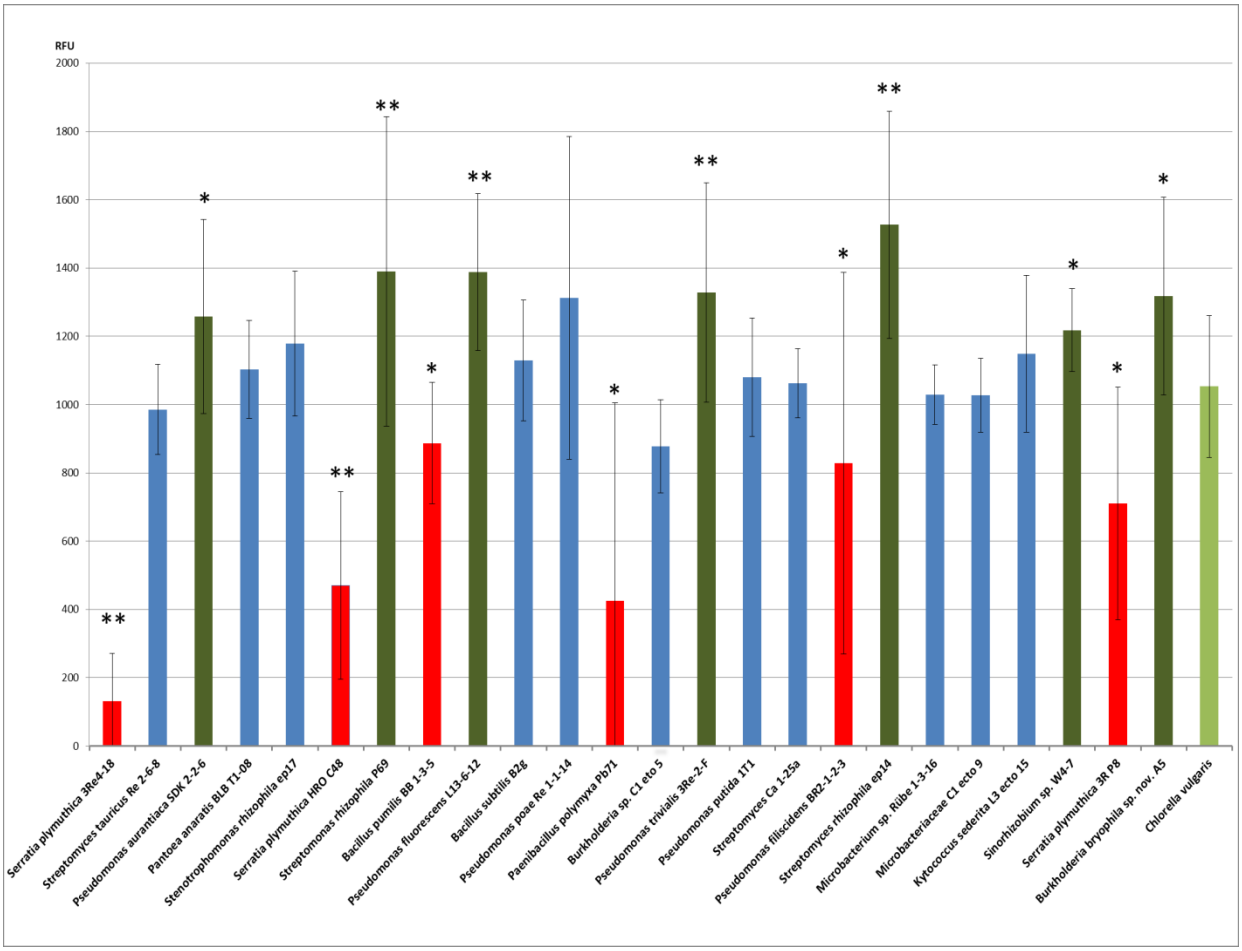

Figure 3.4: *C. vulgaris* cultures co-cultivated with different plant biocontrol strains. An axenic *C. vulgaris* culture served as growth control (light green). Blue colored bars indicate no significant differences in microalgae growth compared to the axenic culture. Red colored bars indicate lower fluorescence intensity than the growth control. Enhanced fluorescence intensity was observed for co-cultivation with biocontrol strains highlighted in dark green. RFU = relative fluorescence units. Statistical significance was determined as follows: p-value < 0.05 = * ; p-value < 0.01 = **.

Through the resulting fluorescence intensity the algae cell number was determined and growth-promoting, growth-suppressing and no growth-affecting bacteria were detected (Table 3.1).

Table 3.1: Results of the microalgae co-cultivation with different BCA. Seven strains showed a growth-promoting effect on *C. vulgaris*, six strains suppressed the algae growth and eleven strains did not affect the microalgae growth.

Growth-promoting BCA		**No algae growth affection**		**Growth-suppressing BCA**	
co-cultivated bacterium	**algae cell number [cfu × mL^{-1}]**	**co-cultivated bacterium**	**algae cell number [cfu × mL^{-1}]**	**co-cultivated bacterium**	**algae cell number [cfu × mL^{-1}]**
Pseudomonas aurantiaca SDK 2-2-6	3.00 × 10^6	*Streptomyces tauricus* RE2-6-8	2.32 × 10^6	*Serratia plymuthica* 3Re4-18	1.78 × 10^5
Stenotrophomonas rhizophila P69	3.33 × 10^6	*Pantoea ananatis* BLBT 1-08	2.61 × 10^6	*Serratia plymuthica* HRO C48	1.03 × 10^6
Pseudomonas fluorescens L13-6-12	3.32 × 10^6	*Stenotrophomonas rhizophila* ep17	2.80 × 10^6	*Bacillus pumilis* BB-1-3-5	2.07 × 10^6
Pseudomonas trivialis 3Re-2-7	3.17 × 10^6	*Bacillus subtilis* B2g	2.68 × 10^6	*Paenibacillus polymyxa* Pb71	9.13 × 10^5
Streptomyces rhizophila ep14	3.67 × 10^6	*Pseudomonas poae* Re × -1-1-14	3.13 × 10^6	*Pseudomonas filiscidens* B2R2-1-2-3	1.92 × 10^6
Sinorhizobium sp. W4-7	2.90 × 10^6	*Burkholderia* sp. C1 ecto 15	2.05 × 10^6	*Serratia plymuthica* 3RP8	1.63 × 10^6
Burkholderia bryophila sp. Nov. A5	3.14 × 10^6	*Pseudomonas putida* 1T1	2.55 × 10^6		
		Streptomyces Ca 1-25a	2.51 × 10^6		
		Micorbacterium sp. Rübe 1-3-26	2.42 × 10^6		
		Microbacteriaceae C1 ecto 9	2.42 × 10^6		
		Kytococcus sedentarius L3 ecto 15	2.73 × 10^6		
axenic *C. vulgaris* cell number [cfu × mL^{-1}]			2.48 × 10^6		

3.2.1 Preliminary results concerning promising beneficial BCAwere dismissed

To confirm the assumed microalgae growth affection the experiment was repeated with the four most promising BCA. The results of the fluorescence intensity measurement can be seen in Figure 3.5. According to the resulting fluorescence intensity *S. plymuthica* 3Re4-18 suppressed *C. vulgaris* growth significantly. *S. rhizophila* ep17, *P. fluorescens* L13-6-12 and *Sinorhizobium sp.* W4-7 did not show a significant effect on microalgae growth.

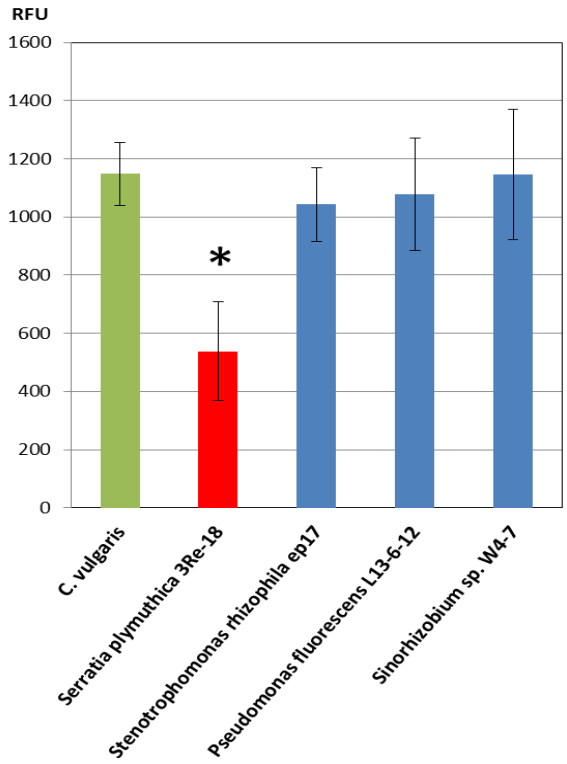

Figure 3.5: *C. vulgaris* cultures co-cultivated with the four most promising growth-affecting biocontrol strains. An axenic *C. vulgaris* culture served as growth control (light green). Blue colored bars indicate no significant differences in microalgae growth compared to the axenic culture. *S. plymuthica* 3Re4-18 showed significantly lower fluorescence intensity than the growth control. Compared to the axenic culture there was no enhanced fluorescence intensity observed. RFU = relative fluorescence units. Statistical significance was determined as follows: p-value < 0.05 = * ; p-value < 0.01 = **.

With the resulting fluorescence intensity the algae cell number was determined and *S. plymuthica* 3Re4-18 was identified as *C. vulgaris* growth-suppressing bacterium (Table 3.2).

Table 3.2: Results of the microalgae co-cultivation with four BCA. Regarding the calculated microalgae cell number *S. plymuthica* 3Re4-18 suppressed the algae growth while *S. rhizophila* ep17, *P. fluorescens* L13-6-12 and *Sinorhizobium sp.* W4-7 did not affect the microalgae growth.

No algae growth affection		**Growth-suppressing BCS**	
co-cultivated bacterium	**algae cell number [cfu × mL^{-1}]**	**co-cultivated bacterium**	**algae cell number [cfu × mL^{-1}]**
Pseudomonas fluorescens L13-6-12	2.55×10^6	*Serratia plymuthica* 3Re4-18	1.20×10^6
Sinorhizobium sp. W4-7	2.71×10^6		
Stenotrophomonas rhizophila ep17	2.46×10^6		
axenic *C. vulgaris* cell number [cfu × mL^{-1}]		2.72×10^6	

3.2.2 The growth of *C. vulgaris* is affected by the cell density of the bacterial inoculum

In order to examine the impact of the initial bacterial cell count during microalgae co-cultivation, *C. vulgaris* was inoculated with a defined number of bacterial cells. Therefore the bacterial OD_{600} was correlated with the respective cfu × mL^{-1} and the resulting equation was used for a defined co-inoculation (Figure 3.6).

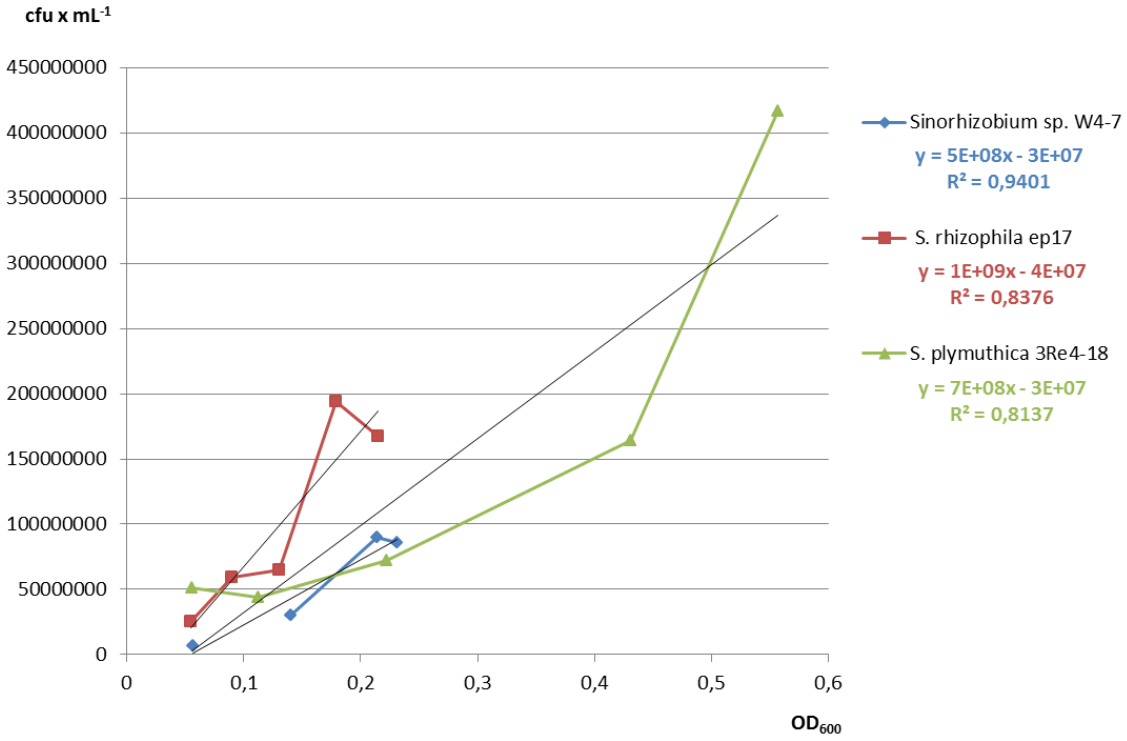

Figure 3.6: Correlated OD_{600} with the respective cfu × mL^{-1} from BCA *Sinorhizobium* sp. W4-7, *S. rhizophila* ep17 and *S. plymuthica* 3Re4-18.

The final fluorescence intensity indicated that *S. plymuthica* 3Re4-18 suppressed microalgae growth when co-cultivated with 10^6 bacterial cells, while co-cultivation with 10^3 bacterial cells did not affect algae growth significantly. Co-cultivation with *S. rhizophila* ep17 resulted in contrary output. When co-cultivated with a low bacterial cell number (10^3 cfu × mL^{-1}) *S. rhizophila* ep17 suppressed *C. vulgaris* growth, while co-cultivation with a higher bacterial cell number (10^6 cfu × mL^{-1}) resulted in growth promotion. In case of *Sinorhizobium* sp. W4-7 both approaches (co-cultivation with 10^3 and 10^6 bacterial cells) resulted in enhanced *C. vulgaris* fluorescence intensity (Figure 3.7).

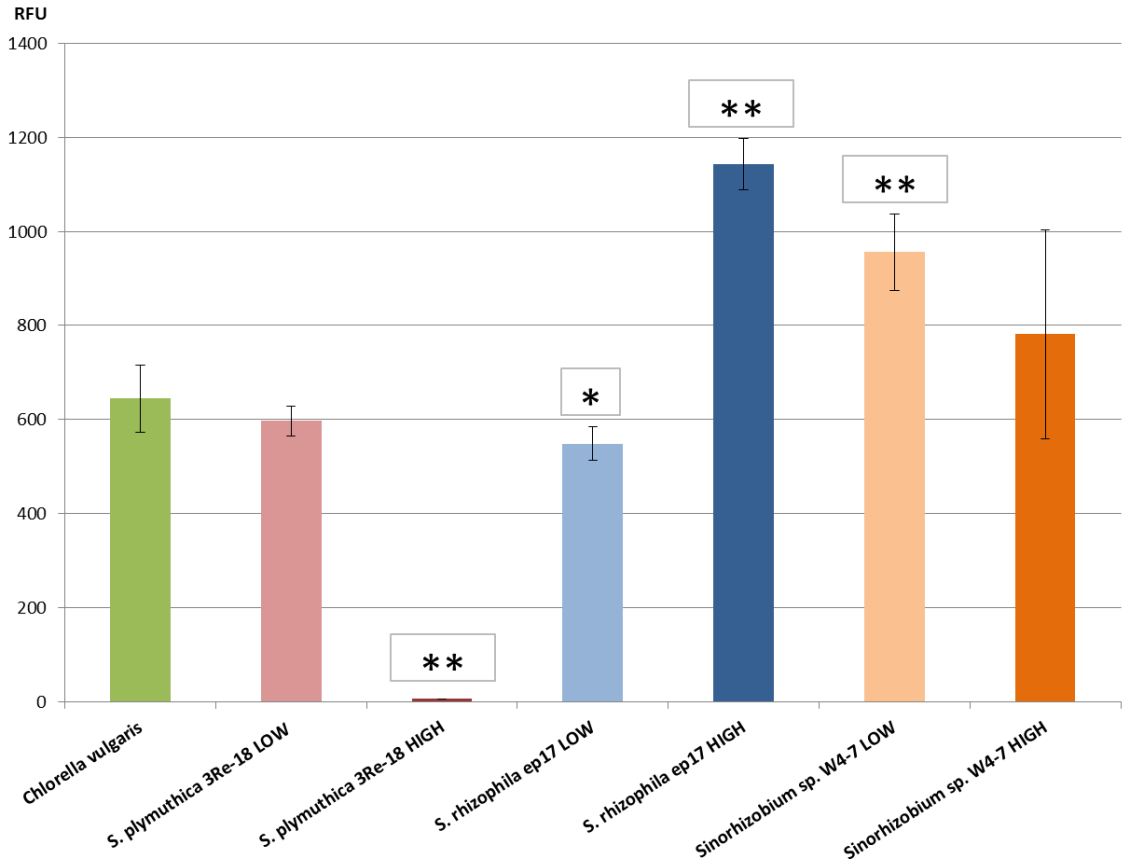

Figure 3.7: Final fluorescence intensity measurement of *C. vulgaris* after eight days of co-cultivation with a defined bacterial cell numbers. LOW = co-inoculation with 10^3 bacterial cells; HIGH = co-inoculation with 10^6 bacterial cells. According to the fluorescence intensity *S. plymuthica* 3Re4-18 suppressed *C. vulgaris* growth, *S. rhizophila* ep17 shows contrary results and *Sinorhizobium* sp. W4-7 promoted microalgae growth. RFU = relative fluorescence units. Statistical significance was determined as follows: p-value < 0.05 = * ; p-value < 0.01 = **.

S. plymuthica 3Re4-18 can be suggested as *C. vulgaris* growth-suppressing strain, while *Sinorhizobium* sp. W4-7 is a *C. vulgaris* growth-promoting bacterial strain. There was not enough data to perform a *S. rhizophila* ep17 growth curve (Figures 3.8; 3.9).

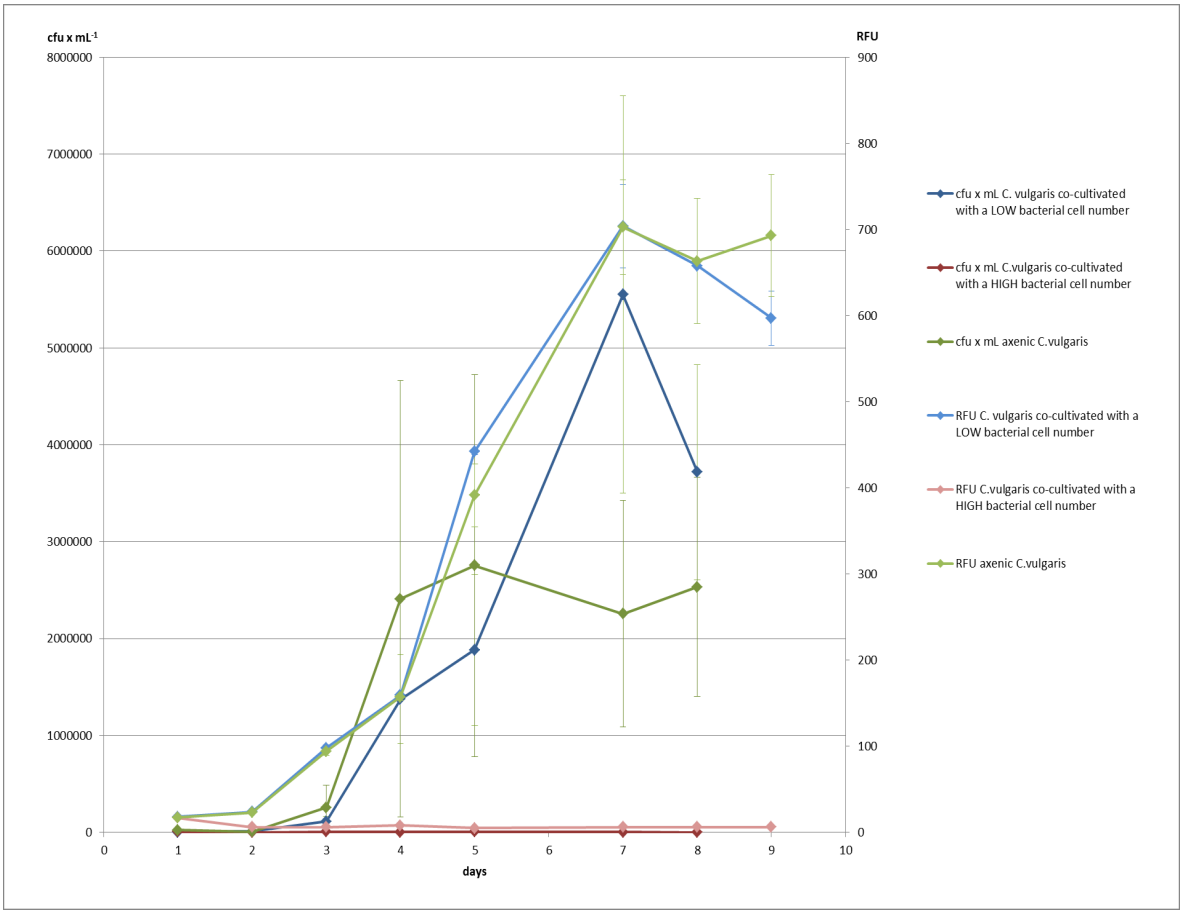

Figure 3.8: Growth curves of *C. vulgaris* when co-cultivated with a LOW (10^3) and a HIGH (10^6) number of *S. plymuthica* 3Re4-18 cells. Co-inoculation with the low bacterial cell number did not affect microalgae growth significantly when compared to the axenic control. The growth of *C. vulgaris* was completely suppressed when co-inoculated with the high bacterial cell number. RFU = relative fluorescence units.

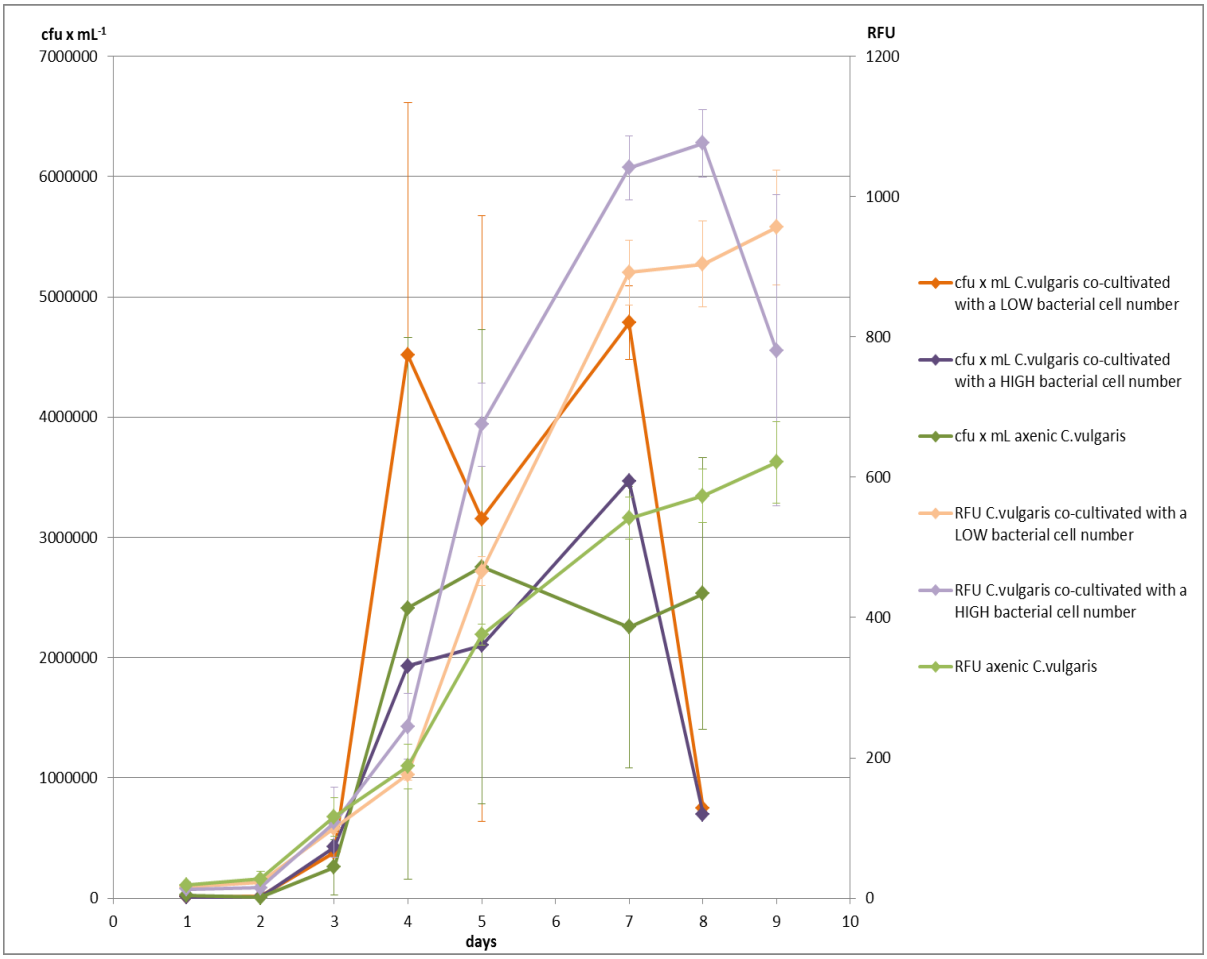

Figure 3.9: Growth curves of *C. vulgaris* when co-cultivated with a LOW (10^3) and a HIGH (10^6) number of *Sinorhizobium* sp. W4-7 cells. Co-inoculation with the low bacterial cell number promoted the microalgae growth significantly when compared with the axenic control. The growth of *C. vulgaris* was not significantly affected when co-inoculated with the high bacterial cell number.

Based on this results *S. plymuthica* 3Re4-18 was chosen as negative co-cultivation control and *Sinorhizobium* sp. W4-7 served as positive co-cultivation control in further growth affection experiments.

3.3 High-throughput screening revealed 106 potential microalgae growth affecting bacterial strains

In a high-throughput prescreening microalgae were co-cultivated in duplicates with unknown bacterial strains from the strain library. Bacteria indicating growth-promotion were further analyzed by repeating the experiment in 18-fold replicates. 726 strains were tested whereby 106 showed potential growth promoting properties.

3.3.1 Further screening with a high replicate number revealed 17 microalgae growth-promoting strains

Based on the initial screening results the most promising bacterial strains were further analyzed in a screening approach including 18-fold replicates. The results can be seen in figures 3.10, 3.11, 3.12 and 3.13. Final fluorescence intensity of co-cultivation approaches was compared with the axenic *C. vulgaris* culture.

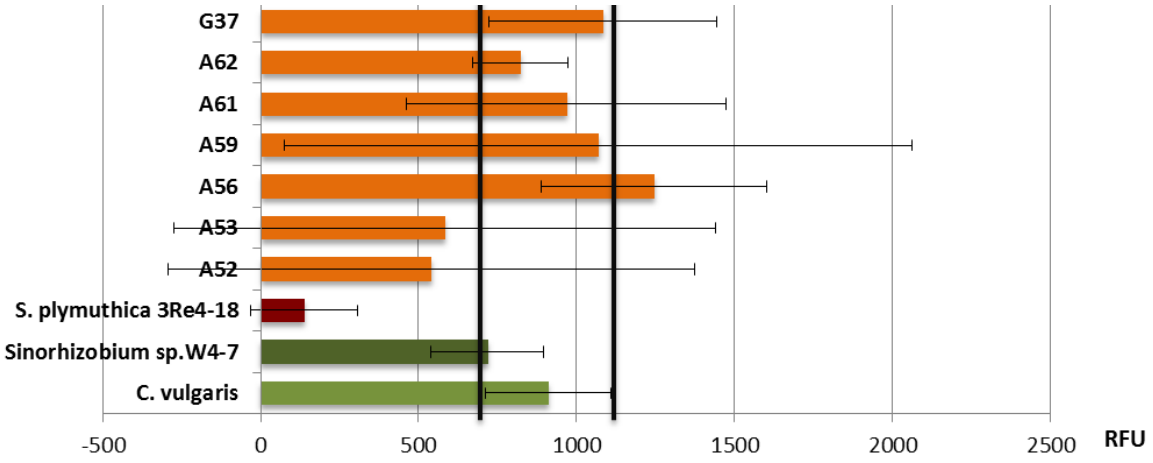

Figure 3.10: Final fluorescence intensity of further growth affection analysis. An axenic *C. vulgaris* culture served as microalgae growth control (light green); *Sinorhizobium* sp. W4-7 served as positive co-cultivation control (dark green); *S. plymuthica* 3Re4-18 served as negative co-cultivation control (red). Unknown bacterial isolates (orange) were picked from PBR A (A) and the suburban region of Graz (G). None of the strains showed significant growth affection on C. vulgaris. RFU = relative fluorescence unit.

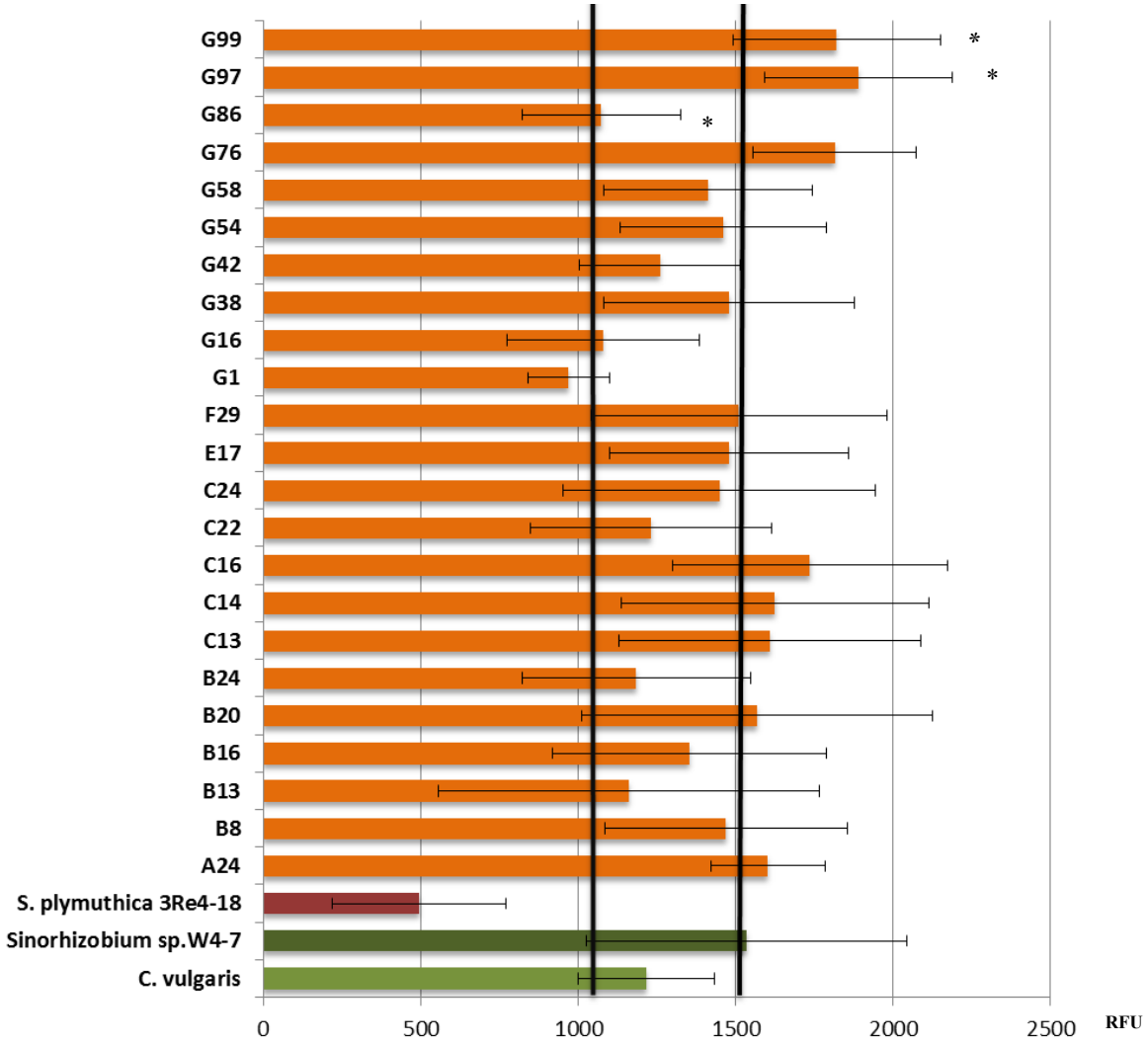

Figure 3.11: Final fluorescence intensity of further growth affection analysis. An axenic *C. vulgaris* culture served as microalgae growth control (light green); *Sinorhizobium* sp. W4-7 served as positive co-cultivation control (dark green); *S. plymuthica* 3Re4-18 served as negative co-cultivation control (red). Unknown bacterial isolates (orange) were picked from PBR A (A), PBR B (B), PBR C (C), PBR E (E), PBR F (F) and the suburban region of Graz (G). Bacterial strains G99, G97, G76 fulfilled the requirements for a growth-promoting microbe. RFU = relative fluorescence unit. Statistical significance was determined as follows: p-value < 0.05 = * ; p-value < 0.01 = **.

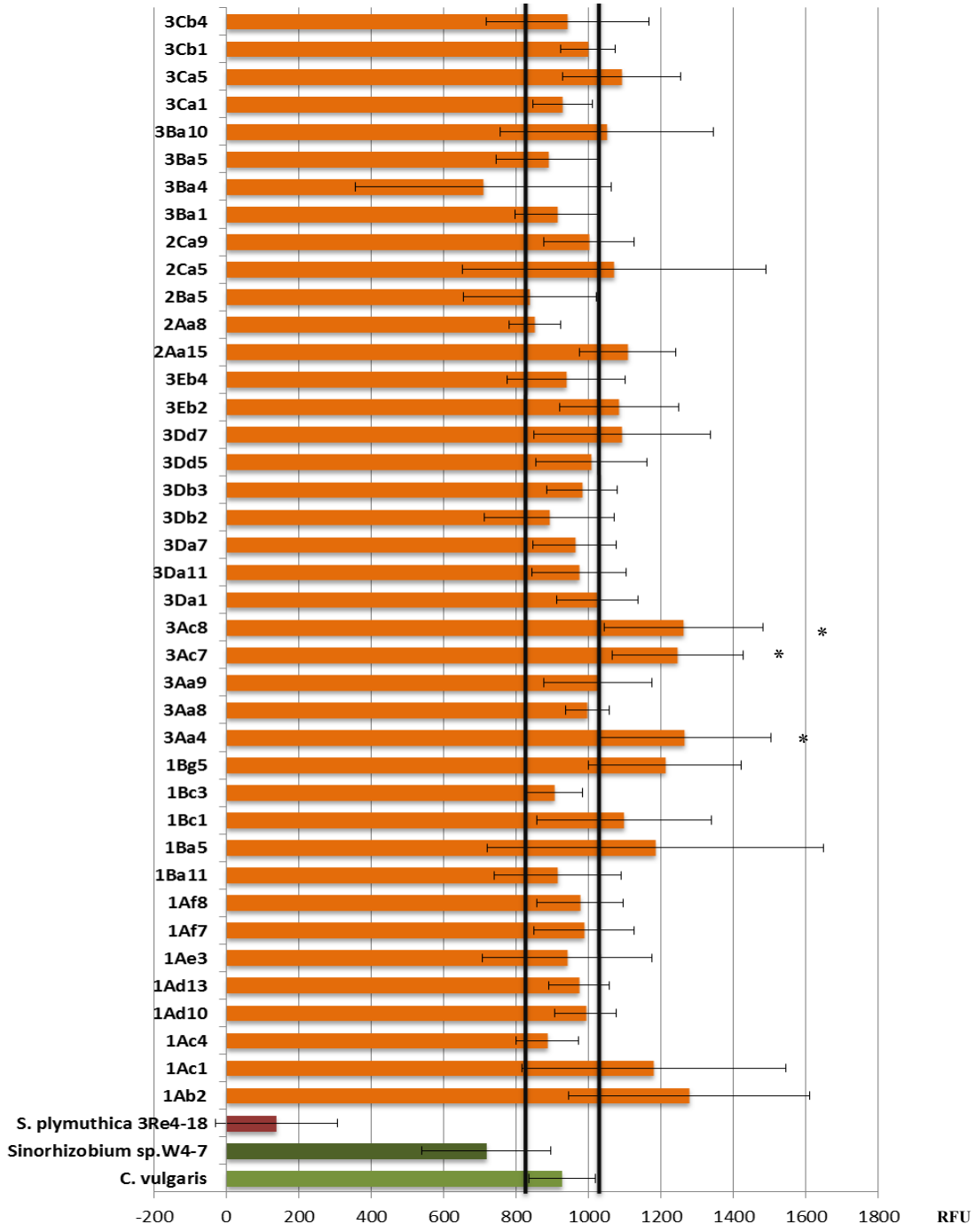

Figure 3.12: Fluorescence intensity of growth affection analysis. An axenic *C. vulgaris* culture served as microalgae growth control (light green); *Sinorhizobium* sp. W4-7 served as positive co-cultivation control (dark green); *S. plymuthica* 3Re4-18 served as negative co-cultivation control (red). Unknown bacterial isolates (orange) were picked from Triebener Tauern (1), Drei Lacken (2) and Seetaler Alpen (3). Bacterial strains 3Ac8, 3Ac7 and 3Aa4 fulfilled the requirements for a growth-promoting microbe. RFU = relative fluorescence unit. Statistical significance was determined as follows: *p*-value < 0.05 = * ; *p*-value < 0.01 = **.

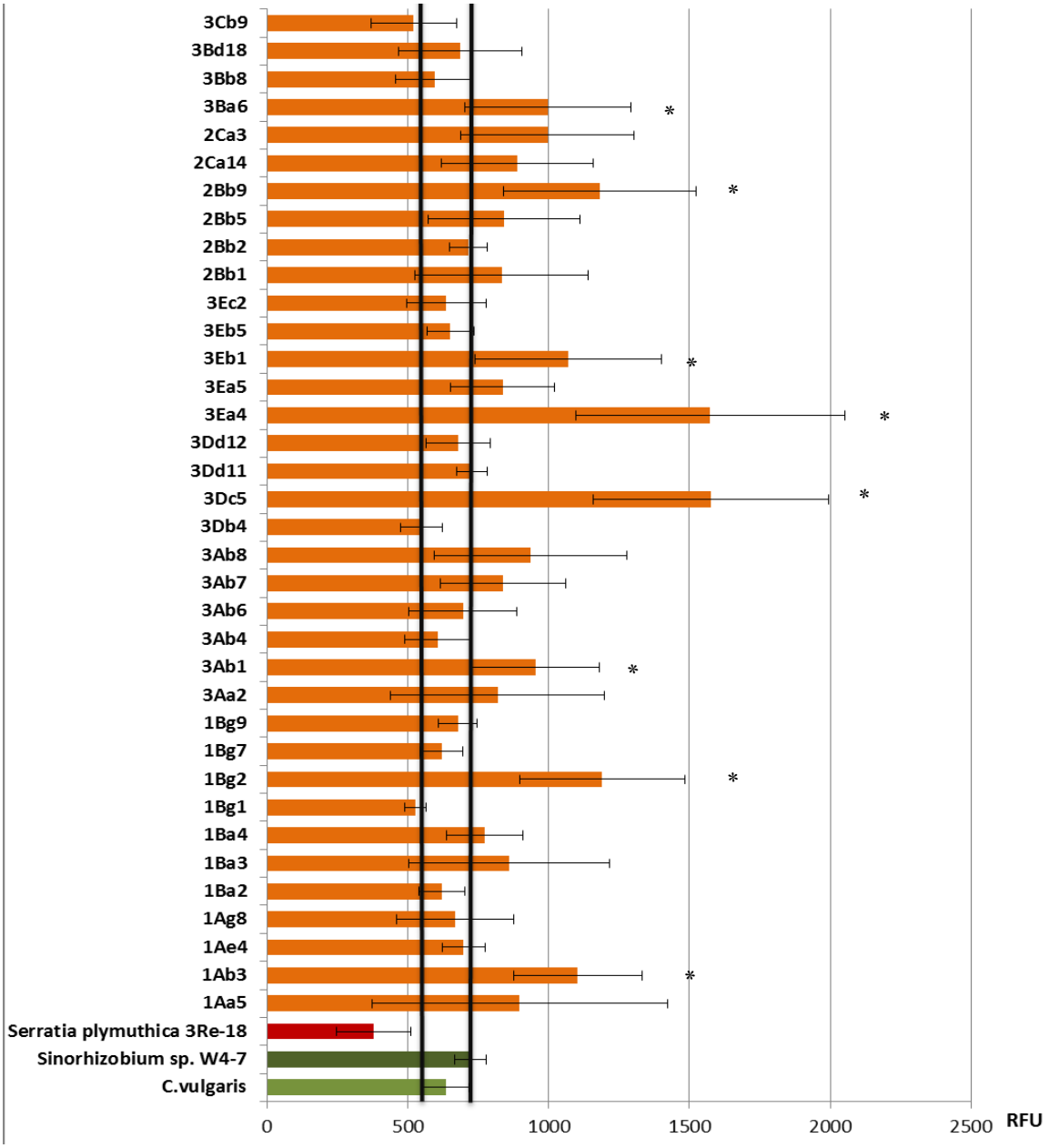

Figure 3.13: Fluorescence intensity of growth affection analysis. An axenic *C. vulgaris* culture served as microalgae growth control (light green); *Sinorhizobium* sp. W4-7 served as positive co-cultivation control (dark green); *S. plymuthica* 3Re4-18 served as negative co-cultivation control (red). Unknown bacterial isolates (orange) were picked from Triebener Tauern (1), Drei Lacken (2) and Seetaler Alpen (3). Bacterial strains 3Ba6, 2Bb9, 3Eb1, 3Ea4, 3Dc5, 3Ab1, 1Bg2 and 1Ab3 significantly fulfilled the requirements for a growth-promoting microbe. RFU = relative fluorescence unit. Statistical significance was determined as follows: p-value < 0.05 = * ; p-value < 0.01 = **.

Additionally to these 14 microalgae growth promoting microbes, the unknown bacterial strains 2Ca3, A24 and C16 were chosen for further analysis.

3.4 Characterization of growth-promoting microbes revealed various properties

3.4.1 Growing on NBRIP media disclosed three phosphate solubilizer

The ability to solubilize phosphate was uncovered by growing the isolated strains on NBRIP media. After the incubation period clear halos at the bacterial growth sites were noted for isolate 2Ca3, 1Ab3 and 3Ba6 (Figure 3.14) indicating the ability to solubilize phosphate.

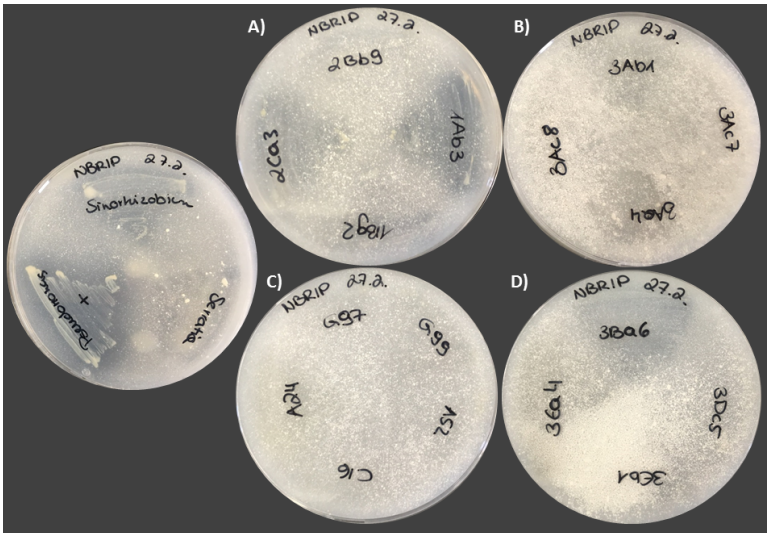

Figure 3.14: *C. vulgaris* growth-promoting strains on NBRIP media after 14 days of incubation at RT. Strains 2Ca3, 1Ab3 (plate A) and 3Ba6 (plate D) show clear halos around their growth sites.

3.4.2 A high proportion of beneficial strains displayed protease activity on skim milk agar

Protease activity of the unknown bacterial strains was determined by growing them on skim milk agar. 13 out of 17 isolates showed visible halos at their growth sites after incubation (Figure 3.15).

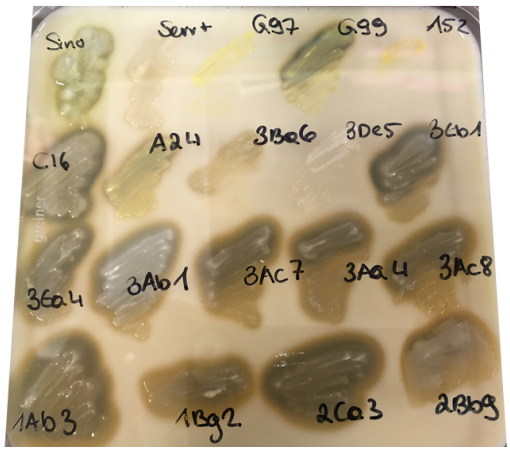

Figure 3.15: Results of the screening for protease activity. Bacterial strains G99, C16, 3Eb1, 3Ea4, 3Ab1, 3Ac7, 3Aa4, 3Ac8, 1Ab3, 1Bg2, 2Ca3 and 2Bb9 showed visible halos on the skim milk plate after two days of incubation.

3.4.3 A low proportion of producers of N-Acylhomoserine lactone was identified

The screening for AHL production discovered microalgae growth-promoting strains 2Bb9 and 2Ca3 as AHL producers (Figure 3.16).

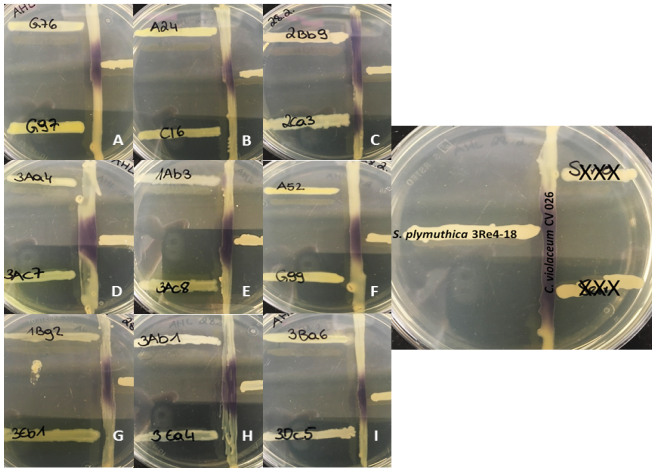

Figure 3.16: Results of the screening for AHL producers. *C. violaceum* 026 turned violet in the presence of strains 2Bb9 and 2Ca3 (plate C).

3.4.4 Siderophore production was prevalent among the tested strains

Nine siderophore producers were identified through the use of respective siderophore agar (Figure 3.17). Microbes 3Ac8, 1Ab3, 3Ac7, 3Aa4, 2Ca3, 3Ea4, 3Ab1 and 1Bg2 formed yellow halos at their growth sites. These indicate for siderophore production.

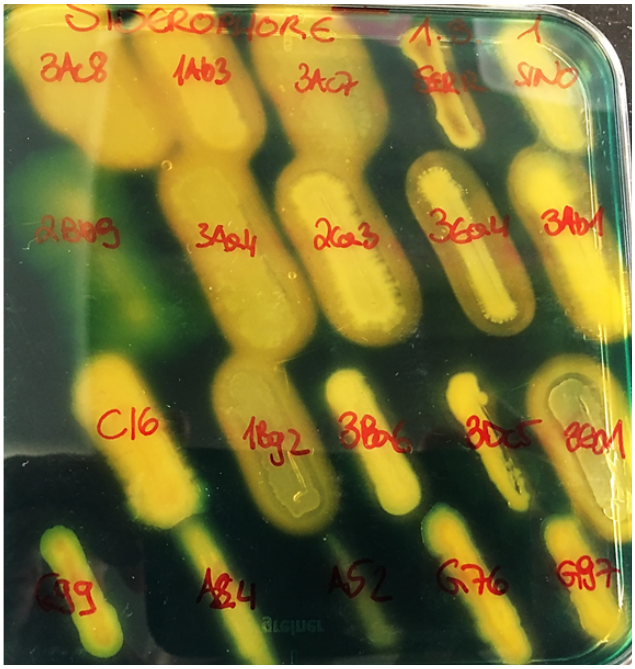

Figure 3.17: Results of the screening for siderophore producers. Isolated microbes 3Ac8, 1Ab3, 3Ac7, 3Aa4, 2Ca3, 3Ea4, 3Ab1 and 1Bg2 formed a yellow halo at their growth sites.

3.4.5 Identification of unknown bacteria revealed *Pseudomonas* sp. as most prominent growth promoter

After sequencing, the unknown growth-promoting bacteria were identified using the BLAST algorithm via the NCBI nucleotide collection database. A complete list of all identified microbes can be seen in Table 3.2. Growth-promoting bacteria originated from environmental sampling sites were mainly members of the genus *Pseudomonas*.

Table 3.2: List of identified *C. vulgaris* growth-promoting microbes, isolated from various environmental sites and photobioreactors.

Sample ID	Origin	Taxon	Class	Identity
1Ab3	Triebener Tauern snowfield A	*Pseudomonas* sp.	*Gammaproteobacteria*	100%
1Bg2	Triebener Tauern snowfield B	*Pseudomonas* sp.	*Gammaproteobacteria*	99%
2Bb9	Drei Lacken pond B	*Aeromonas salmonicida*	*Gammaproteobacteria*	99%
2Ca3	Drei Lacken pond C	*Pseudomonas trivialis*	*Gammaproteobacteria*	99%
3Aa4	Seetaler Alpen snowfield A	*Pseudomonas* sp.	*Gammaproteobacteria*	99%
3Ab1	Seetaler Alpen snowfield A	*Pseudomonas antarctica*	*Gammaproteobacteria*	99%
3Ac7	Seetaler Alpen snowfield A	*Pseudomonas* sp.	*Gammaproteobacteria*	99%
3Ac8	Seetaler Alpen snowfield A	*Pseudomonas* sp.	*Gammaproteobacteria*	99%
3Ba6	Seetaler Alpen water A	*Pseudomonas veronii*	*Gammaproteobacteria*	99%
3Dc5	Seetaler Alpen snowfield B	*Janthinobacterium* sp.	*Betaproteobacteria*	100%
3Ea4	Seetaler Alpen snowfield C	*Pseudomonas* sp.	*Gammaproteobacteria*	99%
3Eb1	Seetaler Alpen snowfield C	*Pseudomonas sp.*	*Gammaproteobacteria*	99%
A24	PBR A	*Stenotrophomonas rhizophila*	*Gammaproteobacteria*	99%
A52	PBR A	*Flavobacterium* sp.	*Flavobacteria*	99%
C16	PBR C	*Stenotrophomonas maltophilia*	*Gammaproteobacteria*	99%
G76	Graz	*Microbacterium* sp.	*Actinobacteria*	99%
G97	Graz	*Microbacterium testaceum*	*Actinobacteria*	99%
G99	Graz	*S. rhizophila*	*Gammaproteobacteria*	99%

3.4.6 *Pseudomonas trivialis* 2Ca3 was uncovered as the most promising growth promoter

Out of the 726 tested bacterial isolates, 18 exhibited a positive impact on *C. vulgaris* growth. These growth-affecting strains were further tested for various plant growth-promoting properties, *e.g.* phosphate solubilization or protease activity (Table 3.3). The isolate 2Ca3, which was identified by 16S rRNA gene fragment sequencing as *Pseudomonas trivialis*, displayed the highest amount of these properties, as it produces AHL and siderophores, is protease active and has the ability to solubilize phosphate.

Table 3.3: Summarized list of *C. vulgaris* growth-affecting isolates including their potentially growth-promoting properties.

Sample ID	Taxon	AHL production	Protease activity	Siderophore production	Phosphate solubilization
1Ab3	*Pseudomonas* sp.	-	+	+	+
1Bg2	*Pseudomonas* sp.	-	+	+	-
2Bb9	*Aeromonas salmonicida*	+	+	-	-
2Ca3	***Pseudomonas trivialis***	+	+	+	+
3Aa4	*Pseudomonas* sp.	-	+	+	-
3Ab1	*Pseudomonas antarctica*	-	+	+	-
3Ac7	*Pseudomonas* sp.	-	+	+	-
3Ac8	*Pseudomonas* sp.	-	+	+	-
3Ba6	*Pseudomonas veronii*	-	-	-	+
3Dc5	*Janthinobacterium* sp.	-	-	-	-
3Ea4	*Pseudomonas* sp.	-	+	+	-
3Eb1	*Pseudomonas sp.*	-	+	+	-
A24	*Stenotrophomonas rhizophila*	-	-	-	-
A52	*Flavobacterium* sp.	-	-	-	-
C16	*Stenotrophomonas maltophilia*	-	+	+	-
G76	*Microbacterium* sp.	-	+	-	-
G97	*Microbacterium testaceum*	-	-	-	-
G99	*Stenotrophomonas rhizophila*	-	+	-	-

3.5 Cultivation approaches provided first insights into the structure of microalgal communities in natural environments

Pure cultures of isolated algae colonies from samples 2B (Drei Lacken, freshwater), 3B and 3C (Seetaler Alpen, both freshwater) were identified by Sanger-sequencing and using the BLAST algorithm via the NCBI nucleotide collection database. The results gave an insight into the cultivable microalgal community of these samples. Sample 2B was dominated by members of the genus *Chlamydomonas* and the phylogenetic family *Scenedesmaceae.* Additionally, *Chlorella emersonii* could be identified (Figure 3.18). The main part of cultivable microalgae colonies of sample 3B belonged to the family *Scenedesmaceae*, especially to the genus *Desmodesmus*. The only exception was one isolate which was identified as *Chlorella sorokiniana*. Sequencing results of sample 3C revealed similar results as for sample 3B: highly dominated by *Scenedesmaceae*, especially by the genus *Desmodesmus*, and a co-occurring member of the genus *Chlorella* (Figure 3.18).

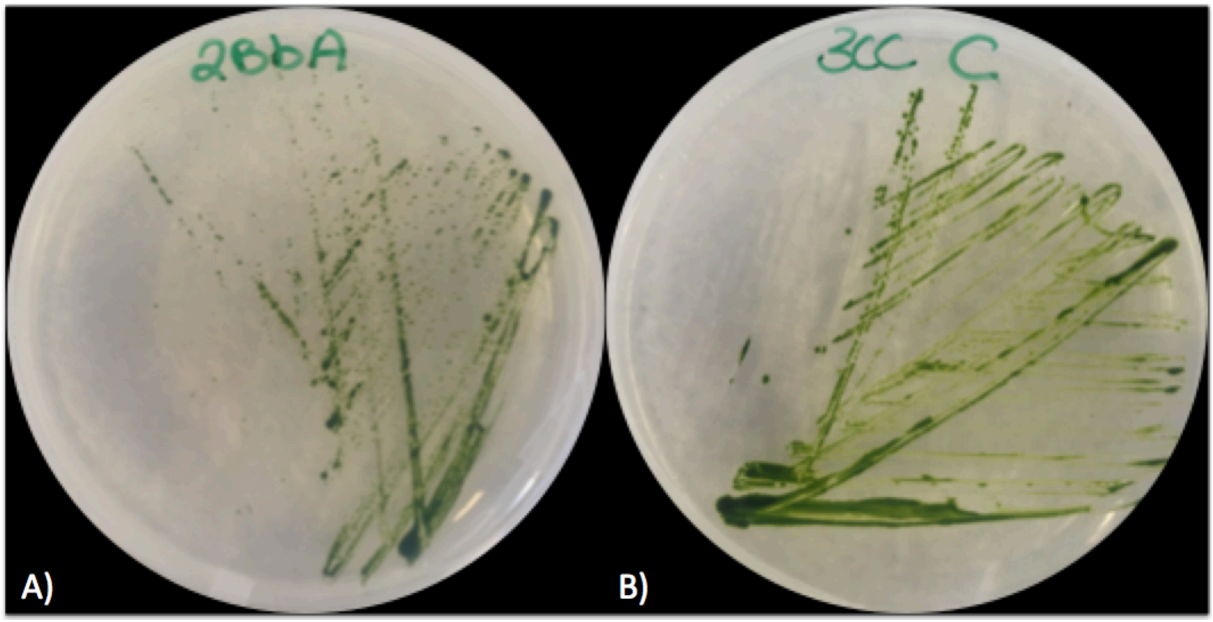

Figure 3.18: Isolated microalgae colonies maintained on solid BBM. Unknown green algae were identified after sanger-sequencing. Sample 2B (A): *Chlorella emersonii*; sample 3C (B): *Chlorella* sp.

3.6 Deepening insights into the bacterial diversity co-occurring with microalgae

To get an insight into the bacterial community of environmental samples taken from snowfields and freshwater (Triebener Tauern, Drei Lacken, Seetaler Alpen) single strand conformation polymorphisms (SSCP) were performed using 16S rRNA gene sequences.

3.6.1 A high bacterial diversity was evident from SSCP profiles

The community patterns of snowfield-associated bacteria showed a high diversity among single sampling spots, but also among different sampling sites. Microbial fingerprints that could be observed in every sample indicated for a specific core microbiome (Appendix 7.6, Figure 7.1). The computer-assisted cluster-analysis of the bacterial SSCP profiles indicated for a general high similarity of snowfield-associated bacterial communities (Figure 3.19).

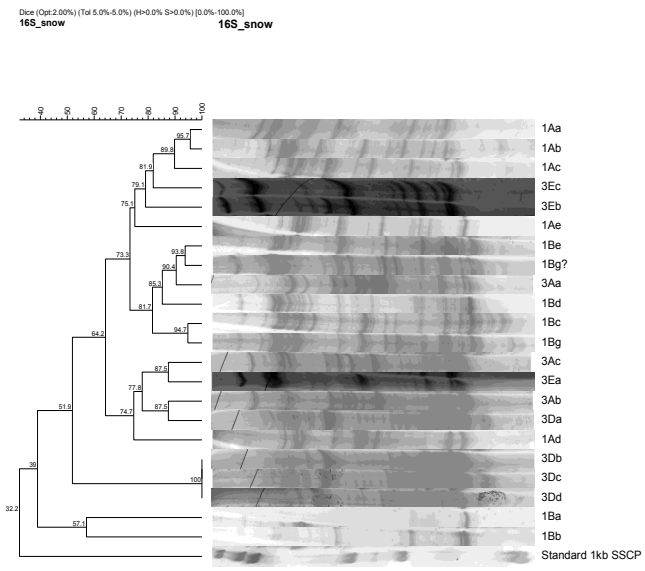

Figure 3.19: Computer-assisted cluster analysis represents the snowfield-associated bacterial communities. Standard: Gene ruler 1 kb ladder.

3.6.2 Freshwater samples harbored less diversified bacteria

Freshwater-associated bacterial communities from sampling sites Drei Lacken (2A; 2B; 2C) and Seetaler Alpen (3B; 3C) were analyzed using SSCP. The community patterns indicated a lower bacterial diversity compared to snowfield-associated fingerprints. SSCP profiles of Drei Lacken displayed a site-specific core pattern (Appendix 7.6, Figure 7.2). The computer-assisted cluster-analysis of the bacterial SSCP profiles indicated for a general low diversity of freshwater-associated bacterial communities (Figure 3.20).

Figure 3.20: Computer-assisted cluster analysis represents the freshwater-associated bacterial communities. Standard: Gene ruler 1 kb ladder.

3.7 The microalgae community was not decodable by 18S rRNA SSCP analyzes

In order to get an insight into the eukaryotic community of snowfield- and freshwater samples from Triebener Tauern, Drei Lacken and Seetaler Alpen SSCP profiles were analyzed. Respective bands were excised from the polyacrylamidegel and subsequently identified by amplification of partial 18S rRNA gene sequencing and aligning them using the BLAST algorithm against the NCBI nucleotide collection database.

The SSCP analysis of snowfield- and high alpine freshwater samples gave an idea of the endemic eukaryotic structure, but hardly any information about the microalgae community. *Scenedesmus* sp. was identified once from a snowfield sample as same as *Ochromonas vasocystis* was identified in a freshwater puddle. Most excised bands and subsequent identified eukaryotes belonged to the phylogenetic kingdom *Animalia* or *Fungi.*

3.7.1 Snowfield-associated eukaryotic communities were dominated by members of the fungal class *Microbotryomycetes*

The snowfield-associated eukaryotic community was analyzed via SSCP fingerprinting and computer-assisted clustering (Figure 3.21; Appendix 7.6, Figure 7.3). In order to identify green microalgae by comparison of their SSCP pattern, pure cultures of *C. vulgaris* and *Haematococcus pluvialis* were additionally applied as references onto the polyacrylamidegel. After amplifying the partial 18S rRNA gene sequence by universal primers covering the V9 region and subsequent sequencing *Scenedesmus sp.* could be identified once. The eukaryotic SSCP profile was dominated rather by members of the fungal class *Microbotryomycetes*. Detailed information about the identified eukaryotes can be observed in Table 3.4.

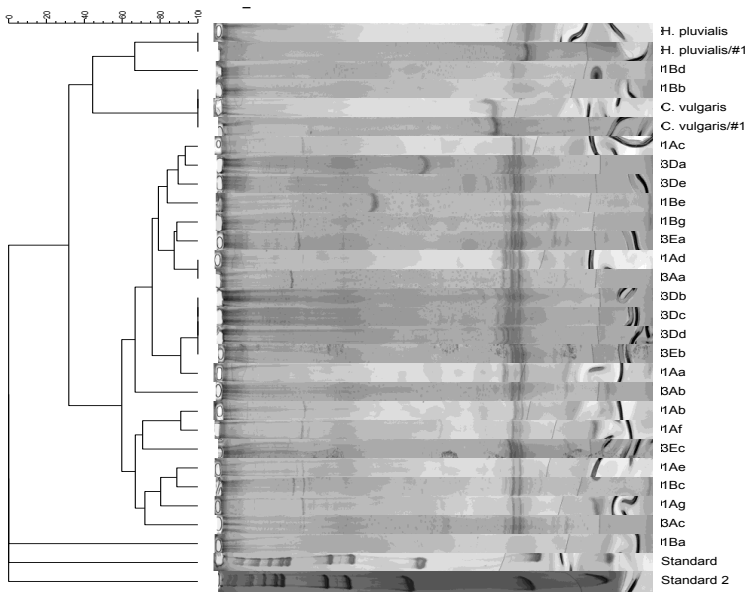

Figure 3.21: Computer-assisted cluster analysis of the snowfield-associated eukaryotic community. References: C.v. = *C. vulgaris*; H.p. = *H. pluvialis*. Standard: Gene ruler 1 kb ladder.

Table 3.4: Taxa present in snowfield-associated eukaryotic profiles.

ID	Taxon	Class	Identity	Origin
H.p.	*Haematococcus pluvialis*	*Chlorophyceae*	100%	Reference
C.v.	*Chlorella vulgaris*	*Trebouxiophyceae*	100%	Reference
1	*Scenedesmus* sp.	*Chlorophyceae*	100%	1Aa
2	*Rhodotorula kratochvilovae*	*Microbotryomycetes*	98%	1Ac
3	*Slooffia cresolica*	*Microbotryomycetes*	96%	1Ac
4	*Lecane inermis*	*Eurotatoria*	100%	1Af
5	uncultured eukaryote clone ALA5117773		100%	1Bc
6	*Pseudohyphozyma pustula*	*Microbotryomycetes*	97%	1Bc
7	*Bradysia hygida*	*Insecta*	99%	1Be
8	*Apanteles* sp.	*Insecta*	94%	3Da
9	uncultured eukaryote clone ALA5117773		100%	1Be
10	*Leucosporidium antarcticum*	*Microbotryomycetes*	98%	1Bg
11	*Rhodotorula kratochvilovae*	*Microbotryomycetes*	98%	3Aa
12	*Slooffia tsugae*	*Microbotryomycetes*	99%	3Ab
13	*Rhodotorula kratochvilovae*	*Microbotryomycetes*	99%	3Ac
14	*Leucosporidium antarcticum*	*Microbotryomycetes*	100%	3Db
15	*Rhodotorula kratochvilovae*	*Microbotryomycetes*	96%	3De
16	*Calycophorae* sp.	*Hydrozoa*	100%	3De
17	*Ustilentyloma graminis*	*Microbotryomycetes*	98%	3Eb

3.7.2 A low diversity was found within freshwater-associated eukaryotes

The freshwater-associated eukaryotic community was analyzed via SSCP fingerprinting and computer-assisted clustering (Figure 3.22; Appendix 7.6, Figure 7.4). In order to identify green microalgae by comparison of their SSCP pattern *C. vulgaris* and *Haematococcus pluvialis* were applied as references onto the polyacrylamidegel. After sequencing *Ochromonas vasocystis* could be identified as part of the eukaryotic community. Details of the identified eukaryotes can be observed in Table 3.5.

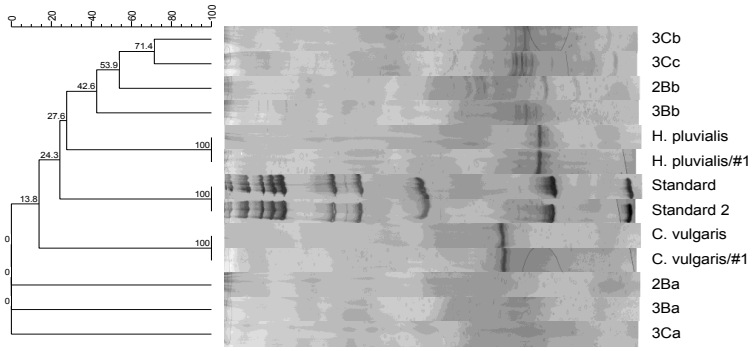

Figure 3.22: Computer-assisted cluster analysis of the freshwater-associated eukaryotic community. References: C.v. = *C. vulgaris*; H.p. = *H. pluvialis*. Standard: Gene ruler 1 kb ladder.

Table 3.5: Eukaryotic taxa identified by Sanger-sequencing in freshwater.

ID	Taxon	Class	Identity	Origin
H.p.	*Haematococcus pluvialis*	*Chlorophyceae*	100%	Reference
C.v.	*Chlorella vulgaris*	*Trebouxiophyceae*	100%	Reference
1	*Ochromonas vasocystis*	*Chrysophyceae*	98%	3Bb
2	*Calycophorae* sp.	*Hydrozoa*	100%	3Cb
3	*Albugo candida*	*Oomycetes*	97%	3Cc
4	*Paralagenidium karlingii*		97%	3Cc

3.8 Illumina MiSeq/HiSeg sequencing revealed potential eukaryotic and prokaryotic interactions

3.8.1 Targeting *Chlorella vulgaris* and closely related microalgae in the amplicon libraries

Unravelling the eukaryotic communities from environmental samples was done by an Illumina-sequencing based amplicon analysis of 18S rRNA gene fragments. The analysis gave insight into the diversity and the composition of the eukaryotic structure and furthermore displayed the abundance of *C. vulgaris* and other closely related microalgae.

3.8.1.1 Snowfield- and freshwater-associated eukaryotes are dominated by *Archaeplastida*, *Opisthokonta* and *SAR*

A general sample overview based on the taxonomic level phylum can be seen in Figure 3.23. Samples taken from the suburban region of Graz and Ennstal showed the highest abundance of *Archaeplastida*, while snowfield and freshwater samples taken from Seetaler Alpen displayed the lowest percentage of *Archaeplastida* (10 - max. 30%). In general samples were dominated by members of the phyla *Archaeplastida*, *Opisthokonta* and members of the *SAR* clade.

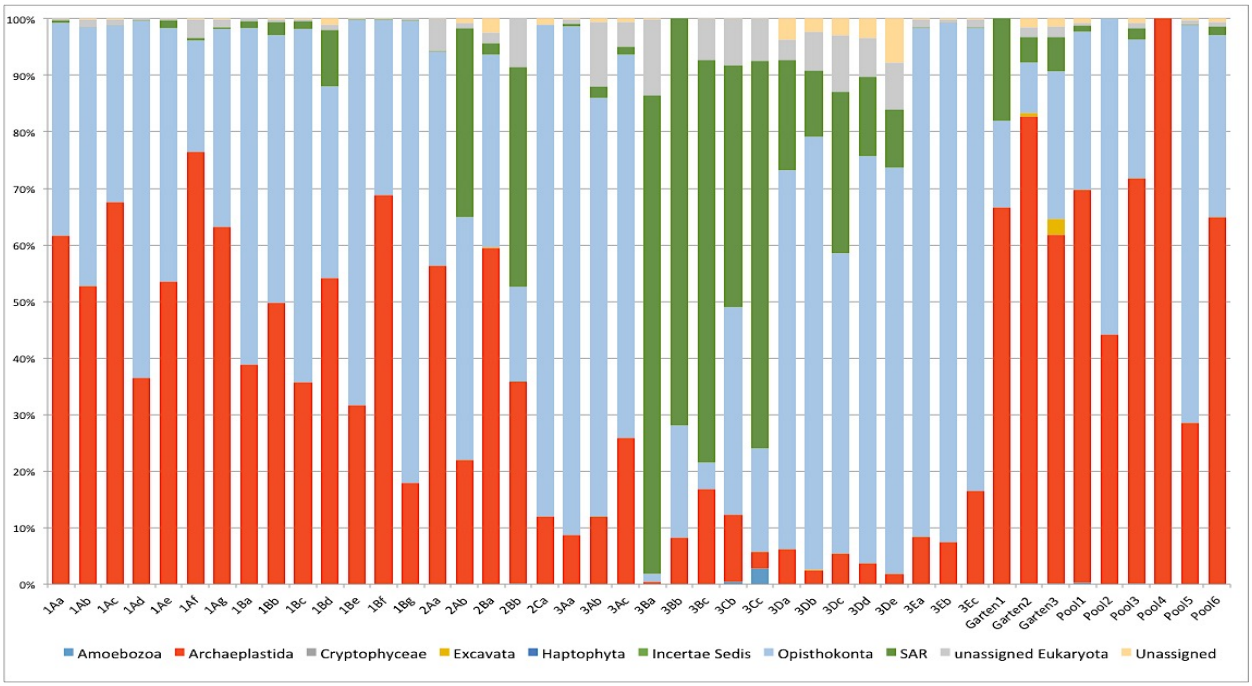

Figure 3.23: Overview on the eukaryotic community composition based on 18S rRNA gene sequencing. 1: Triebener Tauern; 2: Drei Lacken; 3: Seetaler Alpen; Garten: Graz; Pool: Ennstal.

In order to figure out the highest potential of *C. vulgaris* to be present in a sample, the eukaryotic community was examined by grouping the OTUs at taxonomic level class. (Figure 3.24). For that the relative abundance of *Chloroplastida* was estimated more precisely.

Among the snowfield specimen taken from Triebener Tauern, the most dominant subphylum was *Chloroplastida* making up 55% of the total reads, followed by *Nucletmycea* (36%) and *Holozoa* (7%). A similar eukaryotic composition can be observed in freshwater samples from Drei Lacken (48% *Chloroplastida*, 16% *Nucletmycea*, 12% *Holozoa* and 13% *Alveolata*). Stagnant waters and snowfields from Seetaler Alpen exhibited the lowest relative abundance of *Chloroplastida* (8%), but the highest proportion of *Nucletmycea* (50%) and *Stramenopiles* (24%). In contrast sampling sites Graz and Ennstal revealed the highest relative abundance of *Chloroplastida* (71% and 68%) and the lowest of *Nucletmycea* (3% and 10%).

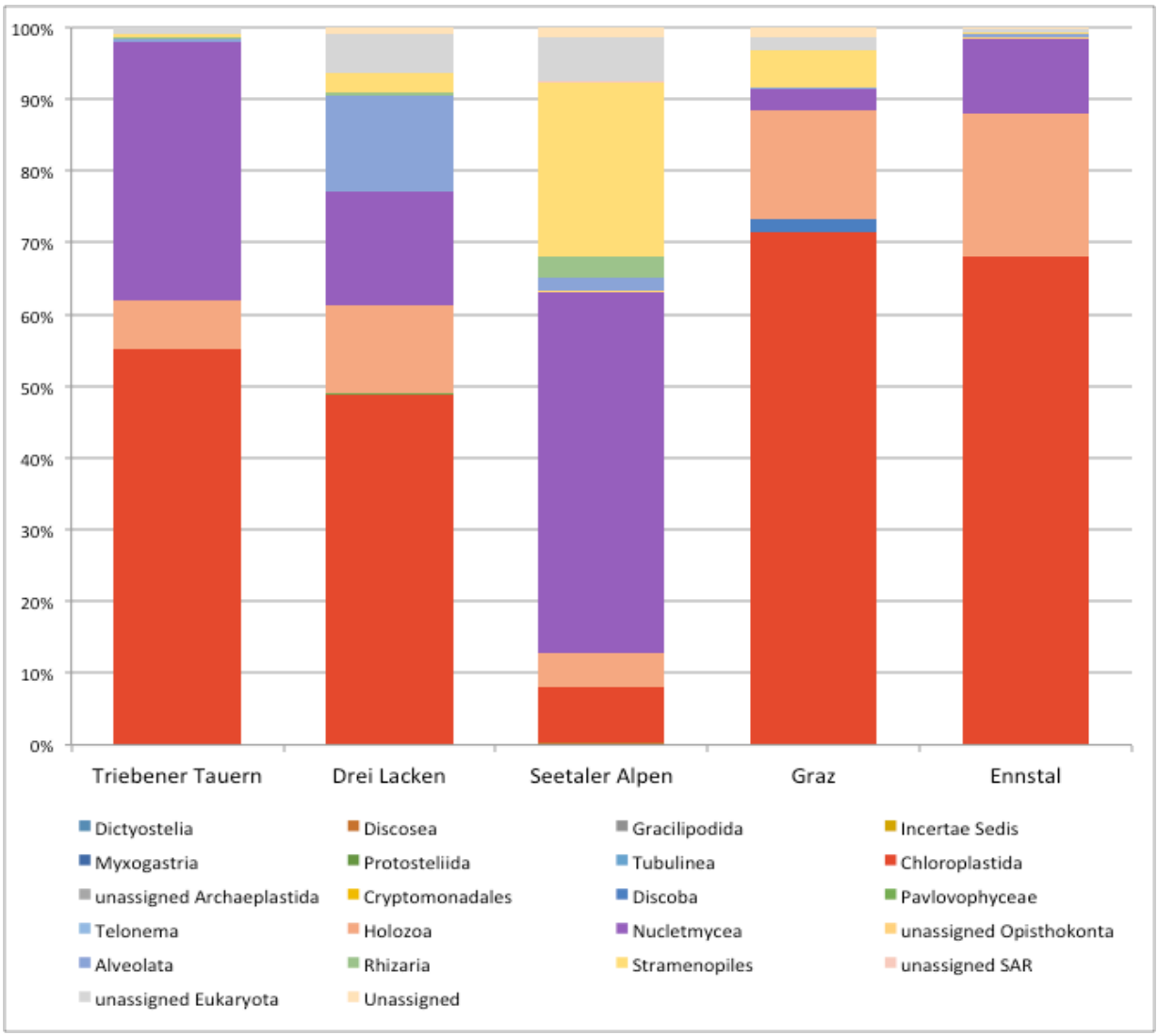

Figure 3.24: Summarized composition of the sampling site specific eukaryotic community represented by grouping at the class level.

3.8.1.2 The relative abundance of *Chlorellales* was determined by generating an archaeplastidome

Of every environmental specimen the archaeplastidome on the phylogenetic level genus was observed to gain a better insight into the plant- and algae composition (Figure 3.25). It was observed that snowfield specimen of Triebener Tauern where highly dominated by algae species of the *Chlamydomonadaceae* family, while samples from Graz and Ennstal were dominated by microalgae species belonging to the *Chlorophyceae* class. Snowfield-associated *Archaeplastida* of Seetaler Alpen consisted mainly of *Chloromonas*, whereas different members of the *Chlorophyceae* class dominated the respective freshwater specimen. *Chlorella emersonii* was detected in a relative abundance of 2% in sample 3Cc.

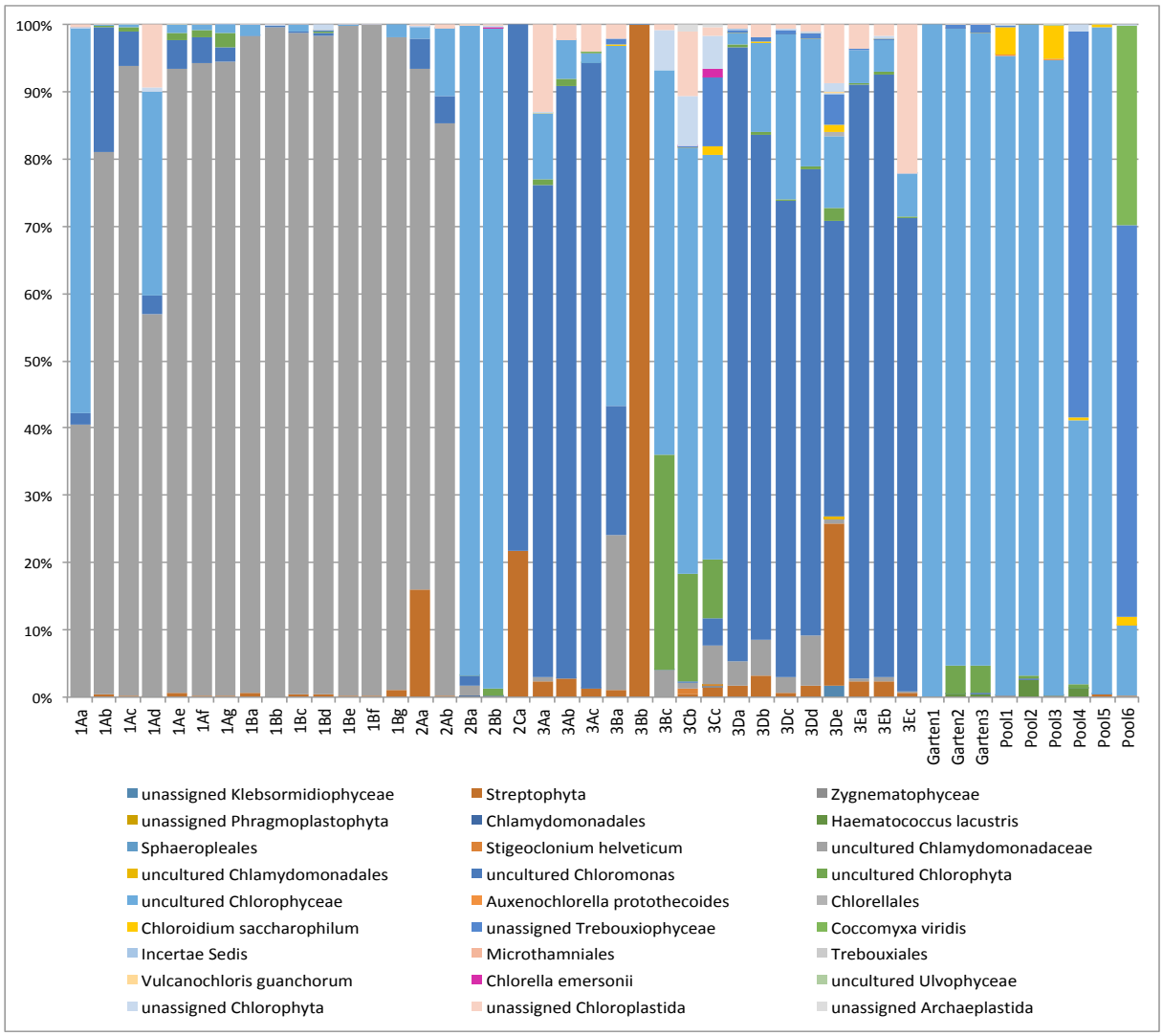

Figure 3.25: *Archaeplastida* diversity and composition of each environmental sample based on 18S rRNA gene sequencing. 1: Triebener Tauern; 2: Drei Lacken; 3: Seetaler Alpen; Garten: Graz; Pool: Ennstal.

Regarding the results of the archaeplastidome, every specimen that comprised members of the order *Chlorellales* were picked out and examined more precisely (Figure 3.26). As already seen in Figure 3.29, sample 3Cc displayed an apparent amount of *Chlorella emersonii* (1.25%). Species of the order *Chlorellales* were found in in sample 3De (0.62%). In general, all selected specimen were dominated by unassigned OTUs of *Chlorophyta*, unassigned OTUs of the classes *Chlorophyceae* and *Trebouxiophyceae.* In samples Pool1 and Pool3 the green algae *Chloroidium saccharophilum*, belonging to the class *Trebouxiophyceae,* occurred as second most abundant. No *C. vulgaris* was found in any of the samples.

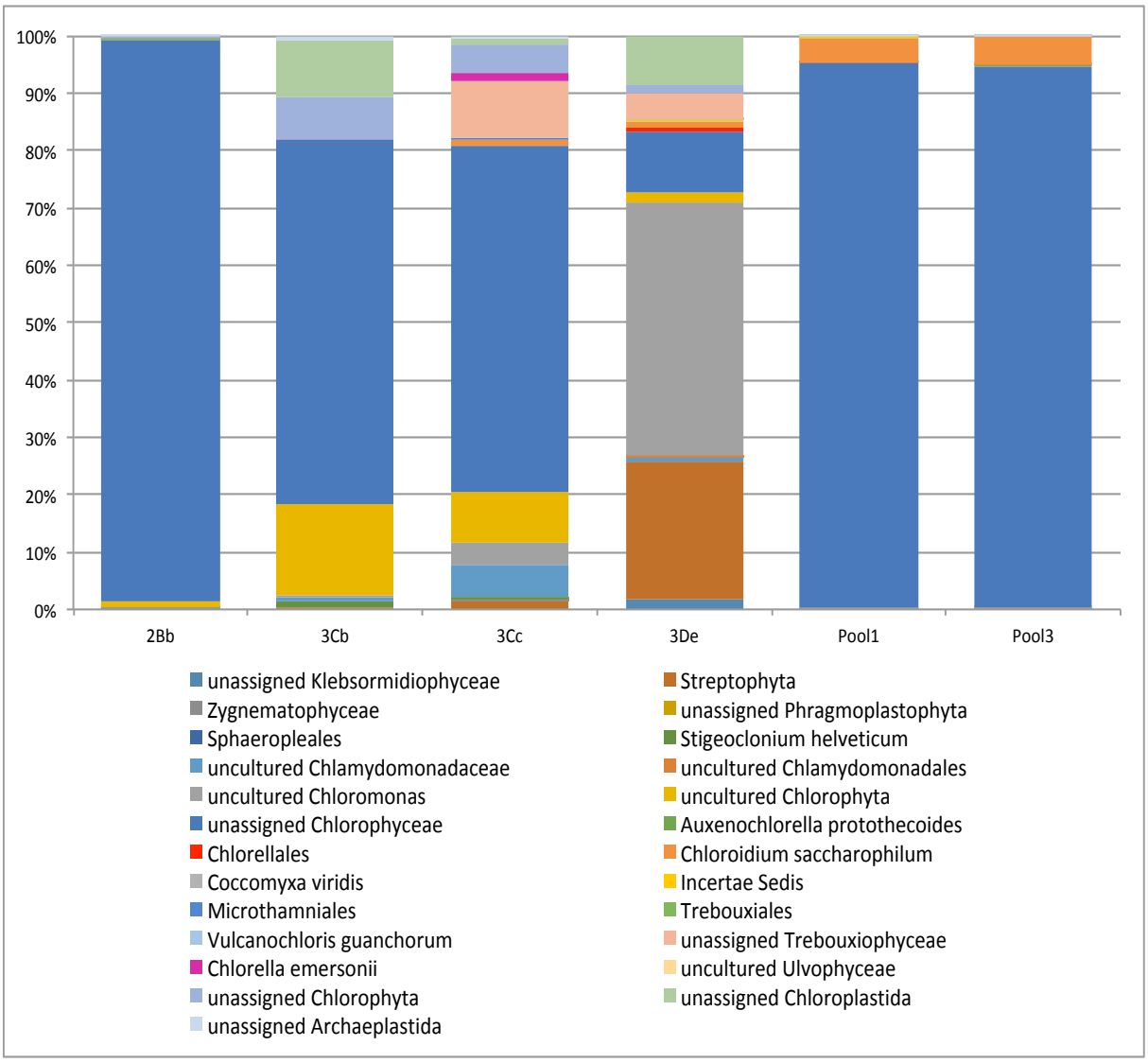

Figure 3.26: *Archaeplastida* community of *Chlorellales* including samples based on 18S rRNA sequencing and grouped by the phylogenetic level genus. 2: Drei Lacken; 3: Seetaler Alpen; Pool: Ennstal.

3.8.2 Unravelling the bacterial community revealed habitat specificity and location independence

An Illumina-sequencing based analysis of the 16S rRNA gene was performed to examine the microalgae-associated microbiome under different environmental conditions.

3.8.2.1 *Proteobacteria* and *Bacteroidetes* dominated the microalgae-associated microbiome

Among the snowfield samples the most dominant phyla were unchanged despite different sampling locations, with *Proteobacteria* and *Bacteroidetes* making up around 90% of all reads (Figure 3.27). Otherwise the four most abundant OTUs in freshwater samples 3B and 3C and also in the environmental samples from Graz and Ennstal were classified as *Proteobacteria*, *Bacteroidetes, Actinobacteria* and *Cyanobacteria*. Freshwater samples originated from Drei Lacken (2A, 2B, 2C) were highly dominated by *Proteobacteria* and *Actinobacteria*, whereas *Bacteroidetes* were detected in trace levels only.

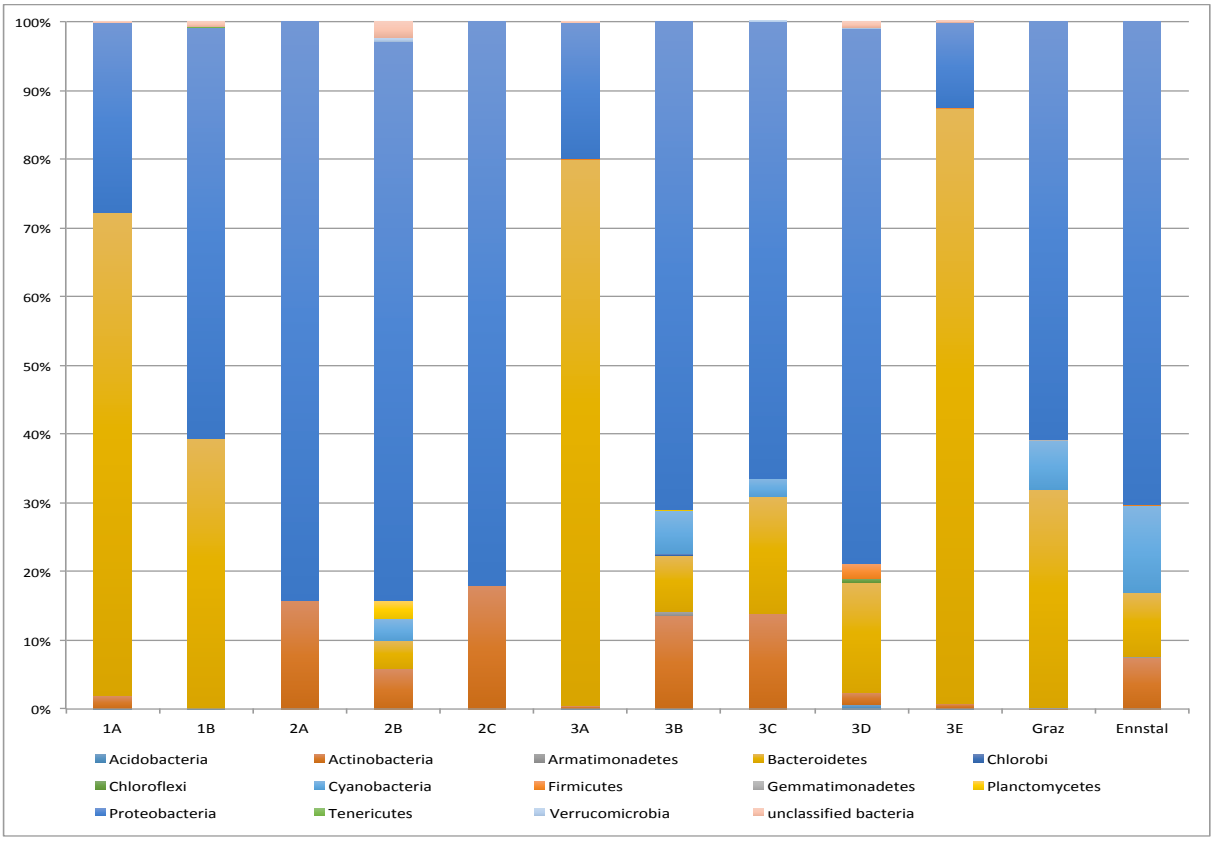

Figure 3.27: 16S rRNA gene sequencing based bacterial community of environmental samples from snowfields (1A, 1B, 3A, 3D, 3E), freshwater (2A, 2B, 2C, 3B, 3C) and suburban regions (Graz, Ennstal). The composition is presented by grouping the OTUs at phylum level.

3.8.2.2 The snowfield-associated microbiome is location-independent

By grouping the identified OTUs at family level a closer look was taken on the snowfield-associated bacterial structure of the different samples (Figure 3.28). Snowfield samples 1A, 3A and 3E were dominated by OTUs classified as *Sphingobacteriaceae* (up to 50%) within the phylum *Bacteroidetes*. *Cytophagaceae*, *Oxalobacteraceae*, *Chitinophagaceae* and in low fractions (under 10%) *Comamonadaceae*, *Sphingomonadaceae* and *Pseudomonadaceae* were detected in these samples. In comparison snowfield 1B was dominated by *Comamonadaceae* (43%), that belongs to the phylum *Proteobacteria,* whereas *Oxalobacteraceae, Sphingomonadaceae, Chitinophagaceae* and *Cytophagaceae* occurred in minor fraction (each 10-12%). Additionally, a valuable count of members belongig to the *Enterobacteriaceae* and the *Bradyrhizobiaceae* family was detected (around 5% each). Members of *Oxalobacteraceae* within the phylum *Proteobacteria* consisted of 62% of the reads in snowfield sample 3D. The other two most abundant families in this sample were classified as *Chitinophagaceae* (10%) and *Comamonadaceae* (8%), while *Cytophagaceae, Sphingomonadaceae, Acetobacteraceae, Sphingobacteraceae* and *Clostridiaceae* represented around 3% of all reads each.

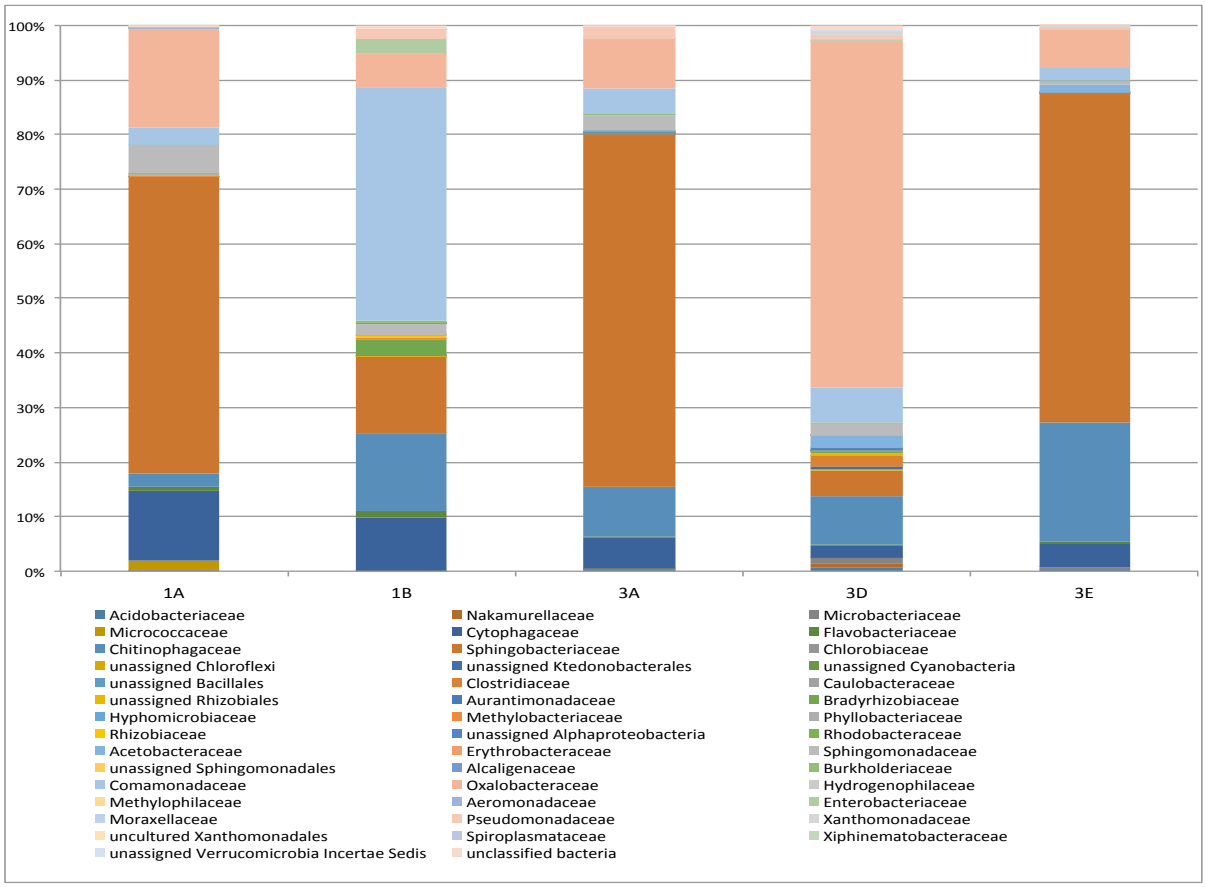

Figure 3.28: Snowfield-associated bacterial community composition based on 16S rRNA gene sequencing. 1: Triebener Tauern; 3: Seetaler Alpen.

3.8.2.3 A sampling site independent bacterial community was found in freshwater samples

The diversity and composition of the bacterial community in freshwater samples was analyzed by grouping them on the phylogenetic level family (Figure 3.29). A low bacterial diversity was detected within samples 2A and 2C, where around 70% of all reads consisted of *Sphingomonadaceae* of the phylum *Proteobacteria.* The second most abundant family was *Micrococcaceae* (15-18%), followed by *Pseudomonadaceae* and *Comamonadaceae*. Other bacterial families were detected in trace levels only. In contrast the freshwater-associated bacterial community of sample 2B consisted of 30% *Sphingomonadaceae*, 23% *Comamondaceae* and 12% *Burkholderiaceae*. *Rhodobacteriaceae, Rhizobiaceae, Bradyrhizabiaceae, Plantomycetaceae, Flavobacteriaceae, Micrococcaceae* and *Sporichtyaceae* represented fractions of under 5% in this sample. About 14% of all occurring *Alphaproteobacteria* could not be classified further. The bacterial community of the freshwater samples 3B and 3C were mainly represented by members belonging to the *Sphingomonadaceae* family (50-65%), followed by *Micrococcaceae, Cytophagaceae, Comamondaceae* and *Flavobacteriaceae*.

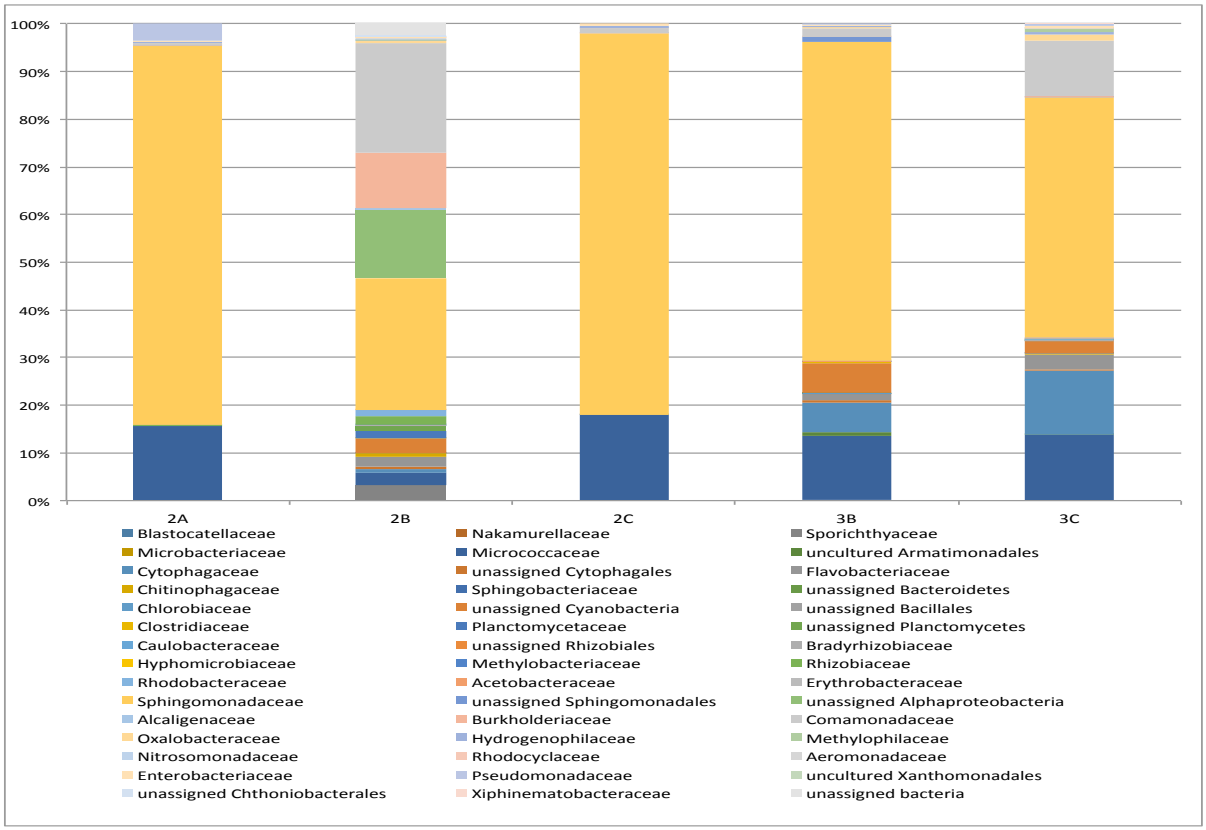

Figure 3.29: Freshwater-associated bacterial community based on 16S rRNA gene sequencing grouped by the phylogenetic level family. 2: Drei Lacken; 3: Seetaler Alpen.

3.9 Alpha rarefaction analysis revealed varying diversity

In order to assess the prokaryotic species richness of the sampling data an alpha rarefaction analysis was performed. The analysis was conducted by using the Shannon index and by examining the observed OTUs. Two different maximum sequencing depths were applied and compared to each other: 800,000 reads (Figure 3.30) and 10,000 reads (Figure 3.31). In both approaches sample 2C displayed the lowest number of observed OTUs (below 20) and a Shannon index of 1.5, which indicated for a low biodiversity. By setting the rarefaction of the OTU table to 10,000 reads sampling site 2C was detected as most diverse sequence collection, with about 800 observed OTUs and a Shannon index of 6.5. Contrarly sampling site 3D was detected as most diverse (Shannon index 8.0) when setting the sequence depth to 800,000 reads. Generally, the results of the Shannon diversity analyses reflect results when assessing the observed OTU counts. Concerning that only one dataset actually had a sequence depth of 800,000 reads, the analysis was more significant by using a sequence depth of 10,000. Results of alpha diversity analyses have to be considered with caution, since for the amplification of 16S gene fragments a nested PCR approach was used for several samples in order to reach sufficient DNA concentrations for sequencing.

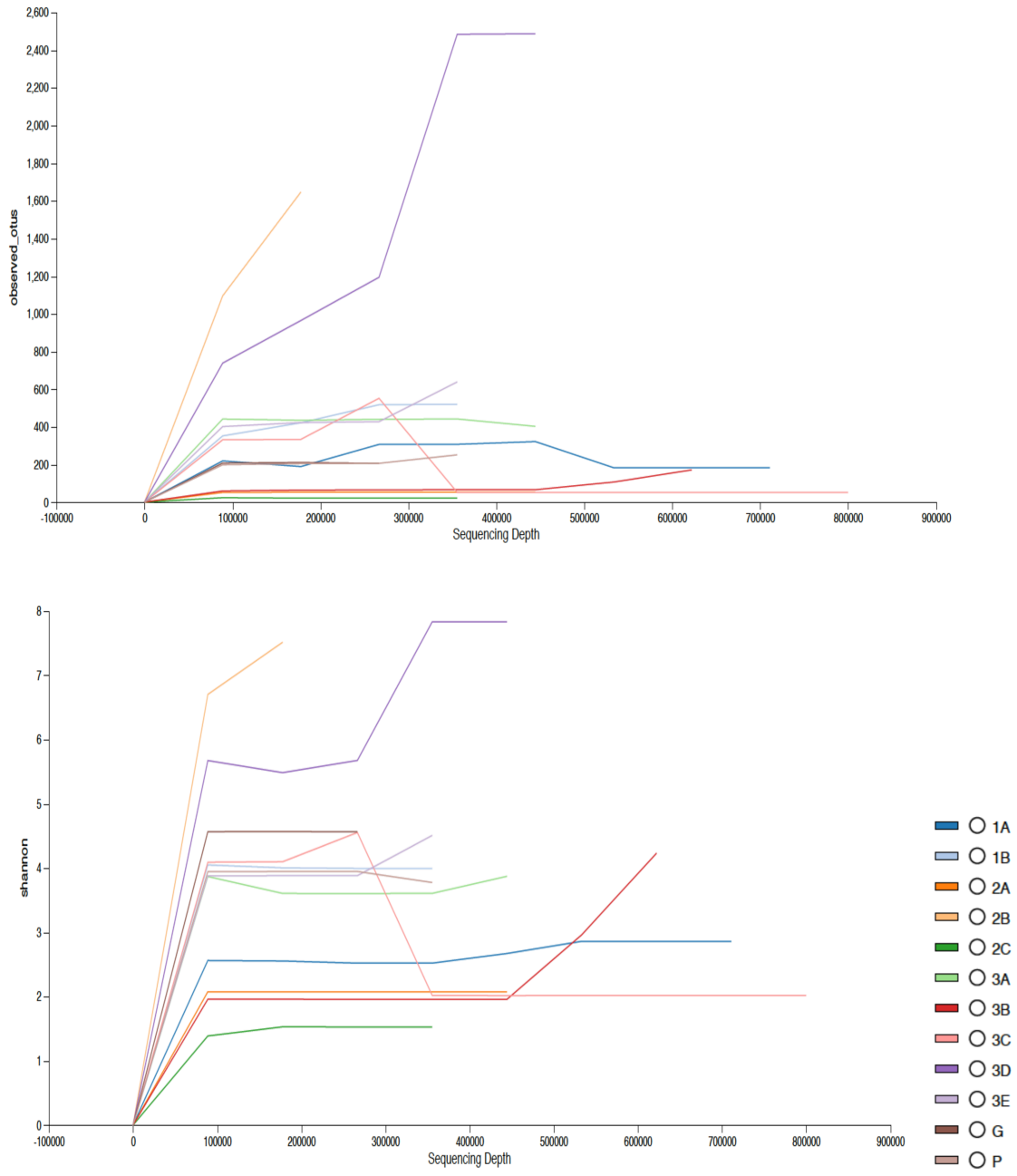

Figure 3.30: Rarefaction curves demonstrating the observed OTUs (above) and the Shannon index (below) of the 16S OTUs identified for the different sampling sites. Rarefaction of the OTU table was set to 800,000. Sampling site 3D revealed 2,500 observed OTUs and a Shannon index of 8.

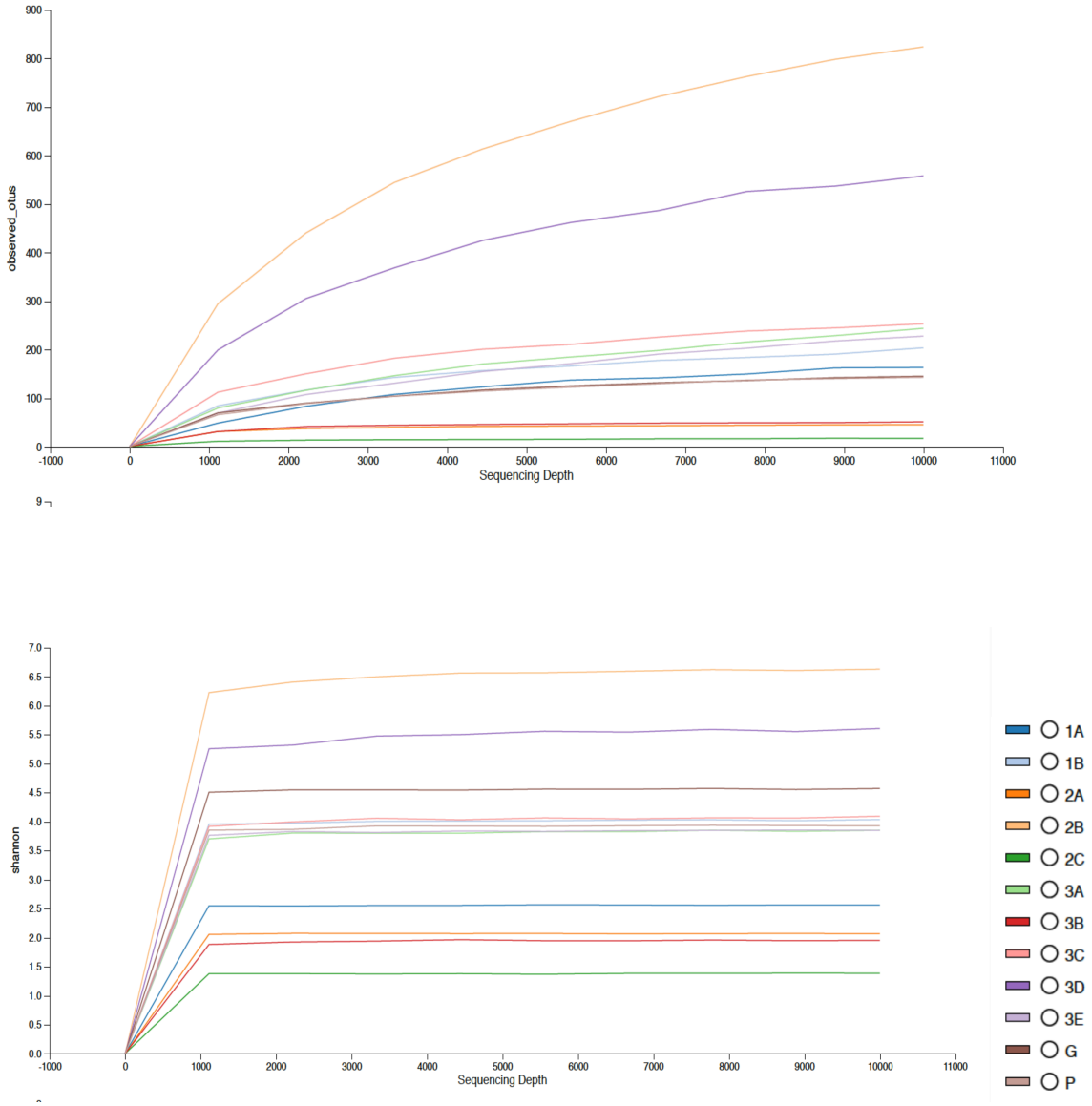

Figure 3.31: Rarefaction curves demonstrating the observed OTUs (above) and the Shannon index (below) of the 16S OTUs identified for the different sampling sites. Rarefaction of the OTU table was set to 10,000. Sampling spot 2B showed the highest number of observed OTUs (around 800) and a Shannon index of 6.5, while in sample 2C only around 20 OTUs were observed, leading to a Shannon index of 1.5.

3.10 PCoA Plot analysis disclosed habitat specific clustering

Principal component analysis was performed to explore the similarities of the 16S rRNA sequencing data (Figures 3.32; 3.33; 3.34). For that purpose, unweighted UniFrac distance metric was used (Lozupone *et al*., 2007).

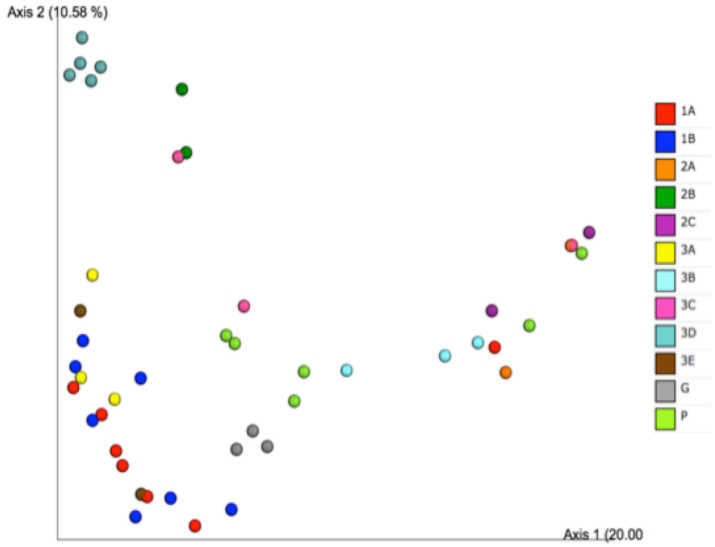

Figure 3.32: Principal coordinate analysis (PCoA) plot using unweighted UniFrac distance matrix based on the 16S rRNA gene sequencing of all environmental samples. 1: Triebener Tauern; 2: Drei Lacken; 3: Seetaler Alpen; G: Graz; P: Ennstal.

Figure 3.36 showed that samples from Triebener Tauern and Seetaler Alpen clustered together while for Graz, Ennstal and Drei Lacken no obvious clustering was detected.

In contrast to that a habitat specific PCoA plot (Figure 3.37) showed snowfield samples clustering together, while (fresh)water samples do not display habitat specificy.

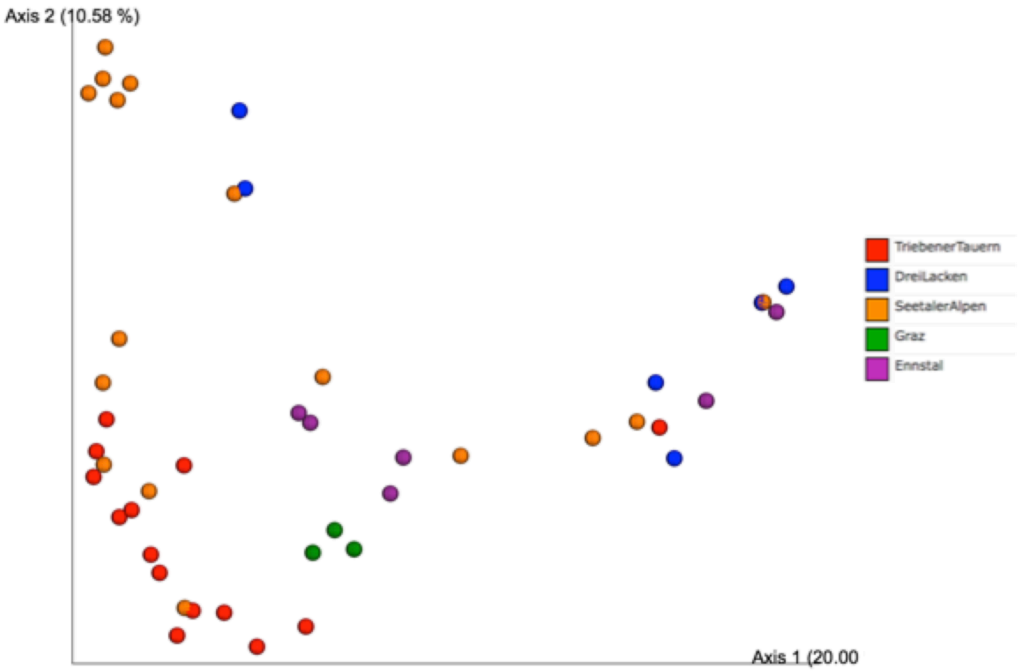

Figure 3.33: Principal coordinate analysis (PCoA) plot using unweighted UniFrac distance matrix based on the 16S rRNA gene sequencing of all environmental samples grouped by sampling site.

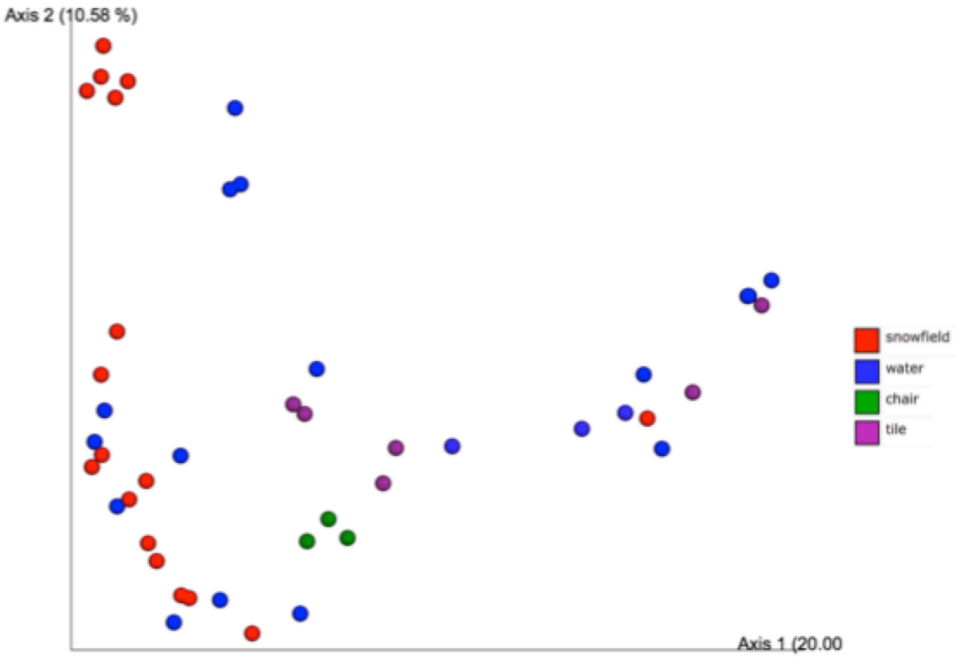

Figure 3.34: Principal coordinate analysis (PCoA) plot using unweighted UniFrac distance matrix based on the 16S rRNA gene sequencing of all environmental samples grouped by kind of habitat. Chair = Graz; tile = Ennstal.

IV. Discussion

In this study the eukaryotic and bacterial communities co-existing in artificial and environmental microalgae habitats were analyzed. Microalgae co-occurring microbes were isolated and subjected to different screenings. Subsequently, growth-affecting strains were identified and further characterized. Amplicon libraries of 16S rRNA gene fragment sequencing gave insight into the microbial community of freshwater and snowfield microalgae environments. They revealed a habitat specific and location independent bacterial diversity. In addition, amplicon sequencing of 18S rRNA gene fragments uncovered that members of the genus *Chlorellales* were only present in 6 out of 44 samples, while *Chlorella vulgaris* was missed in all samples.

4.1 *Pseudomonas trivialis* 2Ca3 was discovered as the most promising microalgae growth-promoting bacterium for biotechnological applications

Characterization of previously identified *C. vulgaris* growth-promoting strains revealed that ten out of 17 microbes belonged to the genus *Pseudomonas*. The genus *Pseudomonas* contains 218 species and is a widespread distributed gram-negative rhizobacterium with versatile attributes concerning plant growth promotion (Peix *et al.*, 2009; Beneduzi *et al*., 2012). Zachow and colleagues (2008) showed that pseudomonads additionally display antagonistic activities against common plant pathogens like *Aphanomyces cochlioides*, *Phoma betae*, *Pythium ultimum* and *Rhizoctonia solani.* Out of 1952 bacterial isolates 75 showed antagonistic activity against at least one of these four pathogens. By sequencing the partial 16S rRNA they identified 70 of them as members of the genus *Pseudomonas*. Furthermore *P. trivialis* in particular provides various plant growth-promoting effects, as Zachow and colleagues (2010) determined enhanced leaf length and -surface of the lettuce *Lactuca sativa* after treatment with *P. trivialis* RE* 1-1-14.

In this study special attention was given to *Pseudomonas trivialis* 2Ca3, which revealed various plant (and microalgae) growth-promoting properties. It was shown to produce siderophores when specific assays were used. As all organisms require iron as cofactor for metabolic enzymes, mainly as a mediator for redox reactions and electron transfer, it is an important micronutrient to maintain functioning in living organisms (Miethke and Marahiel, 2007; Cassat and Skaar, 2013). Considering that iron is often insufficiently available in the environment due to low solubility under physiological conditions, many microorganisms developed high-affinity iron uptake systems to satisfy these nutritional requirements. These

specific pathways include low molecular weight chelators with high affinity to iron called siderophores. Siderophores are secreted by specific microorganisms to solubilize iron from the surrounding environment. Then they form a ferric-siderophore complex that can be taken up again into the cell by diffusion (Andrews *et al*., 2003). Since *P. trivialis* 2Ca3 is capable of secreting one of the various siderophores known to be produced by *Pseudomonas*, it may support iron-uptake in *C. vulgaris* by mutualistic exchange of nutrients. Phosphorus (P) is one of the most essential elements for plant growth and can only be absorbed in soluble form P_i. Under environmental conditions organic P_o is commonly immobilized and not available for eukaryotic organisms like plants or microalgae (Rodriguez and Fraga, 1999). Microbes with the ability to solubilize this P_o are therefore highly important for sufficient phosphorus supply. Illmer and Schinner (1992) investigated the solubilization of P and its release into the culture medium by various microorganisms isolated from forest soil. In 2100 single experiments they found that *Penicillium* sp. (strain 29) and *Pseudomonas* sp. (strain 18) were the most efficient phosphate solubilizers. Gulati and colleagues (2008) reported the solubilization of phosphate substrates by *P. trivialis* for the first time. They isolated and characterized fluorescent *Pseudomonas* sp. with high phosphate-solubilizing abilities from a cold desert with low P availability in the trans-Himalayan region of India. Here *P. trivialis* was discovered as predominant, fluorescent, phosphate solubilizing *Pseudomonas* sp. in the rhizosphere of seabuckthorne. According to these studies *Pseudomonas* is an important rhizobacterium supplying a plant's rhizome with phosphorus, but may also promote microalgae growth by providing soluble phosphorus. *P. trivialis* 2Ca3 was the only among the identified microalgae growth-promoting pseudomonads that was capable of producing N-acylhomoserine lactones. According to Karlsson and colleagues (2012) an AHL-based quorum sensing (QS) system was found in *P. aeruginosa*, from which Roger and Iglewski (2003) suggested to be an antimicrobial target. Obviously also *P. trivialis* 2Ca3 shares an AHL-based QS signaling system, that enables the control of the expression of specific genes. Here these AHL molecules are responsible for coordinated transcription of QS-controlled regulatory genes by binding population-density-depending to intracellular receptors (Roger and Iglewski, 2003). Additionally these QS signals may also affect the performance of eukaryotic cells in an inter-kingdom-signaling process (Pacheco and Speandio, 2009). This provides another explanation of growth promotion by this strain, because AHL molecules may interact with *C. vulgaris* in a beneficial way.

As already mentioned pseudomonads have various abilities to promote plant and furthermore microalgae growth. Considering the ratio of identified *C. vulgaris* growth-promoting

pseudomonads (ten out of 17) it can be assumed that members of the genus *Pseudomonas* are not only highly rated plant growth promoting strains, but may also be promising for prospective *C. vulgaris* biotechnological cultivation approaches.

4.2 A low number of microalgae species were identified by examining the eukaryotic community - *Chlorella vulgaris* was absent in the analyzed environments

The eukaryotic community of environmental samples was investigated via single-strand conformation polymorphism and HiSeq/MiSeq Illumina amplicon sequencing.

SSCP analysis of snowfield-associated and freshwater-associated eukaryotes provided only limited insights into the microalgae community, as only the green microalgae *Scenedesmus* sp. was identified in one sample. Compared to sequencing of 18S rRNA genes, which are highly conserved among algae species, but also include variable regions for species identification (Christner *et al.*, 2003; Martin *et al*., 2002; Bakker *et al*., 1994), SSCP is a more rapid and cheaper method for community analysis (Jernigan and Hestekin, 2015). The low number of identified microalgae species in the present study might be due to a general absence of microalgae in the samples or due to lacking sensitivity of the analysis method. According to Jernigan and Hestekin (2015) detection and differentiation of prokaryotic (cyanobacteria) and eukaryotic algae is possible via SSCP. They performed a CE-SSCP analysis of pure algae cultures on a capillary electrophoresis instrument. This method provides additional advantages like automated loading and laser-induced fluorescence detection, which leads to a more sensitive detection at low concentrations.

In contrast, the SSCP analysis conducted in this study detected a snowfield-associated non-algae eukaryotic profile highly dominated by members of the classes *Microbotryomycetes* and *Insecta*. Fungal members of the class *Microbotryomycetes* were also found as one of the dominating classes in deep groundwater samples of below surface environments in Finland by Sohlberg and colleagues (2015). This may indicate that these fungi are adapted to frigid aquatic environments.

In a complementary approach, the eukaryotic structure of all environmental samples was also unraveled by 18S rRNA gene fragment MiSeq/HiSeq Illumina amplicon sequencing. Taxonomic analysis at phylum level revealed that abundances of *Archaeplastida*, *Opisthokonta* and *SAR* were habitat specific, but not dependent on the sampling site. Freshwater and snowfield samples from the sampling site in Seetaler Alpen (Styria/Austria)

were dominated by *Opisthokonta* and *SAR*, while freshwater samples from Graz and Ennstal as well as snowfield samples from Triebener Tauern were predominated by *Opisthokonta* and *Archaeplastida.* Similar patterns community structures were found by Lutz and colleagues (2015a), when they examined the eukaryotic community on Icelandic glaciers and ice caps.

In order to investigate the algae community, the analysis of the sequencing data focused on the archaeplastidome of all samples. Red and green snow samples were highly dominated by algae species of the family *Chlamydomonadaceae* and from the genus *Chloromonas.* As *Chlamydomonas nivalis* and *Chloromonas nivalis* are two of the most common microalgae species at high altitude red and green snow environments (Fujii *et al.,* 2009; Terashima *et al*., 2017; Newton, 1982; Takeuchi, 2001; Marchant, 1982), it can be assumed that some of the *Chlamydomonadaceae* belong to these species. According to Fujii *et al.* (2009) *Chlorella* sp. can also be found in red snow melt. In order to get an insight on the presence of *C. vulgaris*, samples comprising members of the order *Chlorellales* were examined in more detail. For instance in freshwater sample 3Cc *C. emersonii* (1.25%) was identified. Nevertheless any *C. vulgaris* was found.

4.3 Bacterial communities revealed potential for microalgae growth promotion

Previous 16S rRNA amplicon studies targeting microalgae-associated bacterial communities in snowfields (Terashima *et al*., 2017; Lutz *et al.,* 2015a) and freshwater lakes (Newton *et al.,* 2011) unraveled their bacterial community structure. By comparing their results with this study a similar core-microbiome was detected, consisting of *Proteobacteria, Bacteroidetes, Actinobacteria* and *Cyanobacteria*. In general, it was discovered that the microalgae-associated microbiome composition was independent of sampling location, but habitat-specific.

4.3.1 *Proteobacteria* and *Bacteroidetes* dominated the location-independent snowfield microalgae-associated microbiome

The sequencing of 16S rRNA gene fragments revealed *Proteobacteria* as the most abundant phylum in most of the analyzed samples, excepting samples 1A, 3A and 3E. In contrast, Simek and colleagues (2011) reported *Betaproteobacteria* as most abundant class in xenic algae cultures, since they were specialized and adapted for interaction with co-existing microalgae through a special way of carbon-utilization.

Snowfield-associated microbiomes additionally displayed high relative abundances of *Bacteroidetes*. Another study focusing on microbial communities in colored snowfields also found members of *Proteobacteria* and *Bacteroidetes* to be predominant in communities associated with snow algae (Hamilton and Havig, 2017). Looking at lower taxonomic levels revealed a sampling site independent bacterial community composition. Samples from Triebener Tauern (1A) and Seetaler Alpen (3A and 3E) were dominated by *Bacteroidetes*, especially members of the *Sphingobacteriaceae* family. According to Gomez-Pereira and colleagues (2012) members of *Sphingobacteria* can attach on algae cells as they contain several surface adhesion proteins and peptidases for degradation of algae exudates. Due to this specific attachment mechanisms, *Sphingobacteria* are well-adapted to live in co-existence with microalgae. *Comamonadaceae* from the order *Burkholderiales* within the phylum *Proteobacteria* were highly abundant in the microalgae-associated bacterial community of sample 1B. Further, members of *Oxalobacteraceae* from the order *Burkholderiales* showed major presence in sample 3D. These results are similar to the findings of other studies were *Burkholderiales* were found to be prevalent in colored snow collected from Svalbard and the Pacific Northwest (Lutz *et al.*, 2015b; Hamilton and Havig, 2017).

4.3.2 Freshwater bacterial communities provide high potential for microalgae growth promotion under artificial settings

The bacterial community of high altitude freshwater samples from Drei Lacken (Styria/Austria) were mainly dominated by gram-negative *Proteobacteria* and gram-positive *Actinobacteria*, while in samples from Seetaler Alpen additionally traces of *Bacteroidetes* and *Cyanobacteria* were found. This leads to the hypothesis that the microalgae-associated bacterial community in freshwater environments is not dependent on the sampling site, as well as not on the altitude. Newton and colleagues presented „A Guide to the Natural History of Freshwater Lake Bacteria“ in 2011; they summarized various molecular studies concerning the bacterial community composition in freshwater lakes through construction of a new phylogeny based on previously published 16S rRNA gene sequences from lake epilimnia. According to them and Zwart and colleagues (2002) the most common phyla in freshwater lakes are *Proteobacteria*, *Actinobacteria*, *Bacteroidetes*, *Cyanobacteria* and *Verrucomicrobia*, with *Proteobacteria* and *Actinobacteria* being the most prominent ones. This is in agreement with the community composition found in freshwater samples of this study.

Analyzes at lower taxonomic levels revealed a low bacterial diversity within samples 2A and 2C. They mainly consist of *Sphingomonadaceae* within the phylum *Proteobacteria* and

secondly of *Micrococcaceae* from the phylum *Actinobacteria*. Here the rarefaction curves indicated that their Shannon index is very low when compared to the other samples. In comparison sample 2B displayed the highest diversity on phylogenetic level family within freshwater samples, displaying abundances of *Sphingomonadaceae*, *Comamondaceae*, *Burkholderiaceae*, *Flavobacteriaceae* and *Micrococcaceae.* A similar bacterial community composition was found in freshwater samples 3B and 3C. It may be assumed that the freshwater-associated bacterial community is not dependent from sampling site, but seems to be freshwater habitat-specific. Conversely PCoA plot analysis based on the 16S rRNA sequencing data did not display a freshwater specific clustering.

Since the co-existence of bacteria can have positive effects on algae growth, Cho and colleagues (2014) examined the effect of a consortium consisting of *Flavobacterium, Sphingomonas, Rhizobium* and *Hyphomonas* on *C. vulgaris* performance. They found that implementation of these potentially growth-promoting bacteria in the algae phycosphere leads to an increase in biomass and lipid productivity. These four bacteria belong to phylogenetic bacterial families also found in freshwater specimen of this study. While no *C. vulgaris* sequences were found in this samples, isolation of bacteria and screening for putative *C. vulgaris* growth-promoting strains out of these samples was still a promising approach due to foregoing findings. This assumption was confirmed by identifying *Pseudomonas trivialis* 2Ca3 as *C. vulgaris* growth-promoting strain in freshwater sample 2Ca from Drei Lacken.

V. Conclusions and Outlook

Microalgae growth-promoting strains have the potential to enhance algae growth for industrial purposes in a natural and sustainable way. In this study, various bacteria from photobioreactors as well as bacteria associated with microalgae in their natural habitat were isolated. They were tested for growth-promoting effects on *C. vulgaris*, which is one of the most promising microalgae in industrial-scale algae biotechnology. To characterize these isolates a novel high-throughput screening assay was developed. It was confirmed that fluorescence intensity measurement of the *C. vulgaris* chlorophyll is a simple and rapid method for detection of differences in microalgae growth. Furthermore it allows screening of a high number of bacterial isolates for their potential to promote microalgae growth. Several strains which significantly enhanced *C. vulgaris* growth were identified with the novel assay and further characterized. The most promising candidate *Pseudomonas trivialis* 2Ca3 displayed versatile plant- and microalgae growth-promoting abilities. So far the potential of growth promotion was evaluated only at lab scale. A scale-up to larger volumes will shed light on its applicability in industrial cultivation approaches. Analysis of snowfield and freshwater samples from high altitude exhibited similar results to previously published studies concerning the bacterial and algal community in these habitats. As *C. vulgaris* could not be identified in any of the samples, sampling sites and sampling methods have to be reconsidered and renewed for further studies. The aim of the study – identification of a *C. vulgaris* growth-promoting strain – was fulfilled nevertheless. Different bacterial isolates associated with microalgae species related to *C. vulgaris* were found to promote *C. vulgaris* growth. In order to isolate bacteria which form close symbiotic relationships with *C. vulgaris* sampling should be repeated focusing on natural habitats of *C. vulgaris*. Uncovering evolutionary evolved bacteria-*Chlorella* co-occurrences are a promising way to isolate bacteria promoting *Chlorella* in a natural symbiotic way. In a further study, transcriptome analyses would be useful to unravel modes of interactions between algae and bacteria. Deepening the knowledge of symbiotic algae-bacteria interactions in natural environments might be a promising tool for biocontrol strategies in algae mass cultivation approaches.

VI. References

Adame-Vega, C., Lim, D.K., Timmins, M., Vernen, F., Li, Y., Schenk, P.M. (2011) Microalgal biofactories: a promising approach towards sustainable omega-3 fatty acid production. *Microbial Cell Factories*, 11: 1–11.

Afi, L., Metzger, P., Largeau, C., Connan, J., Berkaloff, C., Rousseau, B. (1996). Bacterial degradation of green microalgae: Incubation of Chlorella emersonii and Chlorella vulgaris with Pseudomonas oleovorans and Flavobacteriumaquatile. *Organic Geochemistry*, 25: 117–130.

Ahmadjian, V. (1967) A Guide to the Algae Occurring as Lichen Symbionts: Isolation, Culture, Cultural Physiology, and Identification. *Phycologia*, 6, 2 and 3: 127-160.

Altschul, S.F., Madden, T.L., Schäffer, A.A., Zhang, J., Zhang, Z., Miller, W., Lipman, D.J. (1997). Gapped BLAST and PSI-BLAST: a new generation of protein database search programs. *Nucleic Acids Research*, 25, 17: 3389–3402.

Amaral-Zettler, L.A., McCliment, E.A., Ducklow, H.W., Huse, S.M. (2009). A Method for Studying Protistan Diversity Using Massively Parallel Sequencing of V9 Hypervariable Regions of Small-Subunit Ribosomal RNA Genes. *PLOS ONE,* 4 (7): e6372.

Amin, S., Hmelo, L., Van Tol, H., Durham, B., Carlson, L., Heal, K. (2015). Interaction and signalling between a cosmopolitan phytoplankton and associated bacteria. *Nature*, 522: 98–101.

Amin, S.A., Green, D.H., Hart, M.C., Kupper, F.C., Sunda, W.G., Carrano, C.J. (2009). Photolysis of iron–siderophore chelates promotes bacterial–algal mutualism. *Proceedings of the National Academy of Sciences of the United States of America*, 106: 17071–17076.

Amin, S.A., Parker, M.S., Armbrust, E.V. (2012). Interactions between diatoms and bacteria. *Microbiology and Molecular Biology Reviews*, 76: 667–684.

Andrews, S.C., Robinson, A.K., Rodríguez-Quiñones, F. (2003) Bacterial iron homeostasis. *FEMS Microbiology Reviews,* 27:215-237.

Ashen, J.B., and Goff, L.J. (2000). Molecular and ecological evidence for species

specificity and coevolution in a group of marine algal-bacterial symbioses. *Applied and Environmental Microbiology*, 66: 3024–3030.

Aslan, S., Kapdan, I.K. (2006). Batch kinetics of nitrogen and phosphorus removal from synthetic wastewater by algae. *Ecological Engineering*, 28: 64–70.

Atkinson, K. M. (1972). Birds as transporters of algae. *British Phyeological Bulletin*. 7: 319–321.

Bakker, F.T., Olsen, J.L., Stam, W.T., van den Hoek, C. (1994). The cladophora complex (Chlorophyta): new views based on 185 rRNA gene sequences. *Molecular Phylogenetics and Evolution*, 3(4): 365–382.

Bassam, B. J., Caetano-Anollés, G., Gresshoff, P. M. (1991). Fast and sensitive silver staining of DNA in polyacrylamide gels. *Analytical Biochemistry*, 196(1), 80-83.

Becker, E.W. (1994). Microalgae: biotechnology and microbiology. Cambridge; New York: *Cambridge University Press*.

Beijerinck M. (1890). Kulturversuche mit Zoochlorellen, Lichenengonidien und anderen niederen Algen. *Botanische Zeitung*, 48: 729.

Beneduzi, A., Ambrosini, A., Passaglia, L.M. (2012). Plant growth-promoting rhizobacteria (PGPR): their potential as antagonists and biocontrol agents. *Genetics and Molecular Biology*, 35: 1044 –1051.

Benemann, J.R., Koopman, B.L., Weissman, J.C., Eisenberg, D.M., Oswald, W.J. (1978). An integrated system for the conversion of solar energy with sewage-grown microalgae. Report, Contract D(0-3)-34, SAN-003-4-2. U.S. *Department of Energy*.

Biondi, N., Cheloni, G., Tatti, E., Decorosi, F., Rodolfi, L., Giovannetti, L., et al. (2017). The bacterial community associated with Tetraselmis suecica outdoor mass cultures. *Journal of Applied Phycology*, 29: 67–78.

Bischoff, H.W., Bold, H.C. (1963). Phycological studies. IV. Some soil algae from Enchanted Rock and related algal species. *University of Texas Publications*, 6318: 1-95.

Borowitzka, M.A., Borowitzka L.J. (1998). Vitamins and fine chemicals from microalgae.

In: Micro-algal biotechnology. *Cambridge University Press*, p. 153–96.

Brennan, L. & Owende, P. (2010). Biofuels from microalgae- a review of technologies for production, processing, and extractions of biofuels and co-products. *Renewable and Sustainable Energy Reviews,* 14: 557–77.

Brenner, K., You, L., Arnold, F.H. (2008). Engineering microbial consortia: a new frontier in synthetic biology. *Trends in Biotechnology,* 26 (9), 483–489.

Callahan, B.J., McMurdie, P.J., Rosen, M.J., Han, A.W., Johnson, A.J.A., Holmes, S.P. (2016). DADA2: High-resolution sample inference from Illumina amplicon data. *Nature Methods*, 13: 581–583.

Caporaso, J.G., Lauber, C.L., Walters, W.A. (2012). Ultra-high-throughput microbial community analysis on the Illumina HiSeq and MiSeq platforms. *The ISME Journal*, 6(8):1621-1624.

Caporaso, J. G., Kuczynski, J., Stombaugh, J., Bittinger, K., Bushman, F. D., Costello, E. K., Fierer, N., Peña, A. G., Goodrich, J. K., Gordon, J. I., Huttley, G. A., Kelley, S. T., Knights, D., Koenig, J. E., Ley, R. E., Lozupone, C. A., McDonald, D., Muegge, B. D., Pirrung, M., Reeder, J., Sevinsky, J. R., Turnbaugh, P. J., Walters, W. A., Widmann, J., Yatsunenko, T., Zaneveld, J., Knight, R. (2010). QIIME allows analysis of high-throughput community sequencing data. *Nature methods*, 7(5), 335-6.

Carney, L.T., Lane, T.W. (2014). Parasites in algae mass culture. *Frontiers in Microbiology*, 5: 278.

Cassat, J.E., Skaar, E.P. (2013). Iron in infection and immunity. *Cell Host Microbe,* 13: 509 –519.

Cha, K.H., Koo, S.Y., Lee, D.U. (2008). Antiproliferative effects of carotenoids extracted from Chlorella ellipsoidea and Chlorella vulgaris on human colon cancercells. *Journal of Agriculture and Food Chemistry*, 56: 10521–6.

Chen, G.-Q., Chen, F. (2006). Growing phototrophic cells without light. *Biotechnology Letters*, 28(9): 607–16.

Chen, W., Sommerfeld, M., Hu, Q. (2011). Microwave-assisted nile red method for in vivo quantification of neutral lipids in microalgae. *Bioresource Technology,* 102: 135–41.

Cho, D.H., Ramanan, R., Heo, J., Lee, J., Kim, B.H., Oh, H.M., and Kim, H.S. (2014). Enhancing microalgal biomass productivity by engineering a microalgal-bacterial community. *Bioresource Technology,* 175c: 578–585.

Christner, B.C., Kvitko, B.H., Reeve, J.N. (2003). Molecular identification of bacteria and eukarya inhabiting an Antarctic cryoconite hole. *Extremophiles*, 7(3):177–183.

Clarens, A.F., Resurreccion, E.P., White, M.A., and Colosi, L.M. (2010) Environmental life cycle comparison of algae to other bioenergy feedstocks. *Environmental Science and Technology,* 44, 1813–1819.

Converti, A., Casazza, A.A., Ortiz, E.Y., Perego, P., Del Borghi, M. (2009). Effect of temperature and nitrogen concentration on the growth and lipid content of Nannochloropsisoculata and Chlorella vulgaris for biodiesel production. *Chemical Engineering and Processsing: Process Intensification*, 48:1146–51.

Cooper, M.B., Smith, A.G. (2015). Exploring mutualistic interactions between microalgae and bacteria in the omics age. *Current Opinion in Plant Biology*, 26, 147–153.

Croft, M.T., Lawrence, A.D., Raux-Deery, E., Warren, M.J., Smith, A.G. (2005). Algae acquire vitamin B12 through a symbiotic relationship with bacteria. *Nature*, 438: 90–93.

de-Bashan, L.E., Bashan, Y., Moreno, M., Lebsky, V.K., J Bustillos, J.J. (2002). Increased pigment and lipid content, lipid variety, and cell and population size of the microalgae Chlorella spp. when co-immobilized in alginate beads with the microalgae-growth-promoting bacterium Azospirillum brasilense. *Canadian Journal of Microbiology*, 48(6): 514-521.

Dittami, S.M., Eveillard, D., and Tonon, T. (2014). A metabolic approach to study algal–bacterial interactions in changing environments. *Molecular Ecology*, 23: 1656–1660.

Evenari, M., Mayer, A.M., Gottesman, E. (1953). Experiments on culture of algae in Israel. *The Scientific Monthly*, 83, 198-203.

Faheed, F., Abdel Fattah, Z. (2008). Effect of Chlorella vulgaris as bio-fertilizeron growth parameters and metabolic aspects of lettuce plant. *Journal of Agriculture and social Science*, 4:165–9.

Feng, Y., Li, C., Zhang, D. (2011). Lipid production of Chlorella vulgaris cultured in artificial wastewater medium. *Bioresource Technology*, 102: 101–5.

Fernandez-Sevilla, J.M., Fernandez, F.G., Grima, E.M. (2012). Obtaining lutein-rich extract from microalgal biomass at preparative scale. *Methods in Molecular Biology*, 892: 307–14.

Foflonker, F., Price, D.C., Qiu, H., Palenik, B., Wang, S., and Bhattacharya, D. (2015). Genome of the halotolerant green alga *Picochlorum* sp. reveals strategies for thriving under fluctuating environmental conditions. *Environmental Microbiology,* 17: 412–426.

Fuentes J. L., Garbayo I., Cuaresma M., Montero Z., González-del-Valle M., Carlos Vílchez C. (2016). Impact of Microalgae-Bacteria Interactions on the Production of Algal Biomass and Associated Compounds. *Marine Drugs*, 14: 100.

Fujii, M., Takano, Y., Kojima, H., Hoshino, T., Tanaka, R., & Fukui, M. (2009). Microbial community structure, pigment composition, and nitrogen source of red snow in Antarctica. *Microbial Ecology*, 59(3), 466-75.

Fulbright, S.P., Robbins-Pianka, A., Berg-Lyons, D., Knight, R, Reardon, K. F., Chisholm S. T. (2018). Bacterial community changes in an industrial algae production system. *Algal Research*, 31: 147–156.

Gendy, T.S., El-Temtamy, S.A. (2013). Commercialization potential aspects of microalgae for biofuel production: an overview. *Egyptian Journal of Petroleum*, 22 :43–51.

Gomez-Pereira, P. R., Schuler, M., Fuchs, B. M., Bennke, C., Teeling, H., Waldmann, J. (2012). Genomic content of uncultured *Bacteroidetes* from contrasting oceanic provinces in the North Atlantic Ocean. *Environmental Microbiology,* 14, 52–66.

Gouveia, L., Raymundo, A., Batista, A.P., Sousa, I., Empis, J. (2005). Chlorella vulgaris and Haematococcus pluvialis biomass as colouring and antioxidant in food emulsions. *European Food Reserach and Technology*, 222: 362–7.

Granado, F., Olmedilla, B., Blanco, I. (2003). Nutritional and clinical relevance of lutein in human health. *British Journal of Nutrition,* 90:487–502.

Grobbelaar, J.U. (2003). Quality, Control and Assurance: crucial for the sustainability of the applied phycology industry. *Journal of Applied Phycology*, 15: 209–15.

Guil-Guerrero, J.L., Navarro-Juarez, R., Lopez-Martinez, J.C., Campra-Madrid, P., Rebolloso-Fuentes, M.M. (2004). Functionnal properties of the biomass ofthree microalgal species. *Journal of Food Engineering,* 65:511–7.

Gulati, A., Rahi, P., Vyas, P. (2008). Characterization of phosphate-solubilizing fluorescent pseudomonads from the rhizosphere of Seabuckthorn growing in the cold deserts of Himalayas. *Current Microbiology*, 56: 73–79.

Gulati, O.P., Berry Ottaway, P. (2006). Legislation relating to nutraceuticals int he European Union with a particular focus on botanical-sourced products. *Toxicology*, 221: 75–87.

Gummert, F., Meffert, M.E., Stratman, H. (1953). Nonsterile large-scale culture of Chlorella in greenhouse and open air. In: Blurlew, J.S. (1953): *Algal culture*, from laboratory to pilot plant, Carnegie Institute of Washington, 600, 166-176.

H. J. Marchant (*1982*) Snow algae from the Australian Snowy Mountains. *Phycologia,* 6, 21, 2: 178-184.

Hamilton, T. L., Havig J. (2017). Primary productivity of snow algae communities on stratovolcanoes of the Pacific Northwest. *Geobiology,* 15, 280–295.

Harun, R., Danquah, M.K., Forde, G.M. (2010). Microalgal biomass as a fermentation feedstock for bioethanol production. *Journal of Chemical Technology and Biotechnology*, 85: 199–203.

Hernandez, J.-P., de-Bashan, L.E., Rodriguez, D.J., Rodriguez, Y., and Bashan, Y. (2009). Growth promotion of the freshwater microalga Chlorella vulgaris by the nitrogen-fixing, plant growth-promoting bacterium Bacillus pumilus from arid zone soils. *European Journal of Soil Biology,* 45: 88–93.

Hirano, A., Ueda, R., Hirayama, S., Ogushi, Y. (1997). CO_2 fixation and ethanol production with microalgal photosynthesis and intracellular anaerobic fermentation. *Energy*, 22:137–42.

Hom, E.F., Aiyar, P., Schaeme, D., Mittag, M., and Sasso, S. (2015). A chemical perspective on microalgal–microbial interactions. *Trends in Plant Science*, 20: 689–693.

Hu, Q., Sommerfeld, M., Jarvis, E., Ghirardi, M., Posewitz, M., Seibert, M. (2008). Microalgal triacylglycerols as feedstocks for biofuelproduction: perspectives and advances. *The Plant Journal*, 54:621–39.

Hu, Q., Sommerfeld, M., Jarvis, E., Ghirardi, M., Posewitz, M., Seibert, M. (2008). Microalgal triacylglycerols as feedstocks for biofuel production: perspectives and advances. *The Plant Journal*, 54: 621-639.

Illmer, P., Schinner F. (1992). Solubilization of inorganic phosphates by microorganisms isolated from forest soil. *Soil Biology and Biochemistry*, 24, 389-395.

Ivanova, J., Stoyancheva, G., and Pouneva, I. (2014). Lysis of Antarctic algal strains by bacterial pathogen. Antonie Van Leeuwenhoek, 105: 997–1005.

Iwamoto, H. (1958). Problems in mass culture of Chlorella. *J. Starch-sugar Tech Association*, 18, 64.

Jernigan, A., Hestekin, C. (2015). Capillary Electrophoresis Single-Strand Conformational Polymorphisms as a Method to Differentiate Algal Species. *Journal of Analytical Methods in Chemistry*, 272964.

Karlsson, T., Turkina, M.V., Yakymenko, O., Magnusson, K.-E., Vikström, E. (2012). The *Pseudomonas aeruginosa N*-Acylhomoserine Lactone Quorum Sensing Molecules Target IQGAP1 and Modulate Epithelial Cell Migration. *PLOS Pathogens,* 8(10): e1002953.

Kim, B.-H., Ramanan, R., Cho, D.-H., Oh, H.-M., and Kim, H.-S. (2014). Role of Rhizobium, a plant growth promoting bacterium, in enhancing algal biomass through mutualistic interaction. *Biomass and Bioenergy*, 69: 95–105.

Kim, M.J., Jeong, S.Y., Lee, S.J. (2008). Isolation, identification, and algicidal activity of marine bacteria against Cochlodinium polykrikoides. *Journal of Applied Phycology*, 20: 1069–1078.

Kononova, S., Nesmeyanova, M. (2002). Phosphonates and their degradation by microorganisms. *Biochemistry (Moscow),* 67: 184–195.

Krediet, C.J., Ritchie, K.B., Paul, V.J., Teplitski, M (2013). Coral-associated microorganisms and their roles in promoting coral health and thwarting diseases. *Proceedings of the Royal Society of London B: Biological Science*, 280: 2012-2328.

Krug L. (2016). Microalgae in an industiral-scale process: analyzing the co-microbiome dynamics. Master thesis, Institute of Environmental Biotechnology, Technical University Graz.

Lau, P.S., Tam, N.F.Y., Wong, Y.S. (1996). Wastewater nutrients removal by Chlorella vulgaris: optimization through acclimation. *Environmental Technology*, 17: 183–9.

Le Chevanton, M., Garnier, M., Bougaran, G., Schreiber, N., Lukomska, E., Berard, J.-B. (2013). Screening and selection of growth-promoting bacteria for Dunaliella cultures. *Algal Research*, 2: 212–222.

Lee, R.E. (2008). Phycology. 4th ed. Cambridge, England; New York: *Cambridge University Press*.

Lee, R.E. (2018). Phycology. *Cambridge University Press*, 5th edition,.

Lian J., Wijffels R., Smidt H., Sipkema D. (2018). The effect of algal microbiome on industrial production on microalgae. *Microbial Biotechnology*, 11(5), 806-818.

Liang, S., Liu, X., Chen, F., Chen, Z. (2004). Current microalgal health food & activities in China. Asian pacific phycology in the 21st century: prospects and challenges. Netherlands, Springer, 45–48.

Liang, S., Xueming, L., Chen, F., Chen, Z. (2004) Current microalgal health food R&D activities in China. *Hydrobiologia*, 512:45–8.

Lim, S.L., Chu, W.L., Phang, S.M. (2010). Use of Chlorella vulgaris for bioremediation of textile wastewater. *Bioresource Technology*, 101: 7314–22.

Lordan, S., Ross, R.P., Stanton, C. (2011). Marine bioactives as functional foodingredients: potential to reduce the incidence of chronic diseases. *Marine Drugs*, 9: 1056–100.

Lozupone, C., Knight, R. (2005). UniFrac: a New Phylogenetic Method for Comparing Microbial Communities. *Applied and Environmental Microbiology,* 71, 12: 8228-8235.

Lozupone, C.A., Hamady, M., Kelley, S.T., Knight, R. (2007). Quantitative and Qualitative β Diversity Measures Lead to Different Insights into Factors That Structure Microbial Communities . *Applied and Environmental Microbiology*, 73(5), 1576–1585.

Lundberg, D. S., Yourstone, S., Mieczkowski, P., Jones, C. D. & Dangl, J. L. (2013). Practical innovations for high-throughput amplicon sequencing. *Nature Methods*, 10(10), 999-1002.

Lutz, S., Anesio, A.M., Edwards, A., Benning, L.G. (2015a). Microbial diversity on Icelandic glaciers and ice caps. *Frontiers in Microbiology,* 6: 307.

Lutz, S., Anesio, A.M., Field, K., Benning, L.G. (2015b). Integrated 'omics', targeted metabolite and single-cell analyses of Arctic snow algae functionality and adaptability. *Frontiers in Microbiology,* 6: 132310.

Luz, E., Gonzalez, L., Bashan, Y. (2000). Increased Growth of the Microalga Chlorella vulgaris when Coimmobilized and Cocultured in Alginate Beads withthe Plant-Growth-Promoting Bacterium Azospirillum brasilense. *Applied and Environmental Microbiology*, 4: 1527–1531.

Martin, W., Rujan, T., Richly, E. (2002). Evolutionary analysis of Arabidopsis, cyanobacterial, and chloroplast genomes reveals plastid phylogeny and thousands of cyanobacterial genes in the nucleus. *Proceedings of the National Academy of Sciences of the United States of America*, 99:12246–12251.

Mata, T.M., Martins, A.A., Caetano, N.S. (2010). Microalgae for biodiesel production and other applications: a review. *Renewable and Sustainable Energy Reviews*, 14: 217–32.

McClean, K.H., Winson, M.K., Fish, L. (1997). Quorum sensing and Chromobacterium violaceum: exploitation of violacein production and inhibition for the detection of N-acylhomoserine lactones. *Microbiology*, 143: 3703–3711.

Mendes, L.B.B., Vermelho, A.B. (2013). Allelopathy as a potential strategy to improve

microalgae cultivation. *Biotechnology for Biofuels*, 6: 1.

Miethke, M., Marahiel, M.A. (2007). Siderophore-based iron acquisition and pathogen control. *Microbiology and Molecular Biology Reviews,* 71: 413–451.

Mitsuya, K., Nyunoyam, T., Tamiya, H. (1953). Pre-pilot plant experiments on algal mass culture. In: Blurlew, J.S. (1953): *Algal culture*, from laboratory to pilot plant, Carnegie Institute of Washington, 600, 273.

Morohoshi, T., Kato, M., Fukamachi, K., Kato, N., Ikeda, T. (2008). *N*-Acylhomoserine lactone regulates violacein production in *Chromobacterium violaceum* type strain ATCC 12472. *FEMS Microbiology Letters*, 279: 124-130.

Mouget, J.L., Dakhama, A., Lavoie, M.C., and Noue, J. (1995). Algal growth enhancement by bacteria: is consumption of photosynthetic oxygen involved. *FEMS Microbiology Ecology*, 18: 35–43.

Nautiyal, C. (1999). An efficient microbiological growth medium for screening phosphate solubilizing microorganisms. *FEMS Microbiology Letters*, 170: 265-270.

Newton, A.P.W. (1982). Red-coloured snow algae in Svalbard—some environmental factors determining the distribution of *Chlamydomonas nivalis* (Chlorophyta volvocales). *Polar Biology*, 1: 167–172.

Newton, R. J., Jones, S. E., Eiler, A., McMahon, K. D., & Bertilsson, S. (2011). A guide to the natural history of freshwater lake bacteria. *Microbiology and Molecular Biology Reviews: MMBR*, 75(1), 14-49.

Oncel, S.S. (2013). Microalgae for a macroenergy world. *Renewable and Sustainable Energy Reviews*, 26: 241-264

Pacheco, A.R., Sperandio, V. (2009). Inter-kingdom signaling: chemical language between bacteria and host. *Current Opinion in Microbiology,* 12: 192–198.

Peix, A., Ramirez-Bahena, H.M., Velázquez, E. (2009). Historical evolution and current status of the taxonomy of genus Pseudomonas. *Infection, Genetics and Evolution*, 9: 1132–1147.

Pienkos, P.T. and Darzins, A. (2009). The promise and challenges of microalgal-derived biofuels. *Biofuels, Bioproduction, Biorefining*, 3: 431-440.

Pribyl, P., Cepak, V., Zachleder, V. (2012). Production of lipids in10 strains of Chlorella and Parachlorella, and enhanced lipid productivity in Chlorella vulgaris. *Applied Microbiology and Biotechnology*, 94:549–61.

Přibyl, P., Cepák, V., Zachleder, V. (2013). Production of lipids and formation and mobilization of lipid bodies in Chlorella vulgaris. *Journal of Applied Phycology*, 25:545–53.

Putt, R., Singh, M., Chinnasamy, S., Das, K. (2011). An efficient system for carbonation of high-rate algae pondwater to enhance CO 2 mass transfer. *Bioresource Technology*, 102: 3240–3245.

Ramanan, R., Kim, B.H., Cho, D.H., Oh, H.M., Kim, H.S. (2016). Algae-bacteria interactions: Evolution, ecology and emerging applications. *Biotechnology Advances,* 34, 14–29.

Rodriguez, H., Fraga, R. (1999). Phosphate solubilizing bacteria and their role in plant growth promotion. *Biotechnology Advances,* 17: 319–339.

Rognes, T., Flouri, T., Nichols, B., Quince, C., Mahé, F. (2016): VSEARCH: a versatile open source tool for metagenomics. *PeerJ*, 4: e2584.

Safi, C., Zebib, B., Merah, O., Pontalier, P.Y.,Vaca-Garcia, C. (2014). Morphology, composition, production, processing and applications of Chlorella vulgaris: A review. *Renewable and Sustainable Energy Reviews*, 35, 265-278.

Schwieger, F., Tebbe, C.C. (1998). A New Approach To Utilize PCR–Single-Strand-Conformation Polymorphism for 16S rRNA Gene-Based Microbial Community Analysis. *Applied and Environmental Microbiology*, 64(12): 4870-4876.

Seymour, J.R., Amin, S.A., Raina, J.-B., and Stocker, R. (2017). Zooming in on the phycosphere: the ecological interface for phytoplankton–bacteria relationships. *Nature Microbiology*, 2: 17065.

Silva-Benavides, A., Torzillo, G. (2012). Nitrogen and phosphorus removal through laboratory batch cultures of microalga Chlorella vulgaris and cyanobacterium Planktothrix isothrix grown as monoalgal and as co-cultures. *Journal of Applied Phycology,* 24: 267–76.

Simek, K., Kasalicky, V., Zapomelova, E., Hornak K. (2011). Alga-derived substrates select for distinct Betaproteobacterial lineages and contribute to niche separation in *Limnohabitans strains*. *Applied and Environmental Microbiology,* 77, 7307–7315.

Singh, A., Nigam, P.S., Murphy, J.D. (2011). Renewable fuels from algae: an answer to debatable landbased fuels. *Bioresource Technology*, 102: 10–6.

Singh, M., Das, K. (2014). Low Cost Nutrients for Algae Cultivation. *Algal Biorefineries*, Dordrecht, The Netherlands: Springer, 69–82.

Sison-Mangus, M.P., Jiang, S., Tran, K.N., and Kudela, R.M. (2014). Host-specific adaptation governs the interaction of the marine diatom, Pseudo-nitzschia and their microbiota. The *ISME Journal*, 8: 63–76.

Smith, R. S., Iglewski, B. H. (2003). Pseudomonas aeruginosa quorum sensing as a potential

Sohlberg, E., Bomberg, M., Miettinen, H., Nyyssönen, M., Salavirta, H., Vikman, M., Itävaara, M. (2015). Revealing the unexplored fungal communities in deep groundwater of crystalline bedrock fracture zones in Olkiluoto, Finland. *Frontiers in Microbiology*, 6, 573.

Solomon, E.P., Berg, L.R., Martin, D.W. (1999) . *Biology*. 5thed, Fort Worth: Saunders College.

Subashchandrabose, S.R., Ramakrishnan, B., Megharaj, M., Venkateswarlu, K., and Naidu, R. (2011). Consortia of cyanobacteria/microalgae and bacteria: biotechnological potential. *Biotechnology Advances*, 29: 896–907.

Takechi, Y. (1965) Present state of mass culture of Chlorella and its application. *Journal of Fermentation Association*, 23, 370.

Takeuchi, N. (2001). The altitudinal distribution of snow algae on an Alaska glacier (Gulkana Glacier in the Alaska Range), *Hydrological Processes*, 15: 3447–3459.

Tanaka, K., Konishi, F., Himeno, K., Taniguchi, K., Nomoto, K. (1984). Augmentation of antitumor resistance by a strain of unicellular green algae, Chlorella vulgaris. *Cancer Immunology, Immunotherapy*, 17: 90–4.

Terashima, M., Umezawa, K., Mori, S., Kojima, H., & Fukui, M. (2017). Microbial Community Analysis of Colored Snow from an Alpine Snowfield in Northern Japan Reveals the Prevalence of *Betaproteobacteria* with Snow Algae. *Frontiers in Microbiology*, 8, 1481.

Valderrama, L.T., Del Campo, C.M., Rodriguez, C.M., de-Bashan, L.E., BashanY. (2002). Treatment of recalcitrant wastewater from ethanol and citric acid production using the microalga Chlorella vulgaris and the macrophyte Lemna minuscula. *Water Research*, 36: 4185–92.

Van den Hoek, C., Mann, D., Jahns, H. (1995). Algae: an introduction to phycology. Cambridge, United Kingdom, *Cambridge University Press*.

Vestheim, H., Jarman, S. N. (2008). Blocking primers to enhance PCR amplification of rare sequences in mixed samples – a case study on prey DNA in Antarctic krill stomachs. *Frontiers in Zoology*, 5(1), 1.

von Ditfurth, H. (1972). Im Anfang war der Wasserstoff, 2.Aufl, Hamburg:Hoffmann und Campe.

Wang, G., Shuai, L., Li, Y., Lin, W., Zhao, X., Duan, D. (2008). Phylogenetic analysis of epiphytic marine bacteriaon Hole-Rotten diseased sporophytes of Laminaria japonica. *Journal of Applied Phycology*, 20: 403–409.

Wang, S., Lambert, W., Giang, S., Goericke, R., and Palenik, B. (2014). Microalgal assemblages in a poikilohaline pond. *Journal of Phycology,* 50: 303–309.

Wangm, K., Brown, R.C., Homsy, S., Martinez, L., Sidhu, S.S.(2013). Fast pyrolysis of microalgae remnants in a fluidized bed reactor for biooil and biochar production. *Bioresource Technology*, 127: 494–9.

White, T.J. (Eds.), Innis, M.A., Gelfland, D.H., Sninsky, J.J. (1990). Amplification and direct sequencing of fungal ribosomal RNA genes for phylogenetics; PCR protocols: a guide to methods and applications. *Academic Press*, San Diego, CA, 315-322.

Widjaja, A., Chien, C-C., Ju, Y-H. (2009). Study of increasing lipid production from freshwater microalgae Chlorella vulgaris. *Journal of the Taiwan Institute of Chemical Engineers*, 40:13–20.

Xie, B., Bishop, S., Stessman, D., Wright, D., Spalding, M.H., Halverson, L.J. (2013). Chlamydomonas reinhardtii thermal tolerance enhancement mediated by a mutualistic interaction with vitamin B12-producing bacteria. *The ISME Journal*, 7, 1544–1555.

Yamamoto, M., Fujishita, M., Hirata, A., Kawano, S. (2004). Regeneration and maturation of daughtercellwalls in the autospore-forming greenalga Chlorella vulgaris (Chlorophyta,Trebouxiophyceae). *Journal of Plant Research*, 117: 257–64.

Yamamoto, M., Kurihara, I., Kawano, S. (2005). Late type of daughter cellwall synthesis in one of the Chlorellaceae, Parachlorellakessleri (Chlorophyta,Trebouxiophyceae). *Planta*, 221: 766–75.

Yao, S., Lyu, S., An, Y., Lu, J., Gjermansen, C., Schramm, A. (2018). Microalgae-bacteria symbiosis in microalgal growth and biofuel production: a review. *Journal of Applied Microbiology*.

Yun,Y.-S., Lee, S.B., Park, J.M., Lee, C.-I., Yang, J.-W. (1997). Carbondioxide fixation by algal cultivation using wastewater nutrients. *Journal of Chemical Technology and Biotechnology,* 69: 451–455.

Yvonne, N., Tomas, K. (2000). Cellwall development, microfibril and pyrenoid structure in type strains of Chlorella vulgaris, C. kessleri, C. sorokiniana compared with C. luteoviridis (Trebouxiophyceae, Chlorophyta). *Archiv für Hydrobiologie*, 100:95–105.

Zachow, C. , Fatehi, J. , Cardinale, M. , Tilcher, R. and Berg, G. (2010). Strain‐specific colonization pattern of *Rhizoctonia* antagonists in the root system of sugar beet. *FEMS Microbiology Ecology*, 74: 124-135.

Zachow, C., Tilcher, R., Berg, G. (2008). Sugar Beet-Associated Bacterial and Fungal Communities Show a High Indigenous Antagonistic Potential Against Plant Pathogens. *Microbial Ecology*, 55: 119.

Zheng, H., Yin, J., Gao, Z., Huang, H., Ji, X., Dou, C. (2011). Disruption of Chlorella vulgaris cells for the release of biodiesel-producing lipids: a comparison of

grinding, ultrasonication, beadmilling, enzymaticlysis and microwaves. *Applied Biochemistry and Biotechnology*, 164:1215–24.

Zhu, Y., Wu, F., He, Z., Guo, J., Qu, X., Xie, F. (2013). Characterization of organic phosphorus in lake sediments by sequential fractionation and enzymatic hydrolysis. *Environmental Science and Technology*, 47: 7679–7687.

Zozaya-Valdés, E., Roth-Schulze, A.J., Egan, S., Thomas, T. (2017). Microbial community function in the bleaching disease of the marine macroalgae *Delisea pulchra*. *Environmental Microbiology*, 19: 3012–3024.

Zwart, G., Crump, B.C., Agterveld, M.P.K.V., Hagen, F., S. K. Han, S.K. (2002). Typical freshwater bacteria: an analysis of available 16S rRNA gene sequences from plankton of lakes and rivers. *Aquatic Microbial Ecology*, 28: 141-155.

VII. Appendix

7.1 Working Solutions

7.1.1 Bold's Basal Medium (BBM)

A1/1	$NaNO_3$ (Carl Roth, Germany)	2.94×10^{-3} mol × L^{-1}
A1/2	KH_2PO_4 (Carl Roth, Germany)	1.29×10^{-3} mol × L^{-1}
A1/3	K_2HPO_4 (Carl Roth, Germany)	4.31×10^{-4} mol × L^{-1}
A1/4	$MgSO_4 \times 7\ H_2O$ (Merck, Germany)	3.04×10^{-4} mol × L^{-1}
A1/5	$CaCl_2$ (Carl Roth, Germany)	1.70×10^{-4} mol × L^{-1}
A1/6	NaCl (Carl Roth, Germany)	4.28×10^{-4} mol × L^{-1}
A2/1	H_3BO_3 (Carl Roth, Germany)	1.85×10^{-4} mol × L^{-1}
A2/2	$FeSO_4 \times 7\ H_2O$ (Carl Roth, Germany)	1.79×10^{-5} mol × L^{-1}
	$ZnSO_4 \times 7\ H_2O$ (Merck, Germany)	3.07×10^{-5} mol × L^{-1}
	$MnCl_2 \times 4\ H_2O$ (Merck, Germany)	7.28×10^{-6} mol × L^{-1}
A2/3	MoO_3 (Carl Roth, Germany)	4.93×10^{-6} mol × L^{-1}
	$CuSO_4 \times 5\ H_2O$ (Merck, Germany)	6.29×10^{-6} mol × L^{-1}
	$Co(NO_3)_3 \times 6\ H_2O$(Merck, Germany)	1.68×10^{-6} mol × L^{-1}
A2/4	EDTA (Carl Roth, Germany)	1.71×10^{-4} mol × L^{-1}
	KOH (Carl Roth, Germany)	5.53×10^{-4} mol × L^{-1}

For solid medium 15 g × L^{-1} Agar-Agar (Carl Roth, Germany) was added and sterilized (120 °C, 15 min). Subsequently 1 μL sterilfiltered (0.20 μm pore size) vitamin stock solution per mL medium was added.

Vitamin H (Biotin)	3.0×10^{-3} g × L^{-1}
Vitamin B (Thiamin-HCL x 2 H_2O)	3.3×10^{-2} g × L^{-1}
Vitamin B_2 (Riboflavin)	1.0×10^{-2} g × L^{-1}
Vitamin B_{12} (Cyanocobalamin)	1.7×10^{-2} g × L^{-1}
Vitamin B_3 (Niacin)	3.3×10^{-3} g × L^{-1}
VItamin B_9 (Folic Acid)	4.0×10^{-3} g × L^{-1}
Vitamin B_6 (Pyridoxamine-HCl)	5.0×10^{-2} g × L^{-1}
Hemicalcium D-(+)-pantothenate	1.7×10^{-2} g × L^{-1}
4-Aminobenzole Acid	1.3×10^{-2} g × L^{-1}
D,L-6,8-Thiotic Acid	1.0×10^{-2} g × L^{-1}

If required Ampicillin (50μg × mL^{-1} BBM) was added.

7.1.2 Reasoner's 2 Agar (R2A) Medium

Reasoner's 2A (Carl Roth, Germany)	18.10 g × L^{-1}

7.1.3 Nutrient Agar (NA) Medium

Noutrient Bouillon II (Sifin, Germany)	15.00 g × L^{-1}
Agar-Agar (Carl Roth, Germany)	18.00 g × L^{-1}

7.1.4 Lysogeny broth Medium

Trypton (Carl Roth, Germany)	10.00 g × L^{-1}
Yeast Extract (Carl Roth, Germany)	5.00 g × L^{-1}
NaCl (Carl Roth, Germany)	10.00 g × L^{-1}

If required 5 mM L-Tryptophan per liter were added.

7.1.5 National Botanical Research Institute's Phosphate growth (NBRIP) Medium

Glucose (Carl Roth, Germany)	10.00 g × L^{-1}
$Ca_3(PO_4)_2$ (Scharlab S.L., Spain)	5.00 g × L^{-1}
$MgSO_4 \times 7\ H_2O$ (Merck, Germany)	0.25 g × L^{-1}
$MgCl_2 \times 6H_2O$ (Carl Roth, Germany)	5.00 g × L^{-1}
KCl (Carl Roth, Germany)	0.20 g × L^{-1}
$(NH_4)_2SO_4$ (neoLab Migge, Germany)	0.10 g × L^{-1}
Agar-Agar (Carl Roth, Germany)	15.00 g × L^{-1}

7.2 Sample overview

7.2.1 Samples from production sites

Table 7.1: Overview of samples taken from photobioreactors: A-F. Specimen were provided by BDI-BioEnergy International GmbH.

Abbrevation	Origin	Growth conditions	Picked bacterial isolates
A	Demo B 10100 green	no data	63
B	5 L PBR	carbon-source CO_2	52
C	5 L PBR	carbon-source Acetic acid	56
D	reactor 4 17016	carbon-source CO_2 + intense light	71
E	reactor 3 17015	carbon source Acetic acid pH 3.9 + intense light	17
F	reactor 3 17015	carbon source Acetic acid pH 7.5 + intense light	34

7.2.2 Overview of high-alpine environmental samples

Table 7.2: Samples taken from Triebener Tauern: 1A and 1B.

Abbrevation	1A	1B
Origin	Snowfield north-eastern incline	Green puddle on snow
Growth conditions	1-2 °C	1-2 °C pH 6.5
Number of replicates	7 abcdefg	6 abcdeg

Table 7.3: Samples taken from Drei Lacken: 2A, 2B and 2C.

Abbrevation	2A	2B	2C
Origin	Green pond	Green pond	Swimming pond
Growth conditions	13 °C pH 6.5	17 °C pH 6.5	15 °C pH 7.2
Number of replicates	2 ab	2 ab	2 ab

Table 7.4: Samples taken from Seetaler Alpen: 3A-3E.

Abbrevation	3A	3B	3C	3D	3E
Origin	Snowfield beside lake	Puddle	Lake	Snowfield on mountain peak	Snowfield
Growth conditions	1-2 °C pH 6.4	14 °C pH 5.5	16 °C pH 7	1-2 °C	1-2° C
Number of replicates	3 abc	4 abcd	4 abcd	5 abcde	3 abc

7.3 Cultivation dependent analysis

7.3.1 Photobioreactor Samples

Table 7.5: Viable cell count after four days of incubation for sample A „Demo B 10100“.

Replicate	Dilution	NA		BBM		R2A	
		CFU × 100 μL^{-1}	bacterial isolates	CFU × 100 μL^{-1}	bacterial isolates	CFU × 100 μL^{-1}	bacterial isolates
A	10^{-0}	>600		>600		>600	
	10^{-1}	>600		>600		>600	
	10^{-2}	213	3	500	2	>600	
	10^{-3}	16	3	58	2	>600	2
	10^{-4}	1	2	12	2	127	2
	10^{-5}	0		4	2	21	4
B	10^{-0}	>600		>600		>600	
	10^{-1}	>600		>600		>600	
	10^{-2}	231	2	>600	2	>600	
	10^{-3}	27	2	60	2	>600	2
	10^{-4}	0		9	2	163	1
	10^{-5}	0		1		2	2
C	10^{-0}	>600		>600		>600	
	10^{-1}	>600		>600		>600	
	10^{-2}	220	2	>600	4	>600	
	10^{-3}	35	2	57	4	>600	
	10^{-4}	6		17	2	96	1
	10^{-5}	0		11	2	18	4
total CFU × mL^{-1}		**2.40×10^5**		**3.40×10^5**		**1.50×10^7**	

Table 7.6: Viable cell count after four days of incubation for sample B „5 L PBR“.

Replicate	Dilution	NA		BBM		R2A	
		CFU × 100 μL^{-1}	bacterial isolates	CFU × 100 μL^{-1}	bacterial isolates	CFU × 100 μL^{-1}	bacterial isolates
A	10^{-0}	>600		>600		>600	
	10^{-1}	>600		>600		>600	
	10^{-2}	213	3	>600		>600	
	10^{-3}	16	3	135		>600	4
	10^{-4}	1	2	91	3	328	2
	10^{-5}	0		7	1	77	4
B	10^{-0}	>600		>600		>600	
	10^{-1}	>600		>600		>600	
	10^{-2}	>600		>600		>600	
	10^{-3}	>600	4	151		>600	
	10^{-4}	166	4	5	2	400	2
	10^{-5}	12	2	3	1	no data	
C	10^{-0}	>600		>600		>600	
	10^{-1}	>600		>600		>600	
	10^{-2}	>600		>600		>600	
	10^{-3}	>600	4	155		>600	
	10^{-4}	185	4	3	1	366	2
	10^{-5}	17	2	7	1	no data	
total CFU × mL^{-1}		**1.60×10^7**		**1.30×10^5**		**4.60×10^7**	

Table 7.7: Viable cell count after four days of incubation for sample C „5 L PBR“.

Replicate	Dilution	NA		BBM		R2A	
		CFU × 100 μL^{-1}	bacterial isolates	CFU × 100 μL^{-1}	bacterial isolates	CFU × 100 μL^{-1}	bacterial isolates
A	10^{-0}	>600		>600		>600	
	10^{-1}	>600		>600		>600	
	10^{-2}	213	3	>600		>600	
	10^{-3}	16	3	374		>600	
	10^{-4}	1	2	61	2	>600	
	10^{-5}	0		5	1	266	4
B	10^{-0}	>600		>600		>600	
	10^{-1}	>600		>600		>600	
	10^{-2}	>600		>600		>600	
	10^{-3}	>600		397		>600	
	10^{-4}	>600	4	55	2	>600	2
	10^{-5}	170	3	8	1	325	4
C	10^{-0}	>600		>600		>600	
	10^{-1}	>600		>600		>600	
	10^{-2}	>600		>600		>600	
	10^{-3}	>600		424		>600	
	10^{-4}	>600	4	51	2	>600	2
	10^{-5}	136	5	9	2	338	4
total CFU × mL^{-1}		**7.66×10^7**		**5.25×10^6**		**3.10×10^8**	

Table 7.8: Viable cell count after four days of incubation for sample D „reactor 4 17016“.

Replicate	Dilution	NA		BBM		R2A	
		CFU × 100 μL^{-1}	bacterial isolates	CFU × 100 μL^{-1}	bacterial isolates	CFU × 100 μL^{-1}	bacterial isolates
A	10^{-0}	>600		>600		>600	
	10^{-1}	>600		>600		>600	
	10^{-2}	>600		>600		>600	
	10^{-3}	>600	3	>600	1	>600	
	10^{-4}	289	3	346	1	142	3
	10^{-5}	150	2	116	3	174	2
	10^{-6}	107	1	56		104	2
B	10^{-0}	>600		>600		>600	
	10^{-1}	>600		>600		>600	
	10^{-2}	>600		>600		>600	
	10^{-3}	>600	2	>600	3	>600	
	10^{-4}	376	3	247	1	223	3
	10^{-5}	95	2	100	3	113	2
	10^{-6}	37	1	33		47	1
C	10^{-0}	>600		>600		>600	
	10^{-1}	>600		>600		>600	
	10^{-2}	>600		>600		>600	
	10^{-3}	>600	2	>600	2	>600	
	10^{-4}	286	3	271	1	260	3
	10^{-5}	88	2	106	3	109	2
	10^{-6}	75	1	62		88	3
total CFU × mL^{-1}		**2.90×10^{8}**		**1.70×10^{9}**		**1.20×10^{11}**	

Table 7.9: Viable cell count after four days of incubation for sample E „reactor 3 17015“.

Replicate	Dilution	NA		BBM		R2A	
		CFU × 100 μL^{-1}	bacterial isolates	CFU × 100 μL^{-1}	bacterial isolates	CFU × 100 μL^{-1}	bacterial isolates
A	10^{-0}	no growth		no growth		>600	
	10^{-1}					>600	
	10^{-2}					34	3
	10^{-3}					4	2
	10^{-4}					2	
	10^{-5}					0	
	10^{-6}					0	
B	10^{-0}	no growth		no growth		>600	
	10^{-1}					>600	
	10^{-2}					60	3
	10^{-3}					4	2
	10^{-4}					0	
	10^{-5}					0	
	10^{-6}					0	
C	10^{-0}	no growth		no growth		>600	
	10^{-1}					>600	
	10^{-2}					29	3
	10^{-3}					0	
	10^{-4}					0	
	10^{-5}					0	
	10^{-6}					0	
total CFU × mL^{-1}						**4.10×10^4**	

Table 7.10: Viable cell count after three days of incubation for sample F „reactor 3 17015“.

Sample	Dilution	NA		BBM		R2A	
		CFU × 100 μL^{-1}	bacterial isolates	CFU × 100 μL^{-1}	bacterial isolates	CFU × 100 μL^{-1}	bacterial isolates
A	10^{-0}	>600		>600		>600	
	10^{-1}	>600		>600		>600	
	10^{-2}	>600		>600		>600	
	10^{-3}	>600		>600		>600	
	10^{-4}	>600		>600		>600	
	10^{-5}	>600	2	>600		>600	3
	10^{-6}	>600	2	316	2	>600	1
B	10^{-0}	>600		>600		>600	
	10^{-1}	>600		>600		>600	
	10^{-2}	>600		>600		>600	
	10^{-3}	>600		>600		>600	
	10^{-4}	>600		>600		>600	
	10^{-5}	>600	2	>600	2	>600	2
	10^{-6}	>600	2	>600	2	>600	1
C	10^{-0}	>600		>600		>600	
	10^{-1}	>600		>600		>600	
	10^{-2}	>600		>600		>600	
	10^{-3}	>600		>600		>600	
	10^{-4}	>600		>600		>600	2
	10^{-5}	>600	2	>600	2	>600	2
	10^{-6}	>600	2	>600	2	>600	1
total CFU × mL^{-1}				**3.16×10^9**			

7.3.2 Environmental Sample from Graz

Table 7.11: Viable cell count after different incubation periods for sample G.

Replicate	Dilution	NA		BBM		R2A	
		CFU × 100 μL^{-1}	bacterial isolates	CFU × 100 μL^{-1}	bacterial isolates	CFU × 100 μL^{-1}	bacterial isolates
A	10^{-0}	>600		>600		>600	
	10^{-1}	>600		>600		>600	
	10^{-2}	128	4	189	3	>600	4
	10^{-3}	22	4	20	2	125	4
	10^{-4}	3	3	13	4	21	4
	10^{-5}	0		0		2	
	10^{-6}	0		0		0	
	10^{-7}	0		0		0	
	10^{-8}	0		19	4	0	
B	10^{-0}	>600		>600		>600	
	10^{-1}	>600		>600		>600	
	10^{-2}	122	4	241	3	>600	4
	10^{-3}	33	4	18	2	215	4
	10^{-4}	4	4	7	4	31	4
	10^{-5}	0		0		10	2
	10^{-6}	0		0		0	
	10^{-7}	0		0		0	
	10^{-8}	0		0		0	
C	10^{-0}	>600		>600		>600	
	10^{-1}	>600		>600		>600	
	10^{-2}	132	4	196	3	>600	4
	10^{-3}	51	4	20	2	80	4
	10^{-4}	6	4	11	3	14	4
	10^{-5}	2		0		3	1
	10^{-6}	0		0		0	
	10^{-7}	0		0		0	
	10^{-8}	0		0		0	
total CFU × mL^{-1}		**2.93×10^5**		**4.78×10^5**		**2.57×10^6**	

7.3.3 High altitude environmental samples

Table 7.12: Viable cell count after different incubation periods for sample 1A.

Sample	Dilution	NA		BBM		R2A	
		CFU × 100 μL^{-1}	bacterial isolates	CFU × 100 μL^{-1}	bacterial isolates	CFU × 100 μL^{-1}	bacterial isolates
1Aa	10^{-0}	no growth		83	8	no growth	
	10^{-1}			0			
	10^{-2}			0			
	10^{-3}			0			
	10^{-4}			0			
	total CFU × mL^{-1}			**8.30×10^2**			
1Ab	10^{-0}	>600		>600		>600	
	10^{-1}	124	4	>600		261	3
	10^{-2}	5	2	0		17	3
	10^{-3}	0		0		0	
	10^{-4}	0		0		0	
	total CFU × mL^{-1}	**8.70×10^3**				**2.15×10^4**	
1Ac	10^{-0}	71	4	146	5	no growth	
	10^{-1}	0		0			
	10^{-2}	0		0			
	10^{-3}	0		0			
	10^{-4}	0		0			
	total CFU × mL^{-1}	**7.10×10^2**		**1.46×10^3**			
1Ad	10^{-0}	no growth		2	2	no growth	
	10^{-1}			0			
	10^{-2}			0			
	10^{-3}			0			
	10^{-4}			0			
	total CFU × mL^{-1}						
1Ae	10^{-0}	59	3	112	4	70	5
	10^{-1}	1		0		5	3
	10^{-2}	1		0		0	
	10^{-3}	0		0		0	

	10^{-4}	0		0		0	
	total CFU × mL^{-1}	590		1120			
1Af	10^{-0}	29	3	418	2	67	3
	10^{-1}	0		26	2	7	1
	10^{-2}	0		1		13	
	10^{-3}	0		1		0	
	10^{-4}	0		0		0	
	total CFU × mL^{-1}	**2.90×10^2**		**3.39×10^3**		**4.79×10^3**	
1Ag	10^{-0}	no growth		42	3	no growth	
	10^{-1}			55	5		
	10^{-2}			4	2		
	10^{-3}			1			
	10^{-4}			0			
	total CFU × mL^{-1}			**2.96×10^3**			

Table 7.13: Viable cell count after different incubation periods for sample 1B.

Sample	Dilution	NA		BBM		R2A	
		CFU × 100 μL^{-1}	bacterial isolates	CFU × 100 μL^{-1}	bacterial isolates	CFU × 100 μL^{-1}	bacterial isolates
1Ba	10^{-0}	6	3	>600		31	3
	10^{-1}	0		3	3	0	
	10^{-2}	0		2	2	0	
	10^{-3}	0		0		0	
	10^{-4}	0		0		0	
	total CFU × mL^{-1}	**60**				**3.10×10^2**	
1Bb	10^{-0}	no growth		50	3	231	5
	10^{-1}			0		0	
	10^{-2}			0		0	
	10^{-3}			0		0	
	10^{-4}			0		0	
	total CFU × mL^{-1}			**5.00×10^2**		**2.31×10^3**	
1Bc	10^{-0}	10	2	19	1	211	2
	10^{-1}	0		1		1	
	10^{-2}	0		0		0	
	10^{-3}	0		0		0	
	10^{-4}	0		0		0	
	total CFU × mL^{-1}	**10^2**		**1.90×10^2**		**2.11×10^3**	
1Bd	10^{-0}	no growth		no growth		no growth	
	10^{-1}						
	10^{-2}						
	10^{-3}						
	10^{-4}						
	total CFU × mL^{-1}						
1Be	10^{-0}	>600		>600		>600	
	10^{-1}	>600		>600		>600	
	10^{-2}	237	2	141	1	191	3
	10^{-3}	17	2	6	2	11	2
	10^{-4}	2		0		0	

	total CFU × mL^{-1}	**2.04 × 10^5**		**1.00 × 10^5**		**1.50 × 10^5**	
1Bg	10^{-0}	>600		>600		>600	
	10^{-1}	>600		11	2	>600	
	10^{-2}	73	3	2		221	2
	10^{-3}	14	2	0		21	2
	10^{-4}	0		0		0	
	total CFU × mL^{-1}	**1.07 × 10^5**		**1.10 × 10^3**		**2.15 × 10^5**	

Table 7.14: Viable cell count after different incubation periods for sample 2A, 2B and 2C.

Sample	Dilution	NA		BBM		R2A	
		CFU × 100 μL^{-1}	bacterial isolates	CFU × 100 μL^{-1}	bacterial isolates	CFU × 100 μL^{-1}	bacterial isolates
2Aa	10^{-0}	19	1	183	1	115	1
	10^{-1}	0		0		0	
	10^{-2}	0		0		0	
	10^{-3}	0		0		0	
	10^{-4}	0		0		0	
	total CFU × mL^{-1}	**1.90×10^2**		**1.83×10^3**		**1.15×10^3**	
2Ab	10^{-0}	no growth		no growth		no growth	
	10^{-1}						
	10^{-2}						
	10^{-3}						
	10^{-4}						
	total CFU × mL^{-1}						
2Ba	10^{-0}	77	2	>600		514	
	10^{-1}	7	1	69	3	7	2
	10^{-2}	0		21	3	0	
	10^{-3}	0		3		0	
	10^{-4}	0		0		0	
	total CFU × mL^{-1}	**7.35×10^2**		**1.40×10^4**		**2.92×10^3**	
2Bb	10^{-0}	93	3	>600		>600	
	10^{-1}	0		>600		14	3
	10^{-2}	0		15	3	0	
	10^{-3}	0		0		0	
	10^{-4}	0		0		0	
	total CFU × mL^{-1}	**9.30×10^2**		**1.50×10^4**		**1.40×10^3**	
2Ca	10^{-0}	176	3	432	2	610	
	10^{-1}	8	2	17	2	>600	
	10^{-2}	0		3		1	
	10^{-3}	0		0		0	

	10^{-4}	0	0	0
	total CFU × mL^{-1}	**1.28×10^3**	**3.01×10^3**	**6.10×10^3**
2Cb	10^{-0}	no growth	no growth	no growth
	10^{-1}			
	10^{-2}			
	10^{-3}			
	10^{-4}			
	total CFU × mL^{-1}			

Table 7.15: Viable cell count after different incubation periods for sample 3A.

Sample	Dilution	NA		BBM		R2A	
		CFU × 100 μL^{-1}	bacterial isolates	CFU × 100 μL^{-1}	bacterial isolates	CFU × 100 μL^{-1}	bacterial isolates
3Aa	10^{-0}	>600		>600		>600	
	10^{-1}	124	1	117	1	46	3
	10^{-2}	10	3	6	2	2	
	10^{-3}	0		0		0	
	10^{-4}	0		0		0	
	total CFU × mL^{-1}	**1.12×10^4**		**8.85×10^3**		**4.60×10^3**	
3Ab	10^{-0}	>600		>600		>600	
	10^{-1}	>600		>600		>600	
	10^{-2}	224	2	352	3	224	2
	10^{-3}	12	3	40	3	15	2
	10^{-4}	0		8	2	0	
	total CFU × mL^{-1}	**1.72×10^5**		**5.17×10^5**		**1.87×10^5**	
3Ac	10^{-0}	>600		>600		>600	
	10^{-1}	>600		>600		>600	
	10^{-2}	43	2	264	1	>600	
	10^{-3}	1		39	3	42	2
	10^{-4}	0		7		5	
	total CFU × mL^{-1}	**4.30×10^4**		**4.51×10^5**		**4.60×10^5**	

Table 7.16: Viable cell count after different incubation periods for sample 3B.

Sample	Dilution	NA		BBM		R2A	
		CFU × 100 μL^{-1}	bacterial isolates	CFU × 100 μL^{-1}	bacterial isolates	CFU × 100 μL^{-1}	bacterial isolates
3Ba	10^{-0}	33	2	>600		321	4
	10^{-1}	0		24	3	1	1
	10^{-2}	0		2	1	0	
	10^{-3}	0		0		0	
	10^{-4}	0		0		0	
	total CFU × mL^{-1}	**3.30×10^2**		**2.40×10^3**		**3.21×10^3**	
3Bb	10^{-0}	119	2	>600		282	3
	10^{-1}	0		231	2	12	4
	10^{-2}	0		2	2	0	
	10^{-3}	0		0		0	
	10^{-4}	0		0		0	
	total CFU × mL^{-1}	**1.19×10^3**		**2.31×10^4**		**2.01×10^3**	
3Bc	10^{-0}	147	3	>600		73	2
	10^{-1}	6		129	3	9	3
	10^{-2}	0		5		0	
	10^{-3}	0		0		0	
	10^{-4}	0		0		0	
	total CFU × mL^{-1}	**1.04×10^3**		**8.95×10^3**		**8.15×10^2**	
3Bd	10^{-0}	33	5	>600		148	3
	10^{-1}	3	2	122	4	11	3
	10^{-2}	0		2		0	
	10^{-3}	0		0		0	
	10^{-4}	0		0		0	
	total CFU × mL^{-1}	**3.30×10^2**		**1.22×10^4**		**1.29×10^3**	

Table 7.17: Viable cell count after different incubation periods for sample 3C.

Sample	Dilution	NA		BBM		R2A	
		CFU × 100 μL^{-1}	bacterial isolates	CFU × 100 μL^{-1}	bacterial isolates	CFU × 100 μL^{-1}	bacterial isolates
3Ca	10^{-0}	800		>600		572	1
	10^{-1}	5	2	67	2	27	3
	10^{-2}	1		4	2	0	
	10^{-3}	0		0		0	
	10^{-4}	0		0		0	
	total CFU × mL^{-1}	**4.25×10^3**		**6.70×10^3**		**4.21×10^3**	
3Cb	10^{-0}	>600		>600		260	2
	10^{-1}	53	2	336	2	4	2
	10^{-2}	0		26	3	0	
	10^{-3}	0		0		0	
	10^{-4}	0		0		0	
	total CFU × mL^{-1}	5300		29800		1500	
3Cc	10^{-0}	>600				>600	
	10^{-1}	116	1			>600	
	10^{-2}	37	2	no growth		22	2
	10^{-3}	0				2	1
	10^{-4}	0				1	
	total CFU × mL^{-1}	**2.43×10^4**				**2.20×10^4**	
3Cd	10^{-0}			>600			
	10^{-1}			>600			
	10^{-2}	no growth		152		no growth	
	10^{-3}			6			
	10^{-4}			0			
	total CFU × mL^{-1}			**1.06×10^5**			

Table 7.18: Viable cell count after different incubation periods for sample 3D.

Sample	Dilution	NA		BBM		R2A	
		CFU × 100 µL^{-1}	bacterial isolates	CFU × 100 µL^{-1}	bacterial isolates	CFU × 100 µL^{-1}	bacterial isolates
3Da	10^{-0}	>600		>600		>600	
	10^{-1}	>600		>600		>600	
	10^{-2}	81	2	85	1	72	2
	10^{-3}	10		7		8	
	10^{-4}	0		0		0	
	total CFU × mL^{-1}	9.05×10^4		7.75×10^4		7.60×10^4	
3Db	10^{-0}	>600		>600		>600	
	10^{-1}	840		>600		>600	
	10^{-2}	0		180	2	82	3
	10^{-3}	1		2	1	0	
	10^{-4}	0		0		0	
	total CFU × mL^{-1}	**8.40×10^4**		**1.80×10^5**		**8.20×10^4**	
3Dc	10^{-0}	>600		>600		>600	
	10^{-1}	>600		>600		>600	
	10^{-2}	118	3	290	1	167	2
	10^{-3}	6	2	27	2	6	1
	10^{-4}	0		0		0	
	total CFU × mL^{-1}	**8.90×10^4**		**2.80×10^5**		**1.14×10^5**	
3Dd	10^{-0}	>600		>600		>600	
	10^{-1}	>600		>600		>600	
	10^{-2}	86	2	>600		33	2
	10^{-3}	20	1	66	2	0	
	10^{-4}	0		8	1	0	
	total CFU × mL^{-1}	**1.43×10^5**		**7.30×10^5**		**3.30×10^4**	
3De	10^{-0}	>600		>600		>600	
	10^{-1}	>600		>600		>600	
	10^{-2}	135	5	>600		145	5
	10^{-3}	10	3	76	4	14	3
	10^{-4}	0		4	1	0	

	total CFU × mL^{-1}	**1.18×10^5**	**5.80×10^5**	**1.43×10^5**

Table 7.19: Viable cell count after different incubation periods for sample 3E.

Sample	Dilution	NA		BBM		R2A	
		CFU × 100 μL^{-1}	bacterial isolates	CFU × 100 μL^{-1}	bacterial isolates	CFU × 100 μL^{-1}	bacterial isolates
3Ea	10^{-0}	230		>600		>600	
	10^{-1}	31	2	>600		51	1
	10^{-2}	1		7	1	11	2
	10^{-3}	0		0		0	
	10^{-4}	0		0		0	
	total CFU × mL^{-1}	**2.70×10^3**		**7.00×10^3**		**8.05×10^3**	
3Eb	10^{-0}	293		>600		>600	
	10^{-1}	0		245		>600	
	10^{-2}	0		26	2	31	2
	10^{-3}	0		7	1	0	
	10^{-4}	0		0		0	
	total CFU × mL^{-1}	**2.93×10^3**		**4.02×10^4**		**3.10×10^4**	
3Ec	10^{-0}	199		>600		>600	
	10^{-1}	15	3	110	3	245	2
	10^{-2}	1	1	14	3	32	3
	10^{-3}	0		6		0	
	10^{-4}	0		0		0	
	total CFU × mL^{-1}	**1.74×10^3**		**2.83×10^4**		**2.83×10^4**	

7.4 Applied plant biocontrol strains

1	*Serratia plymuthica* 3Re4-18
2	*Streptomyces tauricus* RE2-6-8
3	Fau 88 SDK 1-2-18
4	*Pseudomonas aurantiaca* SDK 2-2-6
5	*Pantoea ananatis* SDK BLBT 1-08
6	*Stenotrophomonas rhizophila* ep17
7	*Serratia plymuthica* HRO C48
8	*Stenotrophomonas rhizophila* P69
9	*Bacillus pumilis* BB-1-3-5
10	*Pseudomonas fluorescens* L13-6-12
11	*Bacillus subtilis* B2g
12	*Pseudomonas poae* Re × -1-1-14
13	*Paenibacillus polymyxa* Pb71
14	*Burkholderia sp.* C1 ecto 15
15	*Pseudomonas trivialis* 3Re-2-7
16	*Pseudomonas putida* 1T1
17	*Streptomyces* Ca 1-25a
18	*Streptomyces hasug* Fav2 HRO71
19	*Pseudomonas filiscidens* B2R2-1-2-3
20	*Stenotrophomonas rhizophila* ep14
21	*Micorbacterium sp*. Rübe 1-3-26
22	*Microbacteriaceae* C1 ecto 9
23	*Kytococcus sedentarius* L3 ecto 15
24	*Sinorhizobium sp.* W4-7
25	*Serratia plymuthica* 3RP8
26	*Burkholderia bryophila sp.* Nov. A5

7.5 Chemicals

7.5.1 TBE Buffer [5x conc.]

EDTA [0.5 mM] (Carl Roth, Germany)	0.02 L × L^{-1}
Tris HCl	54.00 g × L^{-1}
Boric Acid	27.50 g × L^{-1}

7.6 Single Strand Conformation Polymorphisms

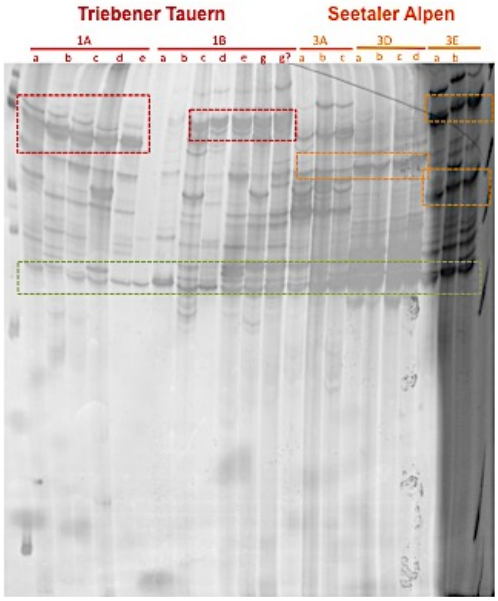

Figure 7.1: SSCP profile of snowfield-associated bacterial communities from sampling sites Triebener Tauern (1A; 1B) and Seetaler Alpen (3A; 3D; 3E). Red and orange dashed boxes point out sampling site specific patterns, while the green dashed box shows a putative snow-associated core pattern. Standard: Gene ruler 1 kb ladder.

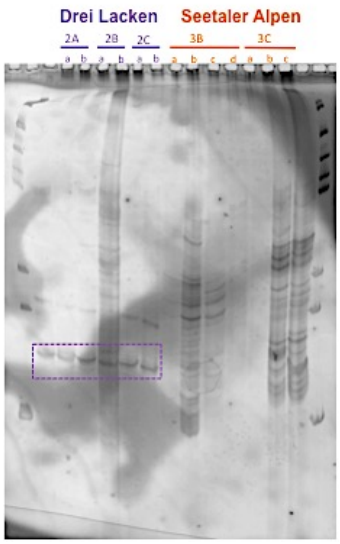

Figure 7.2: SSCP profile of freshwater-associated bacterial communities from Drei Lacken (2A; 2B; 2C) and Seetaler Alpen (3B; 3C). The purple dashed box points out putative site-specific patterns. Standard: Gene ruler 1 kb ladder.

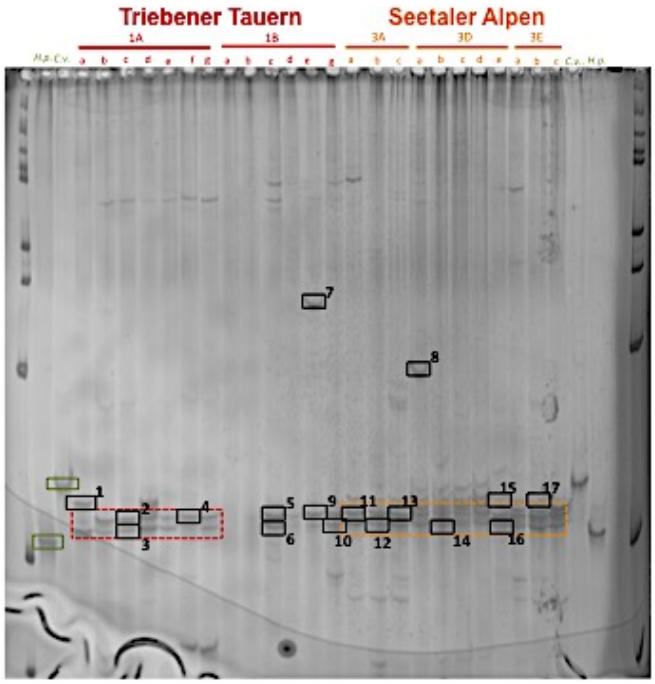

Figure 7.3: 18S rRNA gene fragment SSCP profiles of snowfield-associated eukaryotes from samples 1A and 1B (Triebener Tauern) and samples 3A, 3B and 3D (Seetaler Alpen). References: C.v. = *C. vulgaris*; H.p. = *H. pluvialis*. Standard: Gene ruler 1 kb ladder. Numbered bands were excised for sequencing.

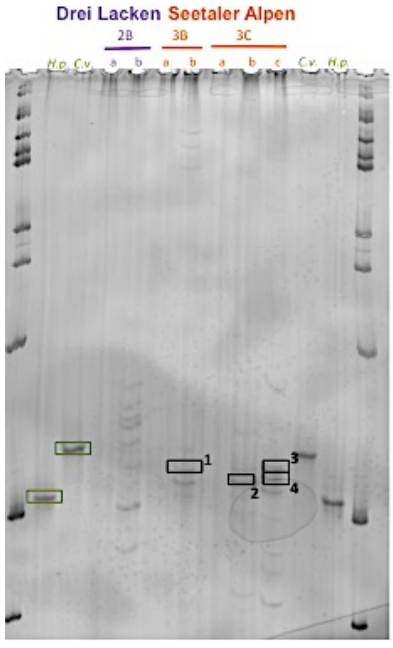

Figure 7.4: 18S rRNA gene fragment SSCP profiles of freshwater-associated eukaryotes from samples 2B (Drei Lacken) and samples 3B and 3C (Seetaler Alpen). References: C.v. = *C. vulgaris*; H.p. = *H. pluvialis*. Standard: Gene ruler 1 kb ladder. Numbered bands were excised for sequencing.

7.7 Amplicon Barcodes

Table 7.20: Primer and barcode-constructs used for amplicon analyzes. Linker sequence used for amplification with golay barcode-constructs GT.

Barcode ID forward	Bardcode ID reverse	Barcode sequence forward	Barcode sequence reverse	Barcode length
golay_bc_97_for	**golay_bc_97_rev**	**ACTCTTACTTAGTATGGTAATTGT**	**ACTCTTACTTAGTATGGTAATTGT**	**24**
golay_bc_98_for	**golay_bc_98_rev**	**CTACAGGGTCTCTATGGTAATTGT**	**CTACAGGGTCTCTATGGTAATTGT**	**24**
golay_bc_99_for	**golay_bc_99_rev**	**CTTGGAGGCTTATATGGTAATTGT**	**CTTGGAGGCTTATATGGTAATTGT**	**24**
golay_bc_100_for	**golay_bc_100_rev**	**TATCATATTACGTATGGTAATTGT**	**TATCATATTACGTATGGTAATTGT**	**24**
golay_bc_101_for	**golay_bc_101_rev**	**CTATATTATCCGTATGGTAATTGT**	**CTATATTATCCGTATGGTAATTGT**	**24**
golay_bc_102_for	**golay_bc_102_rev**	**ACCGAACAATCCTATGGTAATTGT**	**ACCGAACAATCCTATGGTAATTGT**	**24**
golay_bc_103_for	**golay_bc_103_rev**	**ACGGTACCCTACTATGGTAATTGT**	**ACGGTACCCTACTATGGTAATTGT**	**24**
golay_bc_104_for	**golay_bc_104_rev**	**TGAGTCATTGAGTATGGTAATTGT**	**TGAGTCATTGAGTATGGTAATTGT**	**24**
golay_bc_105_for	**golay_bc_105_rev**	**ACCTACTTGTCTTATGGTAATTGT**	**ACCTACTTGTCTTATGGTAATTGT**	**24**
golay_bc_106_for	**golay_bc_106_rev**	**ACTGTGACGTCCTATGGTAATTGT**	**ACTGTGACGTCCTATGGTAATTGT**	**24**
golay_bc_107_for	**golay_bc_107_rev**	**CTCTGAGGTAACTATGGTAATTGT**	**CTCTGAGGTAACTATGGTAATTGT**	**24**
golay_bc_108_for	**golay_bc_108_rev**	**CATGTCTTCCATTATGGTAATTGT**	**CATGTCTTCCATTATGGTAATTGT**	**24**
golay_bc_109_for	**golay_bc_109_rev**	**AACAGTAAACAATATGGTAATTGT**	**AACAGTAAACAATATGGTAATTGT**	**24**
golay_bc_110_for	**golay_bc_110_rev**	**GTTCATTAAACTTATGGTAATTGT**	**GTTCATTAAACTTATGGTAATTGT**	**24**
golay_bc_111_for	**golay_bc_111_rev**	**GTGCCGGCCGACTATGGTAATTGT**	**GTGCCGGCCGACTATGGTAATTGT**	**24**
golay_bc_112_for	**golay_bc_112_rev**	**CCTTGACCGATGTATGGTAATTGT**	**CCTTGACCGATGTATGGTAATTGT**	**24**
golay_bc_113_for	**golay_bc_113_rev**	**CAAACTGCGTTGTATGGTAATTGT**	**CAAACTGCGTTGTATGGTAATTGT**	**24**
golay_bc_114_for	**golay_bc_114_rev**	**TCGAGAGTTTGCTATGGTAATTGT**	**TCGAGAGTTTGCTATGGTAATTGT**	**24**
golay_bc_115_for	**golay_bc_115_rev**	**CGACACGGAGAATATGGTAATTGT**	**CGACACGGAGAATATGGTAATTGT**	**24**
golay_bc_116_for	**golay_bc_116_rev**	**TCCACAGGGTTCTATGGTAATTGT**	**TCCACAGGGTTCTATGGTAATTGT**	**24**
golay_bc_117_for	**golay_bc_117_rev**	**GGAGAACGACACTATGGTAATTGT**	**GGAGAACGACACTATGGTAATTGT**	**24**
golay_bc_118_for	**golay_bc_118_rev**	**CCTACCATTGTTTATGGTAATTGT**	**CCTACCATTGTTTATGGTAATTGT**	**24**
golay_bc_119_for	**golay_bc_119_rev**	**TCCGGCGGGCAATATGGTAATTGT**	**TCCGGCGGGCAATATGGTAATTGT**	**24**
golay_bc_120_for	**golay_bc_120_rev**	**TAATCCATAATCTATGGTAATTGT**	**TAATCCATAATCTATGGTAATTGT**	**24**
golay_bc_121_for	**golay_bc_121_rev**	**CCTCCGTCATGGTATGGTAATTGT**	**CCTCCGTCATGGTATGGTAATTGT**	**24**
golay_bc_122_for	**golay_bc_122_rev**	**TTCGATGCCGCATATGGTAATTGT**	**TTCGATGCCGCATATGGTAATTGT**	**24**
golay_bc_123_for	**golay_bc_123_rev**	**AGAGGGTGATCGTATGGTAATTGT**	**AGAGGGTGATCGTATGGTAATTGT**	**24**
golay_bc_124_for	**golay_bc_124_rev**	**AGCTCTAGAAACTATGGTAATTGT**	**AGCTCTAGAAACTATGGTAATTGT**	**24**
golay_bc_125_for	**golay_bc_125_rev**	**CTGACACGAATATATGGTAATTGT**	**CTGACACGAATATATGGTAATTGT**	**24**
golay_bc_126_for	**golay_bc_126_rev**	**GCTGCCCACCTATATGGTAATTGT**	**GCTGCCCACCTATATGGTAATTGT**	**24**
golay_bc_127_for	**golay_bc_127_rev**	**GCGTTTGCTAGCTATGGTAATTGT**	**GCGTTTGCTAGCTATGGTAATTGT**	**24**
golay_bc_129_for	**golay_bc_129_rev**	**AGATCGTGCCTATATGGTAATTGT**	**AGATCGTGCCTATATGGTAATTGT**	**24**
golay_bc_130_for	**golay_bc_130_rev**	**CATTTCGCACTTTATGGTAATTGT**	**CATTTCGCACTTTATGGTAATTGT**	**24**
golay_bc_131_for	**golay_bc_131_rev**	**ACATGATATTCTTATGGTAATTGT**	**ACATGATATTCTTATGGTAATTGT**	**24**
golay_bc_132_for	**golay_bc_132_rev**	**GCAACGAACGAGTATGGTAATTGT**	**GCAACGAACGAGTATGGTAATTGT**	**24**
golay_bc_133_for	**golay_bc_133_rev**	**AGATGTCCGTCATATGGTAATTGT**	**AGATGTCCGTCATATGGTAATTGT**	**24**
golay_bc_134_for	**golay_bc_134_rev**	**TCGTTATTCAGTTATGGTAATTGT**	**TCGTTATTCAGTTATGGTAATTGT**	**24**
golay_bc_135_for	**golay_bc_135_rev**	**GGATACTCGCATTATGGTAATTGT**	**GGATACTCGCATTATGGTAATTGT**	**24**
golay_bc_136_for	**golay_bc_136_rev**	**AATGTTCAACTTTATGGTAATTGT**	**AATGTTCAACTTTATGGTAATTGT**	**24**
golay_bc_137_for	**golay_bc_137_rev**	**AGCAGTGCGGTGTATGGTAATTGT**	**AGCAGTGCGGTGTATGGTAATTGT**	**24**
golay_bc_138_for	**golay_bc_138_rev**	**GCATATGCACTGTATGGTAATTGT**	**GCATATGCACTGTATGGTAATTGT**	**24**

golay_bc_139_for	**golay_bc_139_rev**	**CCGGCGACAGAATATGGTAATTGT**	**CCGGCGACAGAATATGGTAATTGT**	**24**
golay_bc_140_for	**golay_bc_140_rev**	**CCTCACTAGCGATATGGTAATTGT**	**CCTCACTAGCGATATGGTAATTGT**	**24**
golay_bc_141_for	**golay_bc_141_rev**	**CTAATCAGAGTGTATGGTAATTGT**	**CTAATCAGAGTGTATGGTAATTGT**	**24**
BC_042	**BC_042**	**CAGCATCA**	**CAGCATCA**	**8**
BC_044	**BC_044**	**CGTCATAG**	**CGTCATAG**	**8**
BC_045	**BC_045**	**CTACGAGT**	**CTACGAGT**	**8**
BC_046	**BC_046**	**CTCATGTG**	**CTCATGTG**	**8**
BC_047	**BC_047**	**GACGCATA**	**GACGCATA**	**8**
BC_048	**BC_048**	**GAGCATAC**	**GAGCATAC**	**8**
BC_049	**BC_049**	**GATACGAC**	**GATACGAC**	**8**
BC_050	**BC_050**	**GATGATGC**	**GATGATGC**	**8**
BC_051	**BC_051**	**GCTAGTAC**	**GCTAGTAC**	**8**
BC_052	**BC_052**	**GTAGCATC**	**GTAGCATC**	**8**
BC_053	**BC_053**	**GTGCATGT**	**GTGCATGT**	**8**
BC_055	**BC_055**	**TATGCGAG**	**TATGCGAG**	**8**
BC_056	**BC_056**	**TCAGTGTG**	**TCAGTGTG**	**8**
BC_057	**BC_057**	**TCTACGTC**	**TCTACGTC**	**8**
BC_058	**BC_058**	**TGACTCAC**	**TGACTCAC**	**8**
BC_059	**BC_059**	**TGCATGAG**	**TGCATGAG**	**8**
BC_060	**BC_060**	**TGTCGCTA**	**TGTCGCTA**	**8**
BC_061	**BC_061**	**ACATGCGTA**	**ACATGCGTA**	**9**
BC_062	**BC_062**	**ACTACTGTC**	**ACTACTGTC**	**9**
BC_065	**BC_065**	**AGTGTCAGC**	**AGTGTCAGC**	**9**
BC_066	**BC_066**	**ATCGTCACT**	**ATCGTCACT**	**9**
BC_067	**BC_067**	**ATGAGATGC**	**ATGAGATGC**	**9**
BC_068	**BC_068**	**CACACACGT**	**CACACACGT**	**9**
BC_070	**BC_070**	**CATACATGC**	**CATACATGC**	**9**
BC_071	**BC_071**	**CATGTATGC**	**CATGTATGC**	**9**
BC_075	**BC_075**	**CTCACTGAT**	**CTCACTGAT**	**9**
BC_076	**BC_076**	**CTGTATGCT**	**CTGTATGCT**	**9**
BC_077	**BC_077**	**GACTCGTGT**	**GACTCGTGT**	**9**
BC_079	**BC_079**	**GCACTACTA**	**GCACTACTA**	**9**
BC_080	**BC_080**	**GCATCACGT**	**GCATCACGT**	**9**
BC_081	**BC_081**	**GCGTATATG**	**GCGTATATG**	**9**
BC_082	**BC_082**	**GCTGTACAT**	**GCTGTACAT**	**9**
BC_083	**BC_083**	**GTACGTGAT**	**GTACGTGAT**	**9**
BC_084	**BC_084**	**GTATATGCG**	**GTATATGCG**	**9**
BC_085	**BC_085**	**GTATGTCTC**	**GTATGTCTC**	**9**
BC_086	**BC_086**	**GTCGTATGA**	**GTCGTATGA**	**9**
BC_087	**BC_087**	**TACACATCG**	**TACACATCG**	**9**
BC_088	**BC_088**	**TACGCGTCA**	**TACGCGTCA**	**9**
BC_089	**BC_089**	**TAGCAGTGC**	**TAGCAGTGC**	**9**
BC_090	**BC_090**	**TATCGCACA**	**TATCGCACA**	**9**
BC_092	**BC_092**	**CACATAGTCG**	**CACATAGTCG**	**10**
BC_093	**BC_093**	**CACGTAGCGT**	**CACGTAGCGT**	**10**
BC_094	**BC_094**	**CAGATAGAGA**	**CAGATAGAGA**	**10**
BC_095	**BC_095**	**CATAGCGCAT**	**CATAGCGCAT**	**10**

BC_096	**BC_096**	**CGACTATACT**	**CGACTATACT**	**10**
BC_097	**BC_097**	**CGCATAGCAG**	**CGCATAGCAG**	**10**

VIII. Abbreviations

µ	micro
° C	Grad Celsius
AHL	N-Acyljomoserine lactone
b	base
BBM	Bold's basal medium
BCA	biocontrol agent
BLAST	Basic Local Alignment Search Tool
bp	basepair
CAS	Chrome Azurol-S
cfu	colony forming units
CTAB	cetyltrimethylammonium bromide
CO_2	carbon dioxide
DNA	desoxyribonucleic acid
DOC	dissolved organic carbon
DOM	dissolved organic matter
EDTA	ethylenediaminetetraacetic acid
e.g.	exempli gratia
et al.	et alia
Fig.	Figure
g	gram
h	hour
H_2O	water
k	kilo
L	Liter
LB	lysogeny broth
lm	lumen
m	mili
M	mol
min	minute
n	nano
nm	nanometer
NA	nutrient agar
NaCl	sodiumchloride
NB	nutrient bouillon
NBRIP	National Botanical Research Institute's phosphate growth agar
NCBI	National Center for Biotechnology Information
OD	optical density
OTU	operational taxonomic unit
PBR	photobioreactor
PBS	phosphate-buffered saline
PCoA	Principal Coordinate Analysis

PCR	polymerase chain reaction
pH	pondus hydrogenii
PNA	peptide nucleic acid
PPS	protein precipitation solution
QIIME	quantitative insights into microbial ecology
QS	quorum sensing
R2A	reasoner's 2 agar
rcf	relative centrifugal field
RFU	relative fluorescence units
rpm	revolutions per minute
rRNA	ribosomal ribnulceic acid
RSV	ribosomal sequence variants
RT	room temperature
SAR	Stramenopilen, Alveolata, Rhizaria
SDS	sodium dodecyl sulfate
sec	second
SSCP	single strand conformation polymorphism
t	ton
Tab.	Table
TGGE	temperature gradient gel electrophoresis
UV-Vis	ultraviolet-visible
V	Volt
WHO	world health organisation
wt vol^{-1}	weight per volume

IX. List of Figures

X. List of Tables